UNIVERSITY OF OSLO
Department of Physics

fNIRS and EEG for Detection of Intraoperative Awareness

Master thesis

Magnus Leon
Reinsfelt Krogh

May 2014

Abstract

Background. Patients under general anesthesia have a risk of regaining awareness while being paralyzed and unable to communicate, which may lead to severe psychological trauma. Various methods for monitoring the depth of anesthesia are available, but they rely on measuring biological markers that may be misleading. A new method has been suggested: using a brain computer interface to detect if the patient is attempting to move, because cortical activity as a result of attempted movement can be measured reliably. A system for detection of intraoperative awareness must have a simple generic hardware montage that takes a minimal amount of time to set up, in order to be considered clinically feasible. Electroencephalography (EEG) and functional near-infrared spectroscopy (fNIRS) are two methods for measuring brain activity, which exhibit different advantages and disadvantages. This study investigates if fNIRS may be considered a feasible alternative.

Methods. A combined EEG- fNIRS measurement experiment was conducted on freely informed participants. The participants performed randomly selected, hand and foot movement tasks while brain activity was measured. The data was analyzed post hoc to determine, and compare the performance of the two modalities at detecting these movements.

Results. The average performance rate for EEG at detecting movement, both hand and foot, was higher than for fNIRS, although only significantly for foot movement. Observations made during the analysis suggests that fNIRS could not measure foot movements reliably, and that the performance for the two modalities at detecting hand movements were mutually exclusive, suggesting that only one modality could measure hand movement reliably at a time.

Conclusion. The author will argue, based on aforementioned observations, that using fNIRS or a combination of EEG and fNIRS, in an intraoperative awareness monitoring system reliably, will increase the time and/or complexity of the setup, making it less feasible than a system based on EEG alone. Further research is needed to verify this argument.

Acknowledgments

This thesis is the fulfilling of the Master of Science in Electronics and Computer Technology at the Department of Physics, University of Oslo. It contains work done from August 2013 to June 2014, under the supervision of associate professors Jason Farquhar, Jan Olav Høgetveit and Ole Jakob Elle. The initial research, experiment design, preparations and experiments were performed by the author in collaboration with members of the BCI group at the Donders Institute for Brain, Cognition and Behavior, Radboud University in Nijmegen, the Netherlands. This project is part of a larger research project promoted by Dr. Jörgen Bruhn.

I want to express my sincere gratitude towards my supervisors Jan Olav Høgetveit, Ole Jakob Elle and Jason Farquhar for always being helpful, participating in fruitful discussions, reviewing numerous drafts and assuring my troubled mind at stressful times. Very special thanks to Jason Farquhar, for welcoming me to Nijmegen, where I was invited to stay and learn about the exciting field of brain computer interfaces, from him and his incredibly talented team of researchers. I would like to thank Dr. Bruhn for letting me partake in this exciting project, and for helping with funding for the experiments. I would also like to thank PhD Candidate Yvonne Blokland and Dr. Loukianos Spyrou for all the help I received along the way; Dr. Noël Keijsers and the Sint Maartens Kliniek for lending me the fNIRS equipment; Tormod Gundersen for his maddening attention to detail during the proofreading, engineers and eloquent writing don't always go hand in hand; and last but not least, my wonderful, beautiful and patient Nina Bredesen Hørthe, for all the love and care.

Contents

1 Introduction and motivation **1**
- 1.1 General anesthesia . . . 2
- 1.2 Intraoperative awareness . . . 3
  - 1.2.1 Cause . . . 3
  - 1.2.2 Recollection . . . 3
  - 1.2.3 Sequelae . . . 4
  - 1.2.4 Methods for preventing IOA . . . 4
- 1.3 Brain-Computer Interface . . . 6
  - 1.3.1 Applications . . . 6
  - 1.3.2 The BCI cycle . . . 7
  - 1.3.3 BCI in intraoperative awareness detection . . . 15
- 1.4 Functional near-infrared spectroscopy (fNIRS) . . . 17
  - 1.4.1 Hemodynamics . . . 17
  - 1.4.2 Signal acquisition . . . 17
  - 1.4.3 The modified Beer-Lambert law . . . 21
  - 1.4.4 Advantages and disadvantages . . . 22
- 1.5 Study goals and objectives . . . 23
- 1.6 Study design . . . 25
  - 1.6.1 Sample size determination . . . 25
  - 1.6.2 Inclusion criteria . . . 26
  - 1.6.3 Exclusion criteria . . . 26
  - 1.6.4 Discontinuation/withdrawal of participants from study . . . 26
  - 1.6.5 Participants . . . 26
- 1.7 Data management and statistical analysis . . . 27
- 1.8 Ethical considerations . . . 27
  - 1.8.1 Informed consent . . . 27
  - 1.8.2 Confidentiality . . . 28

2 Methods **29**
- 2.1 Matlab toolboxes . . . 30
- 2.2 Hardware . . . 32
- 2.3 Optode/Electrode placement . . . 34
- 2.4 Software integration . . . 36
- 2.5 Protocol . . . 38

2.6 Data analysis procedures . . . 40
2.6.1 fNIRS data processing and analysis . . . 40
2.6.2 EEG data processing and analysis . . . 41
2.6.3 Classifier . . . 43
2.6.4 Center of Gravity . . . 43

3 Results **45**
3.1 BOLD response . . . 45
3.2 Sensorimotor rhythmic response . . . 46
3.3 Classification rates . . . 51
3.4 Task discrimination using fNIRS . . . 53
3.5 Difference in CoG (ΔCoG) . . . 55

4 Discussion **59**

5 Summary of findings **67**

Appendices **79**

A Declaration of Conformity for Oxymon MKIII **81**

B Oxymon MKIII information leaflet **83**

C WMA Declaration of Helsinki - Ethical Principles for Medical Research Involving Human Subjects **87**
C.1 INTRODUCTION . . . 87
C.2 PRINCIPLES FOR ALL MEDICAL RESEARCH . . . 88
C.3 ADDITIONAL PRINCIPLES FOR MEDICAL RESEARCH COMBINED WITH MEDICAL CARE . . . 92

D Informed consent form and fact sheet **95**

E MATLAB scripts and functions written by the author **101**
E.1 Oxymon to Field Trip script . . . 101
E.2 Analysis control script . . . 105
E.3 fNIRS specific analysis script . . . 109
E.4 fNIRS specific analysis preprocessing function . . . 113
E.5 fNIRS CoG analysis script . . . 117
E.6 BOLD grand average plot script . . . 120
E.7 Analysis saving script . . . 124
E.8 Experiment stimulus script . . . 127
E.9 Experiment signal processing script . . . 132

F MATLAB scripts and functions developed at Donders Inst. **137**
F.1 Shell script to start buffer . . . 137
F.2 Detrend functions . . . 139

F.3 ID outliers functions 142
F.4 Classifier training functions 145

List of Figures

1.1 Graphical representation of the BCI cycle. 7
1.2 Alternative representation of the BCI cycle. 8
1.3 Placement of measurement technologies and level of invasiveness. 9
1.4 Spatial and temporal resolution for various brain signal measurement technologies. 10
1.5 The motor cortex homunculus. 13
1.6 Time frequency plot of a sensorimotor rhythmic response to motor stimulation. 14
1.7 A typical BOLD response to motor stimulation. 18
1.8 Components of a continous wave fNIRS system. 19
1.9 Absorption spectra of chromophores in tissue. 20

2.1 The FieldTrip blackboard buffer structure. 31
2.2 Photos of the measurement hardware used in this study. . . 33
2.3 Electrode/optode placement according to the International 10-20 system for electrode placement. 34
2.4 Photos of the modified cap with attached electrodes and optodes. 35
2.5 Optode channel formation. 36
2.6 Software setup used for the experiments. 37
2.7 Trial sequence. 39
2.8 Analysis pipeline of fNIRS data. 41
2.9 Analysis pipeline of EEG data. 42

3.1 Total grand average of the BOLD response. 46
3.2 Grand average of area under the receiver operating curve (AUC) for hand movement condition for each electrode. . . 47
3.3 Grand average of spectral densities for each electrode, hand movement condition. 48
3.4 Grand average of the area under the ROC curve for each electrode, foot movement task. 49
3.5 Grand average of spectral densities for each electrode, foot movement condition. 50
3.6 Bar diagram showing classification rates for each subject. . . 52

3.7 Center of gravity for hand and foot movement measured by fNIRS. 54
3.8 Grand average CoG, hand movement task, for EEG and fNIRS. 55
3.9 Grand average CoG, foot movement task, for EEG and fNIRS. 56
3.10 Correlation between ΔCoG and classification rate for fNIRS. 57

4.1 Correlation between classification rates for both modalities. 60
4.2 Propagation of vasodilation through the tissue during foot movement, scenario 1. 62
4.3 Propagation of vasodilation through the tissue during foot movement, scenario 2. 63

5.1 Deductions made from observations in objectives 1 and 2. . 69

List of Tables

3.1 Classification rates for each subject. 51
3.2 Coordinates for the center of gravity for each subject, fNIRS, hand and foot movement. 53

Nomenclature

AUC	Area under the receiver operating curve
AWR	Awareness with recall
BCI	Brain-Computer Interface
CoG	Center of gravity
ECoG	Electrocorticography
EEG	Electroencephalography
ERD	Event related de-synchronization
ERP	Event related potential
ERS	Event related synchronization
fMRI	Functional magnetic resonance imaging
fNIRS	Functional near-infrared spectroscopy
HbO	Oxygenated hemoglobin
HbR	De-oxygenated hemoglobin
IOA	Intra-operative awareness
PET	Positron emission tomography
rCBF	Regional cerebral blood flow
rCMRO2	Regional metabolic rate of oxygen consumption
ROC	Receiver operating curve
SMR	Sensorimotor rhythm
SPECT	Single photon emission computed tomography
SSVEP	Steady state visually evoked potential
TFR	Time-frequency representation

Chapter 1

Introduction and motivation

Patients undergoing surgery under general anesthesia have a risk of regaining awareness while being paralyzed and unable to communicate. This might be traumatizing to the patient and may lead to late psychological effects like anxiety, sleep disturbances and post traumatic stress disorder. Various methods for monitoring the depth of anesthesia are available, but they rely on measuring biological markers that may be misleading.

An ongoing research project at the Donders Institute for Brain, Cognition and Behavior suggests an alternative approach; to detect if the patient is trying to move, since this is a natural response for a patient experiencing anesthesia awareness, and attempted movement can be detected reliably with a brain-computer interface (BCI). The system proposed by Donders Inst. is based on measuring the electrical impulses produced in the brain (EEG) when attempting to move. Another method of measuring the brain's activity is functional near infra-red spectroscopy (fNIRS, sometimes denoted as NIRS in more technical context), which is based on measuring the oxygen consumption of particular areas in the brain. These two methods have different advantages and disadvantages.

This study will investigate if fNIRS can be considered a feasible alternative to EEG in regard to how well the two systems can detect attempted movement, and if the system can operate with a minimal, generic setup that will work for all patients. To investigate this a volunteer study with a minimum of 10 healthy participants will be conducted. The participants will be wearing a combined EEG and fNIRS system while performing movement tasks. The gathered data will be analyzed to determine if the system meets the requirements, and whether or not the classification rate of detecting movement will exceed the classification rate of the EEG-based system.

1.1 General anesthesia

When a patient has to undergo surgical treatment, there is often a need to induce unconsciousness so that the patient does not feel or recall any of the procedure. A specially trained medical doctor, the anesthesiologist, will administer several types of medications, in succession, to the patient before the surgical procedure, the basic components being a) a hypnotic component which induces a state of unconsciousness and prevents the formation of memory (amnesia), b) an analgesic component which prevents sensation of pain and stops autonomic reflexes, and c) a neuromuscular blocking agent which paralyzes the patient to prevent any muscular contractions which may complicate the procedure. This combination will lead to a state of unconsciousness not unlike medically induced coma. [1]

When the medications are administered the anesthesiologist will observe the different stages of anesthesia listed below [2]:

- Induction - the patient is able to talk, but slowly loses consciousness.
- Excitement - the patient's muscles begin to convulse, and heartbeat is irregular. This stage passes quickly, and after this stage the patient will have lost consciousness completely.
- Surgical anesthesia - at which the patient's skeletal muscles begin to paralyze and eye movement stops. At this stage the patient is ready for surgery.
- Overdose - this stage is reached if the patient receives too much medication, and may lead to severe brain stem or medullary depression, which can be fatal.

When the patient has reached the stage of surgical anesthesia, the procedure may begin. In this state the patient is often totally paralyzed, unresponsive to reflex activation, and in need of assisted breathing and monitoring of vital organs.

The anesthesiologist's task at this stage is to monitor and balance the administration of the different anesthetics components to keep the patient anesthetized and prevent overdosing. This is typically done by monitoring heart rhythm (ECG), blood oxygen saturation (SpO2), concentration of medication, carbon dioxide levels from expiration, blood pressure and temperature. Additionally there will, in some cases, be some form of awareness monitoring.

1.2 Intraoperative awareness

Undergoing surgery with general anesthesia is not without risks. Many adverse effects may happen in regards to anesthesia as a result of wrongful administration of drugs, human error or imprecise monitoring. One of these adverse effects is a phenomenon called intraoperative awareness (IOA), which manifests in a state where the patient has regained awareness while under surgery, but due to neuromuscular blocking agents is not able to communicate and make the surgery staff aware of the problem. [3, 4, 5, 6]

A prospective, non-randomized cohort study conducted by Sebel at al. [3] on 19,575 patients at seven medical centers in the United States identified 25 cases (0.13%) of awareness occurring at a rate of 0.1-0.2% at each medical facility. Another study conducted by Errando et al. [5] report a number of incidents as high as 1% . The data used in intraoperative awareness studies are often based on different methods of interviewing the patients [7], which might explain the large variation. Nevertheless, IOA is a problem which must be taken seriously, and methods for prevention have a potential for improvement.

1.2.1 Cause

A review study conducted by Ghoneim et al. [4] argues that the number of cases that are reported in prospective studies are insufficient to identify the risks, casual factors and sequelae and they therefore reviewed published cases —from the very first in 1950 to 2005. Comparing 271 reported cases of anesthesia awareness against 19504 control cases without awareness, they found that patients experiencing awareness were more likely to be female, young and to have undergone cardiac and obstretic surgery. They received fewer anesthetic drugs, and were more likely to have episodes of tachycardia and hypertension. The most common causes of anesthesia awareness is a patient history of awareness, in addition to small anesthetic doses and light-anesthetic techniques used as a precautionary measure on sicker patients undergoing major surgery [3, 4, 5].

1.2.2 Recollection

Although more cases of awareness are reported when using the isolated arm technique (which is done by putting a cuff on the patients arm before administering neuromuscular blocking agents so that the patient may move the arm if aware), many of these patients do not recall the events when interviewed after the operation [8].

Explicit memory is the conscious recollection of events that occur, while implicit memory can be described as the changes in behavior produced by occurring events without necessarily recollecting what has

happened. Explicit recollection of awareness is the leading factor for adverse psychological sequelae, but it is conceivable that the implicit memory formation can contribute to this. Although implicit memory is unlikely to cause major psychological problems, the patient might be more anxious and unhappy than they would be otherwise. [8]

Implicit memory formation might be unavoidable, but better monitoring of the patient's mental awareness state might reduce the number of incidences with explicit memory formation and reduce the psychological trauma that is caused.

1.2.3 Sequelae

Experiencing awareness with recall during surgery can be a horrific experience, and in 34% of the reported cases, the patient describe a feeling of helplessness, anxiety, panic, impending death or catastrophe during the episode. This is very traumatizing, and may have adverse postoperative sequelae. 48% of the patients that experienced awareness with recall later reported sleep disturbances, nightmares, daytime anxiety, fear of future anesthetics and other late psychological effects [4].

Although this is a rare phenomenon, the sequelae may be severe and leave patients depending on mental health care for an extended period after surgery as a result of symptoms resembling post traumatic stress syndrome. [4, 9, 10]

1.2.4 Methods for preventing IOA

Methods for preventing intraoperative awareness currently rely on monitoring the physiological factors related to anesthesia. The anesthesiologist will monitor vital signs and different techniques are used in the attempt to monitor the depth of anesthesia, one of which is the Bispectral index (BIS, Aspect Medical Systems, Newton, MA, USA). BIS combines EEG and EMG to estimate the depth of anesthesia based on empirically derived parameters. The index ranges from 0 to 100 where 100 is fully awake and 0 is no EEG signal. The recommended value is between 40 - 60 for adequate depth of anesthesia.

Although BIS was the first available technique for monitoring the depth of anesthesia, and the most frequently used[1], its reliability is disputed. Case studies have reported incidents where the patient has experienced AWR even though they have been in the recommended range of BIS [11] and that the BIS monitoring measures EMG alone instead of depth of anesthesia, which resulted in increased BIS value although concentration of anesthetics was increased [12]. A study by Avidan et al.

[1] http://investor.covidien.com

[13] argues that routine BIS monitoring does not reduce the number of AWR incidences.

Monitoring depth of anesthesia based on measuring auditory evoked potential has also been attempted (A-Line AEP index, AAI), but several studies has shown that it performs even less successfully than BIS and that further improvements are required [14, 15, 16, 17].

The various methods of monitoring depth of anesthesia available today focus on the changes in neural activity as the anesthesia takes effect. Neural correlates to consciousness and awareness have not yet been found, so these monitors are therefore not reliable [6]. A new way to address this problem is clearly needed.

1.3 Brain-Computer Interface

The idea behind a brain-computer interface (BCI) is to create a link between the brain and the environment around the user using thought alone, a communication that bypasses the normal channel of using the peripheral nervous system and muscles to communicate or move around. This can be managed by continuously measuring the brain signals and predicting the user's intentions based on the features hidden within these signals. The predictions can then be used to control a computer which, in turn, performs the desired actions. [18, Chap. 1]

The advances in cognitive neuroscience research have led to a greater understanding of the brain signals and the features they exhibit. The deciphering of these signals is not yet complete, but important components can be extracted and used for different purposes. Creating an interface between brain and machine can be done by harnessing these signals, extracting the features within them and predicting what they mean. [19]

1.3.1 Applications

A BCI can be used for a number of different purposes ranging from recreational use like controlling games and virtual reality to rehabilitation and making life easier for people who cannot make use of their peripheral nervous system. A BCI will harness the brain signals straight from the source and is therefore promising with regards to helping patients who have no muscle control and therefore cannot communicate through normal channels. BCI controlled prosthetics [20], wheelchairs [21, 22], spelling programs [23, 24], and environment control are just a few examples of this.

Some BCI applications demand only a binary selection, for example to turn something on or off. A binary switch system with the use of BCI does not demand great resolution, especially spatial resolution. This makes it possible to limit the number of electrodes being used and as a result it will shorten the setup time and the time it takes to train the algorithm. A binary control system can, for example, be utilized to sound an alarm. [25]

The recent improvements of consumer grade EEG devices[2] has resulted in a massive increase in promising and exciting new BCI applications. Neuro-gaming, for example, is becoming an area with increased growth, with it's own conference exposing many innovative ways of incorporating BCI technology into the entertainment industry[3].

[2]Emotive Systems, NeuroSky, Interaxon

[3]www.neurogamingconf.com

1.3.2 The BCI cycle

The principle of a BCI-system is that it is a continuous loop or cycle that starts and ends with the user. Figure 1.1 and 1.2 on the next page are representations of this cycle from Van Gerven [19] and Shih et al. [26] respectively. The cycle begins by measuring brain signals while the user is performing a mental task and the signals are preprocessed to remove artifacts before the interesting features are extracted. A classifying algorithm predicts what the user intends based on a mathematical model, and the prediction is presented back to the user by some form of sensory feedback (visual, auditory and/or tactile). [19, 26, 18]

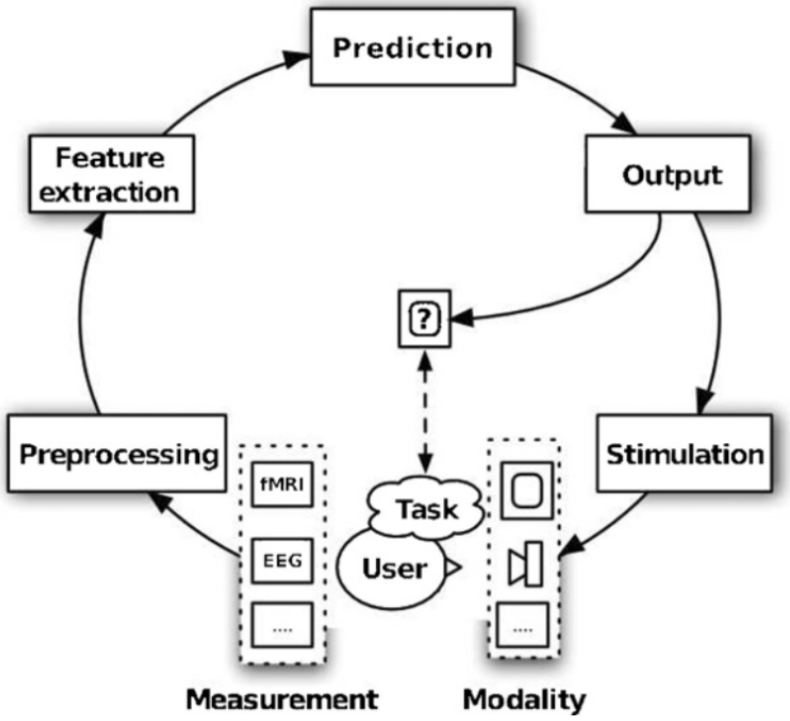

Figure 1.1: Representation of the BCI cycle, from Van Gerven et al. [19]. The measured signal is preprocessed to eliminate noise and artifacts, the features that distinguish the intent of the user is extracted and an algorithm makes a prediction based on these features. The predicted outcome is presented back to the user and is used to determine the success by checking if it was the true intention of the user.

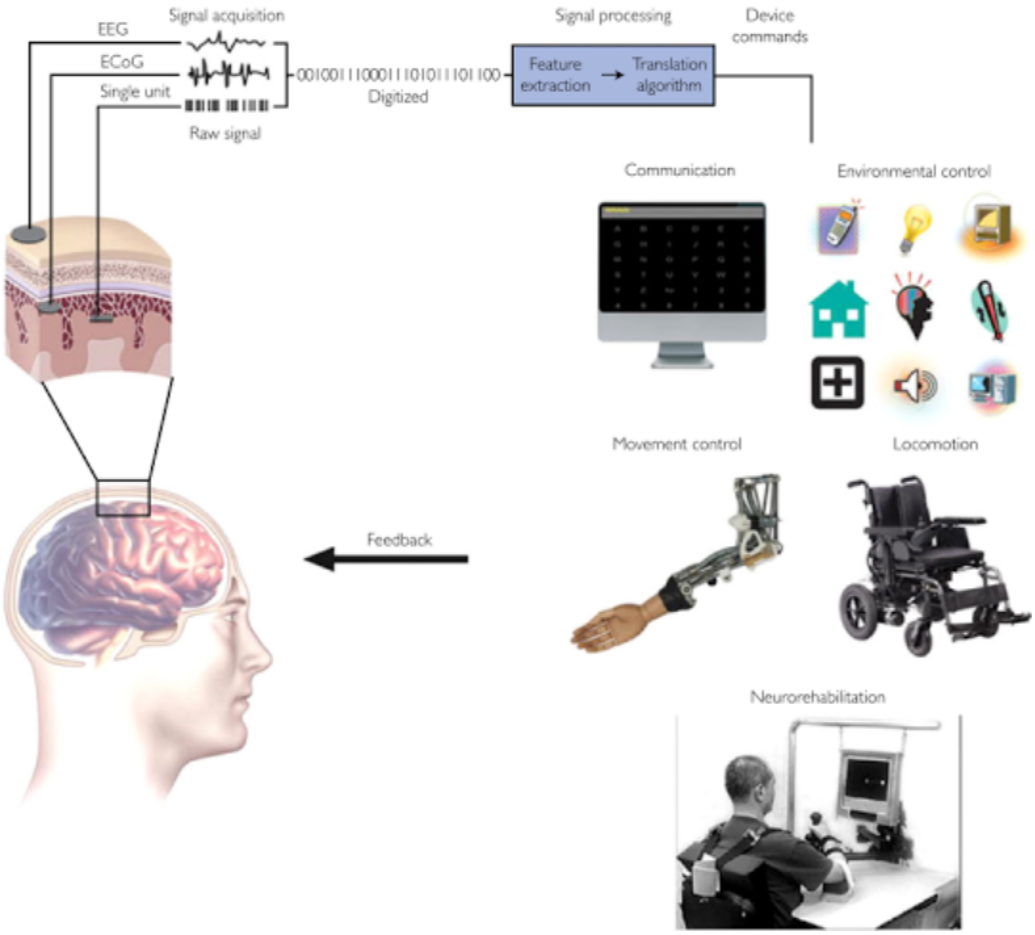

Figure 1.2: Representation of the BCI cycle, from Shih et al. [26].

Signal acquisition and measurement technology

The first step in the BCI cycle is to measure the user's brain signals. There are several methods for acquiring brain signals for assessing cortical activity, and they can be separated into technologies based on measuring electophysiological signals, indirectly measuring the hemodynamic response, i.e. the oxygen consumption within the cortex, or measuring magnetic fields. They are also usually separated into invasive and non-invasive methods.

Methods used for measuring electrical signals are electroencephalography (EEG), electrocorticography (ECoG), microelectrode (ME) or microelectrode array (MEA), and local field potentials (LFP). The concept behind this type of measurement is that it measures the electrical potential which is produced by the ionic currents caused by firing axons in the neurons. The neuronal activity can be measured at different location or scale depending on the purpose, for example the microelectrode array will measure a very small area directly within the cortex, the electrocorticography will measure a large area of the brain with electrodes placed between the dura mater and cortex while EEG will measure the electrical potential that reaches the scalp, see figure 1.3. [18, Chap. 9]

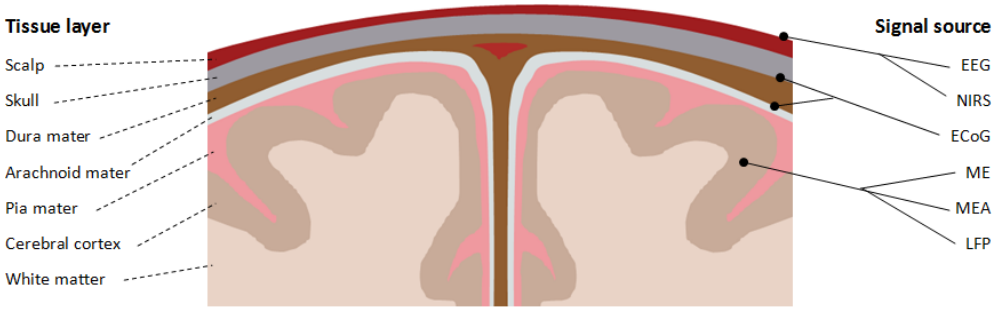

Figure 1.3: This diagram is showing the placement of different measurement modalities in a coronal cross section of the human head. Electroencephalography (EEG) electrodes and functional near-infrared spectroscopy (fNIRS) optodes are placed on the scalp, electrocorticography (ECoG) electrodes are placed epidural or subsural under the skull, micro electrodes (ME), micro electrode arrays (MEA) and local field potential (LFP) electrodes are placed directly within the cortex.

The invasive methods for acquiring brain measurements gives it a very high signal to noise ratio and resolution, both temporal and spatial, but it carries all the risks that implants and brain surgery entail. The invasive methods are therefore best suited for long term users. See figure 1.4 for an overview of the different measurement technologies and their respective resolutions.

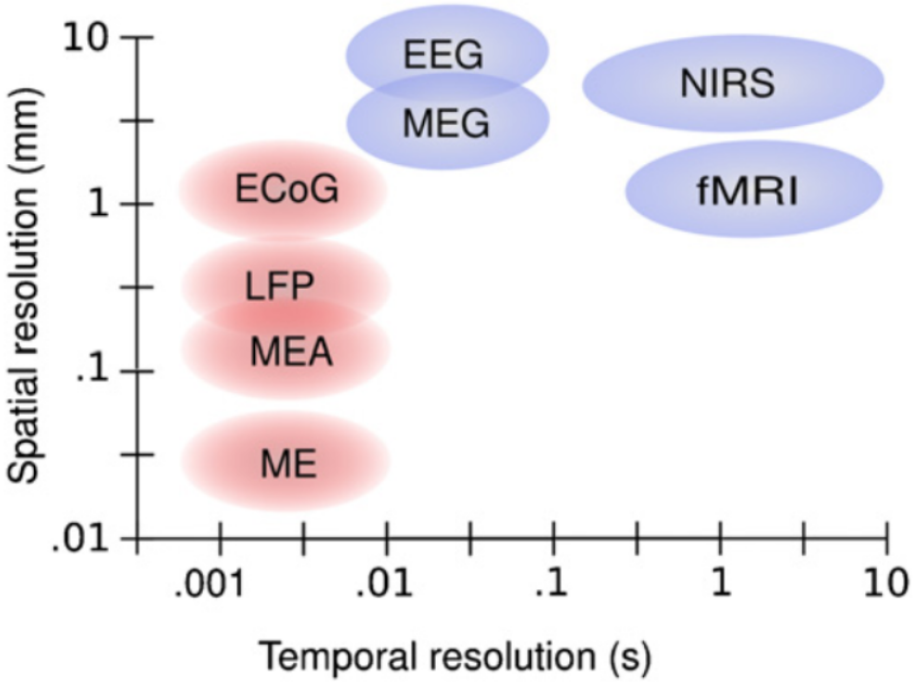

Figure 1.4: Spatial and temporal resolutions of various methods of measuring brain signals. Invasive methods are shown in red and non-invasive in blue. From Van Gerven et al. [19]. The invasive methods have better resolution than the non-invasive in both spatial and temporal resolution.

Methods measuring the hemodynamic changes are functional near-infrared spectroscopy (fNIRS), positron emission tomography (PET) and functional magnetic resonance imaging (fMRI), the concept being that it measures the metabolic rate in the cortical area of interest. The metabolic rate is an indirect sign of cortical activity because the neurons that fire consume more oxygen. PET uses a radioactive tracer which, when injected into the subject, will locate the areas of increased metabolic rate, while fMRI creates an image of tissue based on the amount of hydrogen atoms and measures blood flow and oxygenation by utilizing the blood oxygen level dependent (BOLD) contrast. fNIRS utilizes the absorption of near-infrared light through tissue to measure the concentration of oxygenated and de-oxygenated hemoglobin, and thereby assess the metabolic rate in the cortical areas of interest. [18, Chap. 9]

Although both PET and fMRI can be very useful in BCI research they are too cumbersome and expensive for most BCI applications. The temporal resolution is also very low. fNIRS measurement equipment, on the other hand, is fairly inexpensive and portable while measuring the same hemodynamic changes at the cost of lower spatial resolution.

For brain-computer interfacing the methods of measuring brain signals differ based on the resolution needed for the intended application. Some of the methods require equipment which is too big, expensive and cumbersome to be a feasible alternative in many applications, so the majority of BCI research uses EEG since it has a good temporal resolution [27] and is fairly cheap and portable compared to fMRI, PET and other methods requiring large equipment. The fact that it is non-invasive also makes it a good alternative for short term users.

Signal preprocessing

The electrical brain signals measured with EEG contain considerable noise and artifacts which is caused by electrical interference, myoelectrical activity from eye blinks and movement which has to be removed to get a clear signal which, in turn, can be used for feature extraction. For electrical measurements the data will usually be filtered and the common average potential will be removed, which removes most of the external noise and interference. A reference electrode placed near the eye, recording myoelectrical potential, might also be used to subtract the electrical signal, caused by movement artifacts, from the measurements.

For hemodynamic signals measured with fNIRS the response is slow (approx. 0.2Hz [28]) and high frequency noise can easily be removed with a lowpass filter. The slow drifts are removed with a highpass filter and the use of a reference channel can improve the signal to noise ratio further by subtracting the hemodynamic signal from more shallow tissue like scalp and skull [29].

Feature translation

The features that are hidden in the neurological signals must be translated into meaningful commands to be further processed. This can be done by using an algorithm based on a mathematical model which describes the relationship between the intent of the user and the set of features the signal exhibits. The mathematical models can either be discriminant or based on regression. A discriminant model will translate the observations into discrete categories of output whilst a regression model will translate the features into a continuous variable. [18, Chap. 8]

The algorithm must be trained to recognize the different outputs, called classes. During a training block, the user is told what to do while the data is recorded, in this way the intentions of the user, i.e. classes, and the data

associated with them are known. Given this information a linear logistic regression model will calculate the feature coefficients based on the known output. [30]

The feature coefficients are saved as a classifier for that particular user during that particular session. Think of this classifier as the function that relates the data to the output, or class, that is associated with it. The classifier can then be used on further data recordings to predict the output, analogous to a decryption key used on encrypted data.

Biological data has a high degree of variation, so to be sure that the algorithm will perform well on future data it needs to be tested with data other than the data used to parameterize it. This is done by separating the data into a training set and a test set. The training set is used to parameterize, i. e. make a classifier, and the classifier is applied to the test set to evaluate the performance. To further improve the evaluation the data is divided into subsets using one subset for training and the rest for testing. This cross validation is done X-fold (10-fold used in this study) meaning that all except one subset (X-1) is used to train a classifier and then tested on the remaining subset, this is done for each subset. After the performance tested on each subset has been evaluated the score is averaged over all folds and the best one is a measure of the performance where 1.0 is perfect discrimination between classes and 0.5 is random chance, i. e. the classifier can not predict the users intent. [18, Chap. 8]

Neurological signal features

The brain signals will show different patterns based on what the person is thinking or what sensory input the person is subjected to. For example, when a person moves the right arm, or even imagines to move the right arm, there is a change in the power spectrum of the sensorimotor rhythms (SMR) recorded on the motor cortex in the left brain hemisphere. This is an example of an *induced* signal feature meaning that the response is produced by the user actively thinking about something, in this case movement. Another example: when a person is subjected to a sequence of short sounds, where a few of the sounds are of a different pitch (called an oddball paradigm [31]), an event related potential (ERP) can be detected as an increase in amplitude approximately 300 ms after the odd sounds (P300). This is an example of an *evoked* response meaning that the feature is produced as a response to external stimulus. Another evoked response worth mentioning, is the steady state visually evoked potential (SSVEP) which, when recorded on the visual cortex, will show the same repeating structure in the brain response as a regularly repeating stimulus presented to the user. Since this study is focusing on SMRs and hemodynamic responses as a result of movement, the evoked responses will not be introduced further.

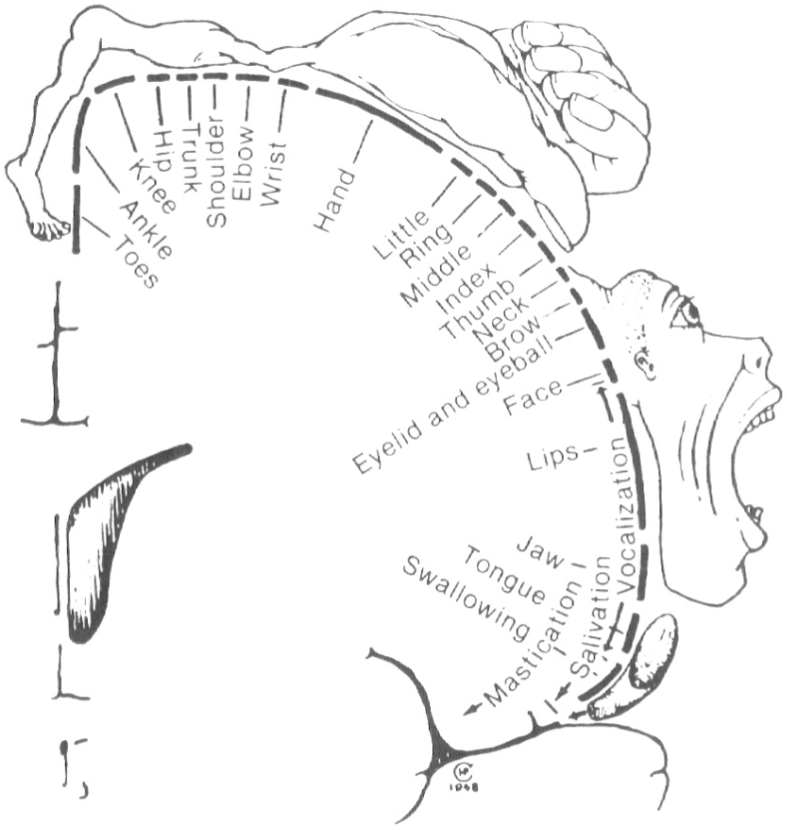

Figure 1.5: Diagram showing a coronal cross section of the motor cortex homunculus, from Penfield and Rasmussen [32]. It shows the cortical areas in the motor cortex which is associated with movement of different parts of the body. Note that the location for foot movement is further from the skull than hand movement.

SMRs are electrical oscillations that can be recorded over the sensorimotor cortices, figure 1.5 on the preceding page is Penfield and Rasmussen's [32] representation of the motor cortex and the areas associated with movement of different body parts. The oscillations that EEG can detect are in the frequency groups of the mu-band (8-12 Hz) and the beta-band (18-30 Hz). When a person is moving, or imagining a movement, the power of these frequencies will decrease. This is called an event related desynchronization (ERD) and is a clear correlate to the users intent to move. Immediately after movement, or imagined movement, the SMR may increase and this is called an event related synchronization (ERS). These responses can be clearly identified by looking at a time-frequency plot of the power spectrum, see figure 1.6. [18, Chap. 13]

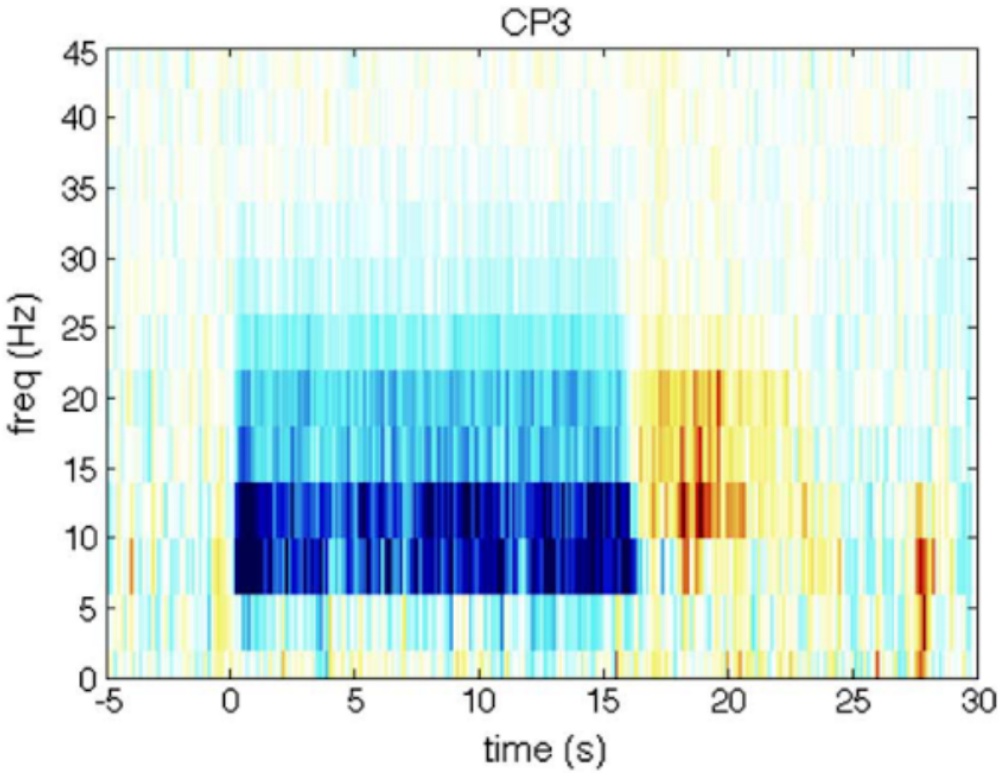

Figure 1.6: Time frequency plot of sensorimotor rhythmic ERD/ERS recorded near the motor cortex (CP3, 10-20 electrode position system [33]). Blue and red represents a decrease and increase in frequency power respectively. Task duration is, in this case, from 0 - 15 s and a clear ERD/ERS pattern can be seen for the mu (8 - 12 Hz) and beta (18 - 30 Hz) bands. This plot is from Blokland et al. [28] and it is used here only to illustrate a typical SMR response.

The hemodynamic response is another feature that correlates to cortical activity. When neural activity increases, the demand for oxygen is increased in the relevant area. This blood oxygen level dependent (BOLD) response is a change in concentration of oxygenated (HbO) and de-oxygenated (HbR) hemoglobin and can be detected as a change in amplitude of the optical density through the cerebral cortex. This is explained in detail in section 1.4 on page 17.

1.3.3 BCI in intraoperative awareness detection

When moving or attempting to move parts of the body the neural activity will increase in the respective areas of the motor cortex, see figure 1.5 on page 13. The electrical signals produced in these areas will have features that distinguish between relaxation and attempt to move. A brain-computer interface translates these signals into control signals which can be used for different purposes, in this case to give a signal if the patient is trying to move. There are several different methods for acquiring brain signals (e.g. EEG, fMRI, ECoG, PET, fNIRS), each with its own advantages and disadvantages. For this purpose ECoG, ME and MEA can be excluded since they are invasive, fMRI and PET can be excluded due to the size and cost of the equipment/procedure which leaves EEG and functional near-infrared spectroscopy (fNIRS).

An on-going research project at Donders Institute for Brain, Cognition and Behavior[4] suggests an alternative to existing methods: using a brain-computer interface (BCI) to detect if the patient tries to move his or her limbs, rather than monitoring the depth of anesthesia, since trying to move has consistently been reported by patients experiencing intraoperative awareness and attempted movement has clear neural correlates which can be detected reliably.

Blokland et al.[6] further suggests requirements for this system to be clinically feasible: The system must have a standardized setup of electrodes which must work for all patients. The algorithm for decision making must have a very low false positive rate and a high true positive rate. The acceptable rate of false positives is one per 2 hours operating time and the time to detect awareness must not exceed 2.5 min. Although this may increase the reaction time for the system, the accuracy is here prioritized over speed, considering that the anesthesiologist must remain focused at all times and that more than one false alarm during 2 to 3 hours operating time does not seem to be clinically acceptable according to Blokland et al.'s experience. The suggested detection paradigm is a "four-in-a-row" selection which means the system must detect four attempted movements in a row to set of the alarm –this will lower the chance for false positive detections. Ideally, the system would be asynchronous, but

[4]Radboud University, Nijmegen, the Netherlands

this establishes a much more complicated signal processing procedure. A synchronous model is therefore suggested using an auditory cue to time lock the task, i.e. the patient must attempt movement in sync with an auditory cue.

EEG is the most commonly used measurement technology in BCIs because it has a high temporal resolution which makes it fast enough for real-time processing and able to detect frequency changes with high accuracy. These features, however, may not be that important in a system for detecting intraoperative awareness where the only necessary distinction is between attempted movement and no movement. fNIRS, which has a lower temporal resolution than EEG but can measure brain activity with a smaller number of channels, and may therefore be a feasible alternative to EEG in this application.

1.4 Functional near-infrared spectroscopy (fNIRS)

Functional near-infrared spectroscopy is, as previously mentioned, an alternative method of indirectly assessing cortical activity by measuring the haemodynamic response (much similar to fMRI) rather than electrical activity [34]. By emitting near-infrared light into the scalp and measuring the reflected light it is possible to determine the amount of blood oxygenation and thereby measure the oxygen consumption of activated neurons in a particular area of the brain. This measurement technique has been implemented in BCI applications, both as an alternative to EEG [25], and as a combination of the two resulting in a hybrid BCI-system [28, 35].

1.4.1 Hemodynamics

When neurons create action potentials the demand for energy increases, and more oxygen is consumed. This increase in regional cerebral metabolic rate of oxygen consumption (rCMRO2) will change the regional cerebral blood flow (rCBF) and result in an increase of oxygenated hemoglobin (HbO) and a decrease of de-oxygenated hemoglobin (HbR) as the cortical region is active [27]. After the region stops being active the hemoglobin levels will fall back to baseline within a few seconds. This response is often called the blood oxygen level dependent (BOLD) response and a typical response can be seen in figure 1.7 on the following page.

During movement or imagined movement the corresponding area of the motor cortex will accelerate its metabolism, which results in an increase of venous HbR, the vascular system responds by dilating to increase the flow of oxygenated blood to prevent oxygen deprivation in the area and supplies more oxygen than needed, the HbR level drops significantly and the level of HbO rises [36]. An attempted movement can thereby be classified by measuring a decrease of HbR and an increase in HbO by a 2- to 3-fold magnitude [37].

1.4.2 Signal acquisition

Near-infrared light ranges from 700 nm - 1000 nm in the optical spectrum and has the ability to pass through tissue like skin and bone and reach the cerebral cortex if projected into the scalp. The light will scatter through the tissue and some of it will be absorbed by chromophores (light absorbing molecules) like oxygenated and de-oxygenated hemoglobin. The light that is reflected will be picked up by a receiving fiber optic cable and transported to a photomultiplier amplification. The signal is then digitally converted and can be further processed, see figure 1.8 on page 19. [18, 38, 25, 39, 34, 37]

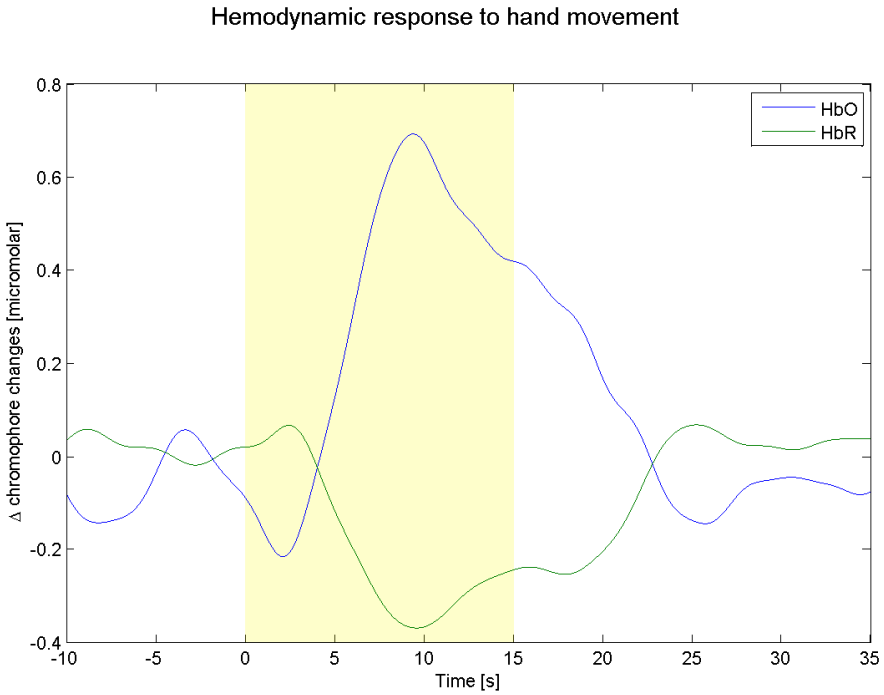

Figure 1.7: A typical BOLD response to motor stimulation during actual movement of the hand. The BOLD response to imagined movement will show a similar characteristic, although less prominent. The motor stimulation cue is, in this case, from 0 - 15 s, marked with yellow. The concentration of oxygenated hemoglobin (HbO) will increase as the stimulation progresses while the de-oxygenated hemoglobin (HbR) concentration will decrease, although to a lesser extent. Note that the BOLD response is rather slow, taking approx. 7 - 10 seconds to reach peak value and approx. the same to return to baseline after stimulus ends.

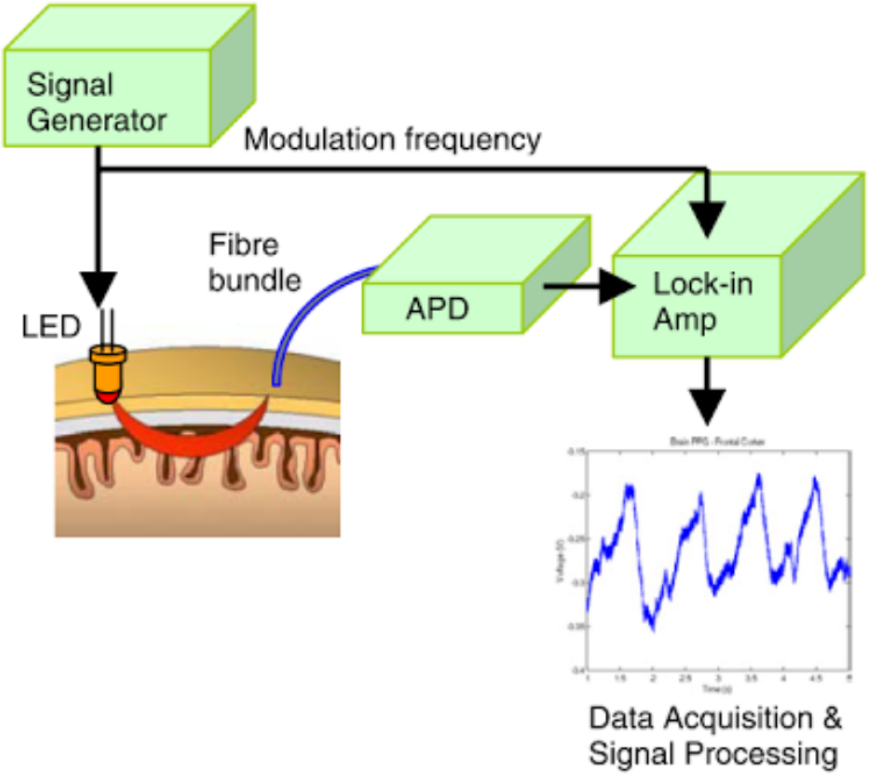

Figure 1.8: Components of a continous wave fNIRS system, from Coyle et al. [25]. The signal generator produce a sinus signal which is sent into the scalp as light through an optode. A receiving optode picks up a portion of the light which scatters through the tissue and sends it to a photo amplification unit. A lock-in amplifier extracts the signal and removes the common noise and the data is digitally converted for further processing.

The absorption spectra, within the NIR range, of oxygenated and deoxygenated hemoglobin, as seen in figure 1.9 by Rolfe [40], has a distinct difference and by sending beams of light at two different wavelengths, one on each side of the isobestic point (the frequency where absorption is equal for both chromophores), the chromophores can be measured individually.

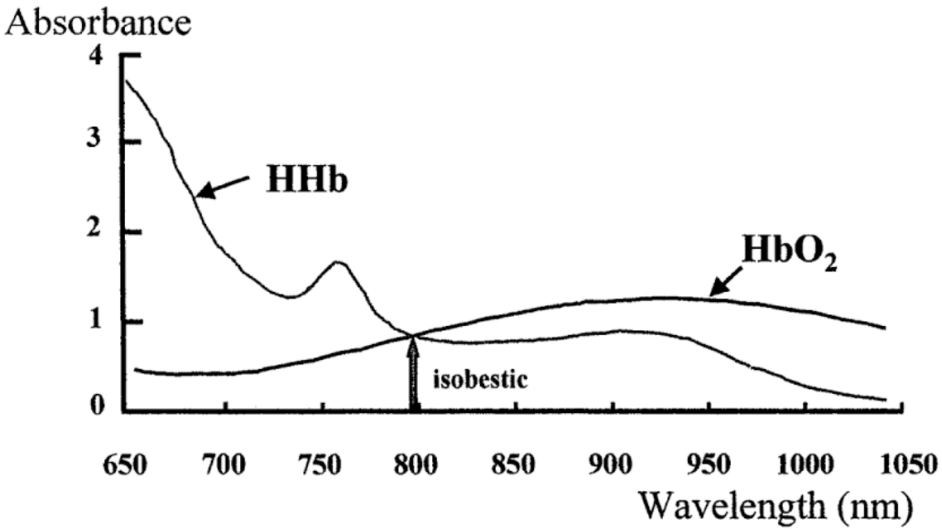

Figure 1.9: Absorption spectra of chromophores in tissue, from Rolfe. [40]. By applying the modified Beer-Lambert law to measurements done with light frequencies on each side of the isobestic point, the concentration of HbO and HbR (HbO2 and HHb in this figure) can be extracted.

There are three different techniques for fNIRS measurements which utilizes different properties of the absorption of light through tissue:

1. Time resolved spectroscopy which uses a pulse of light to measure how much time the photons use to get through the tissue.

2. Frequency domain spectroscopy measures both the phase delay and attenuation of the reflected light, by using intensity modulated light. The phase delay is related to the time delay through the tissue and the path length can be calculated.

3. Continuous wave spectroscopy uses a continuous emission of light modulated at low frequency, the changes in magnitude in the received light is a measure of absorption in the tissue.

Although the first two methods can give more information like better depth resolution and measurement of the path length, the instrumentation is much more complex and expensive and the continuous wave method is therefore most commonly used. [25, 27]

1.4.3 The modified Beer-Lambert law

The absorption of light through matter is described by the Beer-Lambert law and relates the transmission of light to a product of the matter's absorption coefficient and the distance the light travels. This, however, is only applicable in a setting where the absorbing matter is homogeneous, does not scatter the radiation, and light is projected straight through the matter (often through a cuvette). The layers of tissue from scalp to cortex is much more complex than a liquid or gas sample in a cuvette, and the light beam is scattered by different interfaces and absorbed by several different chemical compounds. fNIRS does not measure straight through the tissue, but utilizes this back-scattering in order to get an elliptical beam of light from the receiver to the transmitter, which are placed ipsilaterally next to each other. [40]

A modified Beer-Lambert equation which takes the aforementioned into account is therefore applied to convert the optical density data to changes in hemoglobin. From Coyle et al.[25] "The attenuation due to absorption and scattering effects may be described by a modified version of the Beer–Lambert law:

$$A = log_{10}\frac{l_o}{l} = \alpha cLB + G \tag{1.1}$$

where A is attenuation, Io is the incident light intensity (mW), I is the transmitted light intensity (mW), α is the specific extinction coefficient (mol-1 m-1), c is the concentration of the absorber (mol), L is the distance between the source and the detector (m), B is the differential path length factor and G is a term to account for scattering losses."

The differential path length factor (DPF) differs according to age and is calculated individually for each subject based on an empirical study [41]. The attenuation, A, is also referred to as optical density (OD).

A multivariate analysis can be used to calculate the concentration of both chromophores by assuming that the total attenuation at each wavelength is equal to the sum of the attenuations of each absorber [40]. Coyle et al. [25] implemented an algorithm to calculate the changes in hemoglobin based on an algorithm by Cope and Delpy [42] which relies on the modified Beer-Lambert law and is the same principle for measuring fNIRS used in this study:

$$\Delta A = (\alpha_{HbO}\Delta c_{HbO} + \alpha_{HbR}\Delta c_{HbR})BL \tag{1.2}$$

where ΔA is the change in optical density, α_{HbR} and α_{HbR} are extinction coefficients for the two chromophores, B is the differential pathlength factor and L is the distance between transmitter and receiver. By applying this algorithm to two wavelengths on each side of the isobestic point the changes in concentration of HbO and HbR can be extracted.

1.4.4 Advantages and disadvantages

fNIRS, compared to EEG, has a greater latency (range of seconds) and more limited spatial resolution (cm range), but it may have advantages in that it is unaffected by the immense electrical noise within a clinical environment since the measurement is optical as opposed to electrical, and that it can be used inside an MRI. It may also have an advantage regarding set-up time if the system can give reliable results with a smaller number of sensors.

An estimated portion of EEG-based BCI users (15 to 30%) are "BCI-illiterate" meaning that BCI control does not work for the user [43]. EEG-based BCIs often require a lengthy training period where the user has to learn a new thought process to control their brain's electrical signals reliably, which might cause this problem. The hemodynamic changes, however, are directly coupled to the cognitive activity and is therefore relatively easy for the user to control [38]. fNIRS may therefore be feasible in that it may work for a larger portion of the population, although further studies are needed to verify this. On the other hand, the optical signals are affected by the hair color and the skull thickness of the user, which decreases the signal to noise ratio. This may affect NIRSs ability to work for the general population, since the signal to noise ratio will be decreased for users with dark hair color or thick skulls. Experiments have also shown that operation of a fNIRS-BCI under continuous background auditory noise decreases the specificity by an average of 19% [44].

1.5 Study goals and objectives

The goal of this study is to produce evidence on whether fNIRS may be considered a feasible alternative to EEG for detection of intraoperative awareness based on the fNIRS's ability to detect attempted movement. In addition to the criteria for clinical feasibility, that is, the optode setup must be generic and working for all subjects, the false positive rate must not exceed one per two hours working time and the time to detect awareness must not exceed 2.5 min after the subject is trying to activate using a "four-in-a-row" paradigm, i.e. four successful detected attempted movements in a row.

The first objective is to assess the performance of EEG and fNIRS at detecting actual hand and foot movement by measuring the classification rates, as explained in section 1.3.2 on page 11. The classification rate is a measure of the probability for true positive detection. It is essential for an anesthesia monitor to perform well generically among patients, the evidence will therefore be used to compare fNIRS to EEG which is the gold standard in these kinds of BCI applications. The number of participants is to small to verify the performance in a general population, but the evidence produced can be used to argue the reliability of the two modalities compared to each other.

The second objective will be to investigate if fNIRS has the ability to discriminate between hand and foot movement using a center of gravity (CoG) approach [45] to locate where the hemodynamic response is originating. Although this may not be relevant for the implementation of fNIRS in an anesthesia monitor where hand movement is enough, it will give valuable insight into the spatial resolution of fNIRS based on the specific optode setup that is used in this study. A minimal setup of optodes/electrodes that works for the general population is essential for this system to be clinically feasible. This study will, based on this objective, hopefully be able to draw conclusions on whether or not a generic optode setup can target the cortical area of interest reliably.

If a combination of fNIRS and EEG were to be used for anesthesia monitoring, a standardized cap or fixture must be used to incorporate both electrodes and optodes. This cap must therefore be placed on the head according to the International 10-20 system for electrode placement [33]. By calculating the difference in spatial location of center of gravity between EEG and fNIRS (ΔCoG), this will give a measure of how well the two modalities agree on where the response is located. The 10-20 system, being the most established method for electrode placement, will make EEG the most reliable source in this regard. Comparing ΔCoG with

the performance of fNIRS will produce evidence as to whether or not the difference in CoG affects the performance. If the ΔCoG anti-correlates with the performance of fNIRS it will mean that optode placement is highly individual, will affect the performance and the optodes can therefore not be placed according to the 10-20 system. This may give additional insight into the suitability of fNIRS when it comes to the importance of optode/electrode setup.

To address these objectives three hypotheses will be stated:

- Hypothesis 1: fNIRS has a higher classification rate, i.e. the systems ability to correctly predict the users intention, than EEG when detecting movement of hand and feet.
- Hypethesis 2: The difference in location of center of gravity, i.e. where the hemodynamic response originates, for hand and foot movement will be significant when measured with fNIRS. The location for hand movement is expected to be significantly more lateral than the location for foot movement.
- Hypothesis 3: The difference in location of center of gravity, i.e. where the brain signals originate, between EEG and fNIRS will anti-correlate with the performance of fNIRS.

In addition to these objectives, a real time testing block will be performed during the experiment to test if the system meets the requirements of low false positive rate, and if it can detect a "four-in-a-row" activation. This real time block is meant solely as a proof of concept.

1.6 Study design

This is a basic research study to compare one type of signal acquisition, namely fNIRS, to EEG for the end purpose of detecting intraoperative awareness. A volunteer study was conducted in close collaboration with the BCI research group at Donders Institute for Brain, Cognition and Behavior at their facilities at Radboud Uni. in Nijmegen, the Netherlands. The protocol and analysis procedures are based on similar studies performed by Blokland et al. [6, 28] at this institute.

The volunteer study had to include a minimum of 10 healthy male and female participants aged 18 - 60. The measurement devices used (TMSI Mobita EEG, Artinis Oxymon NIRS) are non-invasive and electronically safe according to several standards. The NIRS device is not CE-approved as a medical device but has been declared to conform with all relevant standards by the manufacturer, see Appendix A on page 81. The Donders Inst. has laboratories set up specifically for BCI research with auditory and electrically isolated rooms, a standardized system for enrollment of voluntary participants and a research team with considerable expertise regarding BCI research.

1.6.1 Sample size determination

BCI studies are usually novel and to prove a concept, the sample size is therefore of less importance in most studies. Although the sample size is usually accepted to be 10, it is here determined using binomial response [46, Chap. 9]:

1. From Blokland et al.[6], it is assumed that the classification rate of the EEG-based system is 92% , $P_s = 0.92$.

2. Second assumption is that the classification rate for the fNIRS-based system will be over 75%, $P_n = 1 - 0.75 = 0.25$.

3. The significance level is chosen to be 0.01 and the power to be 0.95 which gives a determination constant $C = 17.8$. The sample size can be determined from the following formula:

$$
\begin{aligned}
N &= \frac{P_n \cdot (1 - P_n) + P_s \cdot (1 - P_s)}{(P_n - P_s)^2} \cdot C \\
&= \frac{0.25 \cdot (1 - 0.25) + 0.92 \cdot (1 - 0.92)}{(0.25 - 0.92)^2} \cdot 17.8 \\
N &= 10.35 \\
N &\approx 10
\end{aligned}
$$

1.6.2 Inclusion criteria

The participant could be included given all of the following:

- Participant is willing and able to give informed consent for participation in the study.
- Male or Female, aged 18 to 60.
- Participant is in good health and has normal or corrected-to-normal vision and hearing.

1.6.3 Exclusion criteria

The participant could not enter the study given any of the following:

- Participants who are hearing impaired. *There were plans to use auditory cues during the experiments, but it was later changed to visual cues.*
- Participants with any form of neurological impairment.
- Any other significant disease or disorder which, in the opinion of the investigator, may either put the participants at risk because of participation in the study, or may influence the result of the study, or the participant's ability to participate in the study.

1.6.4 Discontinuation/withdrawal of participants from study

Each participant had the right to withdraw study at any time. In addition, the investigator could discontinue a participant from the study at any time if the investigator considers it necessary for any reason, including:

- Ineligibility (either arising during the study or retrospectively having been overlooked at screening)
- Significant protocol deviation
- Significant non-compliance with study requirements
- Consent withdrawn

1.6.5 Participants

The study was advertised at Radboud University[5] and 16 participants signed up. One participant failed the screening process and three participants did not show up to the assigned timeslot. The twelve remaining participants (7 female) was of age from 22-60 (mean $30 \pm 10.3SD$).

[5]SONA study participant system

1.7 Data management and statistical analysis

No person-identifiable data other than the form for informed consent was collected. Any participant with a deviation from the screening criteria was not included and it was therefore not necessary to collected any data of medical history for statistical analysis. The data collected from the trials is linked to the participant through a non-decipherable code number and can not be traced back to the participant. The data is stored on a server located at the University of Oslo. The list of names with number codes, along with the forms for informed consent is stored securely and is only accessible to the head investigators.

1.8 Ethical considerations

The study was carried out in accordance with the World Medical Association Declaration of Helsinki on Ethical Principles for Medical Research Involving Human Subjects (Appendix C on page 87). Since the study was carried out at Radboud Uni. in Nijmegen, Holland where similar studies are approved and carried out at a daily basis, the protocol was not sent to the Regional Ethical Commitee in Norway.

Although no adverse effects are anticipated, the well-being of the participant takes precedence over all other interests. This is ensured by seeking the potential participant's freely-given informed consent, the freedom to withdraw from the study at any time without prejudice, the confidentiality of personal information and giving adequate information about the study to the participant.

1.8.1 Informed consent

The participant had to personally sign and date the latest approved version of the informed consent form before any study specific procedures were performed. Written and verbal versions of the participant information and informed consent was presented to the participants detailing no less than: the exact nature of the study; the implications and constraints of the protocol; the known side effects and any risks involved in taking part. It was clearly stated that the participant is free to withdraw from the study at any time for any reason without prejudice, and with no obligation to give the reason for withdrawal.

The participant was allowed as much time as needed to consider the information, and the opportunity to question the investigator or other independent parties to decide whether they wanted to participate in the study. Written informed consent was then obtained by means of participant dated signature and dated signature of the person who presented and obtained the informed consent. The person who obtained

the consent was suitably qualified and experienced, and was authorized to do so by the Principal Investigator. The original signed form is retained at the University of Oslo. The forms are appended, see appendix D on page 95.

1.8.2 Confidentiality

The investigators are subjected to strict confidentiality as per the regulations stipulated by Oslo University Hospital. As mentioned in section 1.7 on the previous page the informed consent forms and all other personal data is stored at a secure location only accessible to the head investigator. The raw data from the trials are all anonymous and can not be traced back to the participant.

Chapter 2

Methods

This chapter will introduce the tools and methods used to carry out the experiment and data analysis for this study. As previously mentioned, the objective of this experiment is to measure the brain activity that is produced by hand and foot movement, using both EEG and fNIRS simultaneously, for the purpose of comparing the two.

Using two measurement devices simultaneously is challenging. Customized solutions must be implemented to ensure proper handling of data, integration of hardware and software, and synchronization between the individual data streams.

The fNIRS and EEG measurement devices had to be integrated physically by making a prototype cap, which is placed on the head of the participants, incorporating both EEG electrodes and fNIRS optodes. This cap ensures a uniform setup for all participants. The measurement devices' recording software had no built in common platform for synchronization of the two data streams, so a software buffer structure, explained in detail in the next section, was used to handle all the data and sample markers (also called events) to ensure proper synchronizations.

A software program exporting the EEG data from the measurement software to the buffer continuously, was already available. This, however, was not the case for the fNIRS measurement software. To solve this issue, the author wrote a function that decrypts the binary output from the fNIRS measurement software and exports it to the buffer continuously.

During the experiment sessions, brain activity is recorded while the participant is asked to perform 15 second movement tasks (either hand movement, foot movement or no movement), when visual cues are presented on a monitor placed in front of the participant. Between each trial there is a semi-random resting period to ensure that the brain signals return to baseline (idle state). The tasks are randomly selected and evenly distributed over 6 sequences of 6 trials, resulting in a total of 36 trials per subject. The stimulus presentation, i.e. visual cues and instructions, were implemented in Matlab [47] with PsychToolbox.

The data recorded with both modalities during the experiment sessions

is processed and analyzed post hoc in Matlab, individually. Several tools made specifically for analyzing brain signal data are used, most of which are developed at Donders Inst., in addition to some written by the author. The processed data is used to visualize the average recorded brain responses among all subjects, and to determine the performance of the two modalities.

2.1 Matlab toolboxes

FieldTrip is an open source Matlab toolbox developed at the Donders Centre for Cognitive Neuroimaging which provides a high level interactive environment for developing algorithms, data analysis and visualization of numerous types of neuroimaging data. It is primarily intended for electrophysiological data, like EEG, ECoG, etc., but it can be used on any kind of time series data. It is therefore able to analyze hemodynamic data like fNIRS. In addition to many tools for offline analysis of physiological data, it is an environment for online real time processing which is ideal for BCI research. [48]

Matlab is a single thread application, and though it is able to gather a stream of real time data it is not able to gather the data and process it at the same time. To solve this issue, the people behind FieldTrip developed a buffer structure which is a cross between the acquisition of data and the Matlab processing. The buffer receives the data and keeps track of the sample number and timing, so that the Matlab data processing can retreive data from the buffer at it's own pace [48]. The FieldTrip buffer is a TCP server and works like a blackboard structure —data and events can be sent and retrieved from the buffer by several applications at once, see figure 2.1 on the facing page.

The visual stimulus and on-screen instructions were written in Matlab using the Psychophysics Toolbox developed by Brainard [49], Pelli [50] and Kleiner et al. [51]. This toolbox is designed for low latency real time visualization.

Most of the tools for data preprocessing and analysis are based on the FieldTrip toolbox and further developed at Donders Inst. by Dr. Jason Farquhar[1]. These tool are published under the GNU general public license for open source software.

[1] github.com/jadref

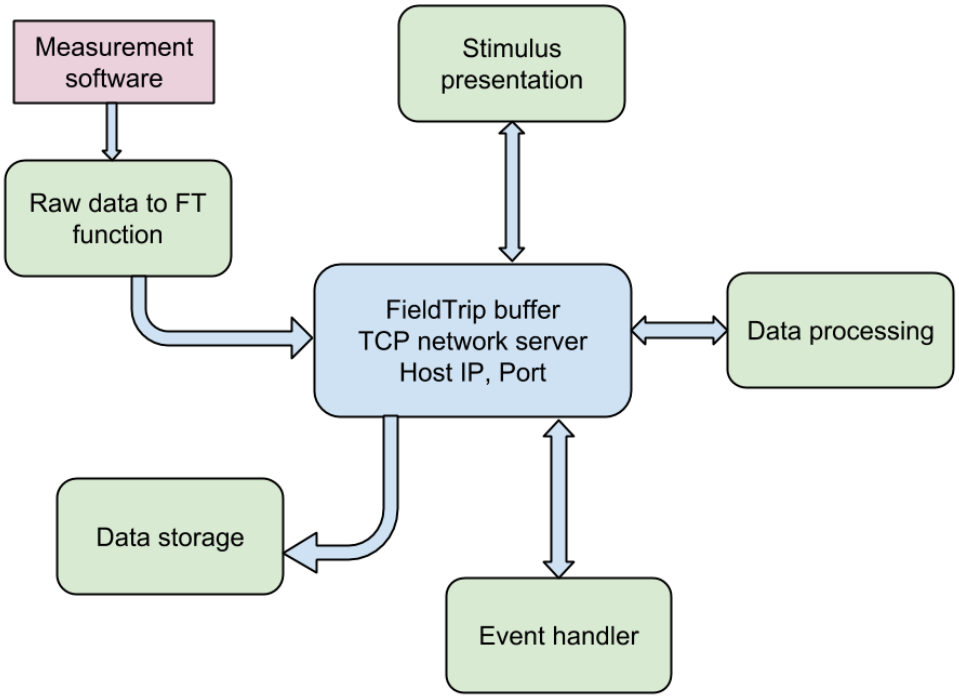

Figure 2.1: Diagram showing an example of a blackboard structure. The buffer (blue square) acts as a common hub for external programs. Other programs can read and write data and events to the buffer and it will affect the other programs. In this example the measurement data is sent to the buffer through a driver, the stimulus script sends events when stimulus is shown to the participant and the data processing script listens to the buffer and starts processing when the events are written to the buffer. The buffer will also send raw data to storage, and a separate event handler can be implemented to perform further actions when events occur.

2.2 Hardware

fNIRS. The Oxymon MK III (Artinis, Zetten, the Netherlands) is a NIRS measurement system that has two receivers and up to eight transmitters and is shown in figure 2.2a on the next page. The Oxymon NIRS system is not invasive or electrochemically connected to the research participant, the intensity of the light source is under the threshold for harmful exposure, and the device can therefore be considered safe in an investigative setting. As previously stated, the device is not CE-approved as a medical device, but has been declared to conform with all relevant standards.

Raw optical density data is recorded at 250 Hz, with two wave lengths per channels (765 and 855 nm for HbR and HbO respectively). The hardware has the option to include analog signals from external devices, which was utilized to check the synchronization between the systems by using a hardware marker, i.e. a short voltage pulse.

Connected to the device is fiber-optic cables which sends out and receives near-infrared light. The device is capable of recording 16 channels with the use of split fiber-optic cables, but only 2 split and 2 regular cables were available resulting in a maximum of 8 channels, which in the opinion of the author were sufficient.

EEG. The TMSI Mobita is a wireless EEG data acquisition system, and is shown in figure 2.2b on the facing page. It is capable of transferring 32 channels of DC recording with a 24 bit data resolution over WiFi and is CE-certified as a medical device (class 2A, type CF). The data was recorded with a sampling frequency of 250 Hz.

The device is compact, battery-driven, portable and uses waterbased electrodes, which makes the setup fast and relatively easy compared to systems that use gel based electrodes. The cap that comes with this system is flexible and relatively inexpensive, which was important for this study since it had to be modified to incorporate both EEG and fNIRS without having to decrease the number of electrodes.

(a) Photo of the Artinis Oxymon NIRS data acquisition system.

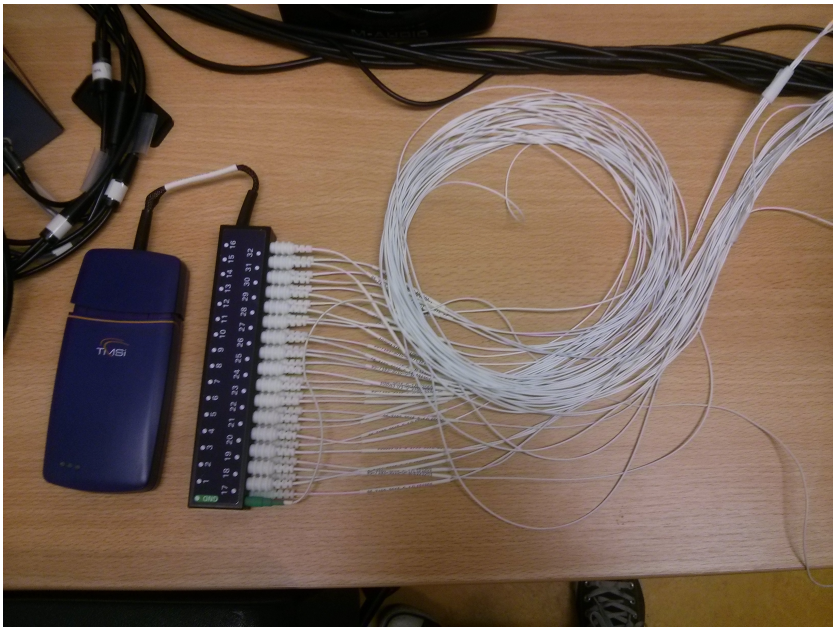

(b) Photo of the Mobita EEG data acquisition system.

Figure 2.2: Photos of the hardware used in this study. a) Fiber optic cables transmit and receive the near-infrared light. The light is transmitted through the eight connectors on the right and received through the two on the left. The device has the capacity to transmit light through 8 channels if the transmitting cables are split, in this study there were 2 split and 2 single ended cables. b) 32 electrode channels measure data which is received by the EEG data acquisition device. The data is sent to a computer with WiFi.

2.3 Optode/Electrode placement

The electrode placement follows the international 10-20 electrode placement system [33]. The motor cortex, which is associated with movement of the body, expands laterally from the central midline towards the ears. The locations associated with hand movement is denoted with C3 and C4 for right and left hand respectively, see figure 2.3. The location associated with foot movement is denoted with Cz. These are standard notations in the 10-20 electrode system. The EEG electrodes are positioned to cover the motor cortex on both hemispheres, while the fNIRS optodes are covering the motor cortex on left hemisphere only, placed uniformly around C3.

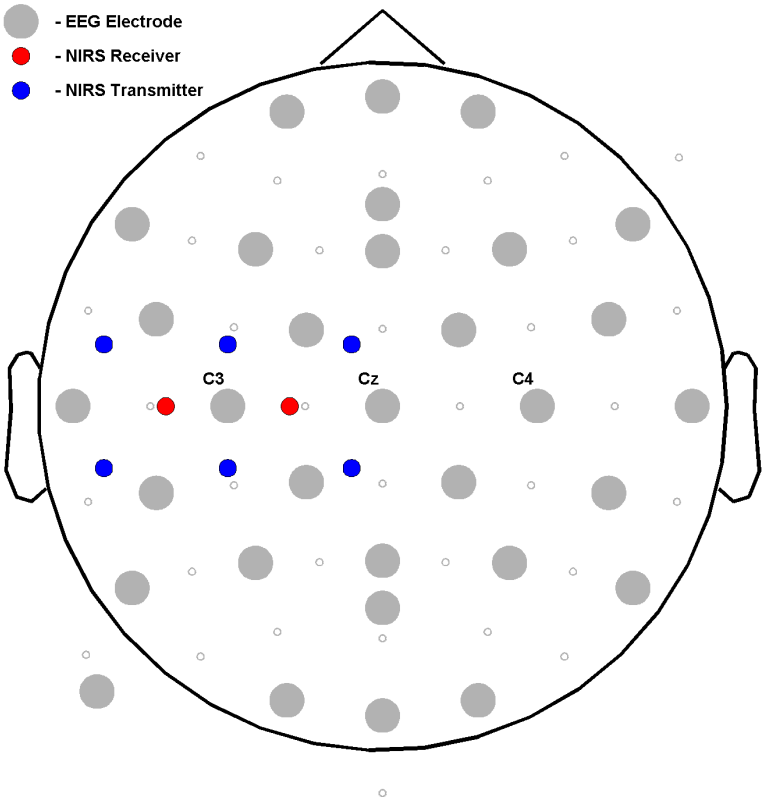

Figure 2.3: Diagram showing the placement of optodes and electrodes. The grey circles represent the EEG electrodes placed according to the international 10-20 system. The red and blue circles represent the placement of the fNIRS receivers and transmitters respectively. The fNIRS receivers and transmitters form 8 channels covering the left hemisphere motor cortex, focusing on the center for right hand movement.

An already made EEG cap was modified to incorporate the fNIRS optodes. The optodes and fiber optic cables are relatively heavy, so a

styrofoam pad, approx. 1 cm thick, was glued to the inside of the fabric with holes for the optodes and the electrode over C3, see figure 2.4 for photos of the modified cap.

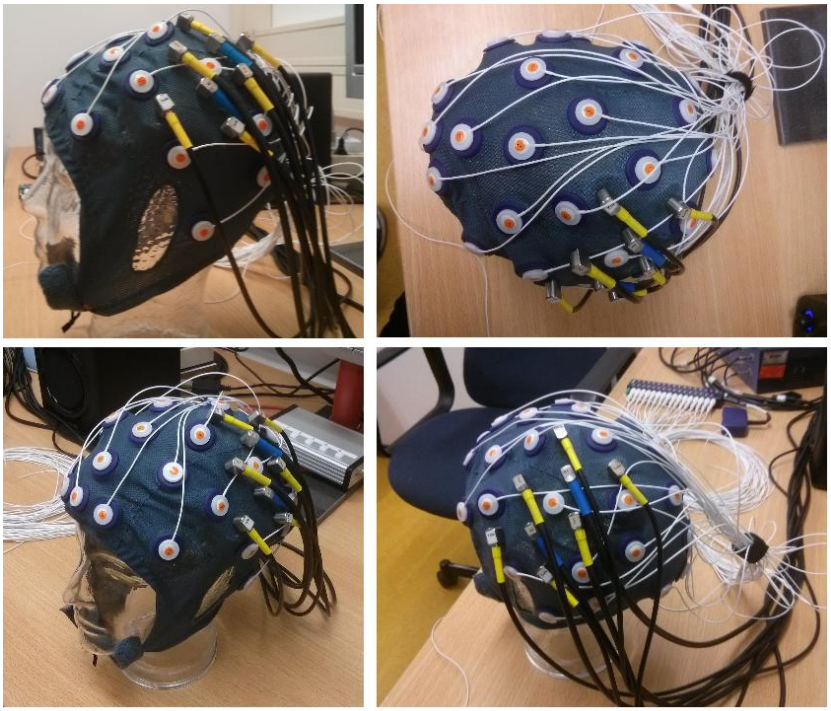

Figure 2.4: Photos of the modified cap with attached electrodes and optodes. The cap was modified using a styrofoam pad with holes placed underneath the fabric. This foam, approx. 1 cm thick, holds the optodes in place during the experiment. A tooth pick was used to move hair to the side under the holes before the optodes were placed, to achieve a better connection. To ensure that the optodes were in contact with the scalp a band was secured around the head, putting pressure on the optodes.

Hair under the holes for the optodes is moved to the side using a toothpick before the optodes were placed and a band is fastened around the subjects head to increase the pressure of optode to the scalp. This ensures that the optodes are firmly placed with sufficient rigidity to be in contact with the scalp during the experiment. A detailed view of the optode setup is shown in figure 2.5 on the next page, showing how the channels are formed.

Relying on the 10-20 framework may result in inaccuracies in optode placement, and it is often necessary to adjust the placement manually during a practice run until a detectable signal can be achieved. This is not doable in this particular case since the optodes are incorporated into the electrode cap. To counter this problem, the fNIRS channels have to cover as much area as possible. The receivers and transmitters are spaced

30 mm from each other with a 45° angle, which makes an area of coverage at approx 44 x 88 mm around C3. This area of coverage is as large as our equipment will allow, so to be sure that it covers the area of interest the center of gravity is determined post hoc for the EEG, to see if the location for the two movement conditions falls within the covered area. From this analysis it will be determined if the difference between the two CoG locations has any correlation to the performance for each subject.

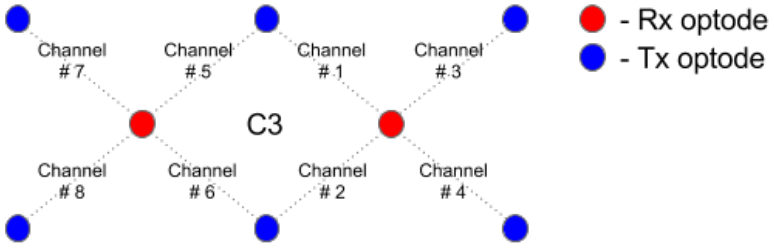

Figure 2.5: Diagram showing the optodes and how the channels are formed. The transmitters (blue circles) sends light which scatters in the tissue beneath, some of this light is absorbed by HbO and HbR and the rest is picked up by the receivers (red circles). This results in a channel formed by the arched beam of light between the transmitter and receiver that reaches the cortex underneath. The optodes are placed uniformly around C3, the area associated with hand movement, covering the motor cortex strip.

2.4 Software integration

FieldTrip buffers, which is explained in section 2.1 on page 30, were used to handle the events and the data from the EEG and fNIRS measurement systems simultaneously. A driver for the Mobita to send the data stream to the buffer was already available but there was no such driver for the Oxymon. So to send the data from the Oxysoft measurement software to the FieldTrip buffer, a program which translates the data and feeds it to the buffer in real time had to be implemented. This was done by decrypting a binary temp file, which is produced and constantly updated by the Oxysoft data acquisition software during the measurement. After comparing data read by the implemented program with the data from Oxysoft a function run in Matlab which reads the data from the oxymon and exports it to the FieldTrip buffer online was implemented, see Appendix E.1 on page 101. The transfer rate is determined by the operating system's capacity to write to file and was in this case written in blocks of 50 samples at a frequency of 5 Hz. Since the expected

hemodynamic response in motor cortex is well under 1 Hz a 5 Hz transfer rate is sufficient.

A representation of the software setup of this experiment is shown in figure 2.6. The data from the EEG and fNIRS measurement softwares is sent to two separate buffers, which handle the data flow and events. The stimulus presentation script sends events to both buffers when the visual cues are presented to the subject. These events are associated with the respective sample number in both buffers, and can therefore be used as a synchronization between the two data streams. The data and events are further processed and stored by the signal processing scripts and a backup storage of the raw data is saved by the buffers. The EEG and fNIRS measurement softwares are written for Windows XP but the laboratory computer ran Apple OS X, which is better suited for running multiple Matlab instances at the same time. This was solved by running the measurement software in a Virtual Windows XP inside OS X, where the data is transferred to the buffers through the internal network between the Virtual Machine and the Mac.

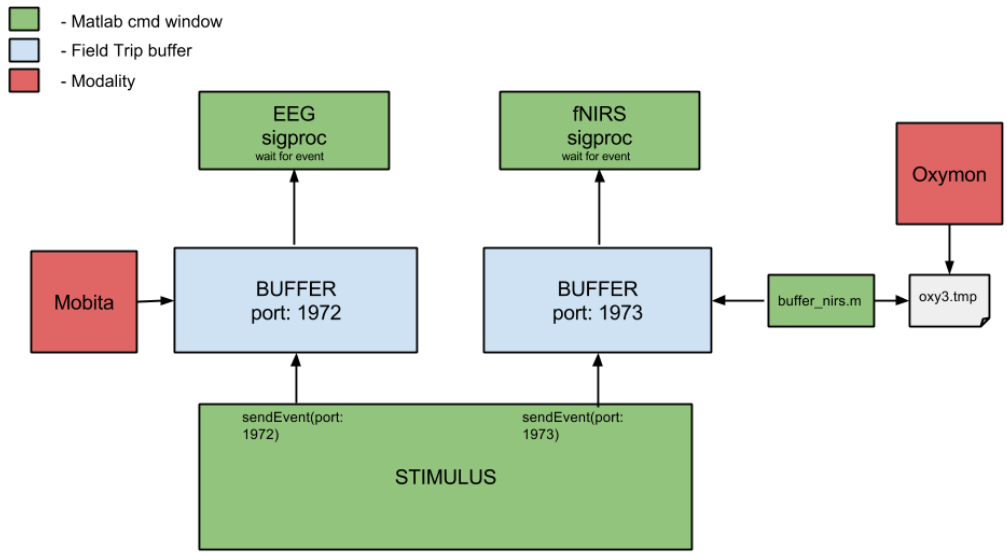

Figure 2.6: Diagram showing the software setup used for the experiment. The data from the data acquisition software (red square) are sent to each respective buffers (blue squares), these buffers get events from the same stimulus presentation script to ensure synchronization. The data is processed exclusively by one script each. The drivers for the acquisition hardware is run in a Windows XP virtualbox, the rest is run in Apple OS X.

2.5 Protocol

The whole experiment can be divided into three blocks:

1. The setup block
2. The trial block
3. The online block

Setup block

The participant is seated in a comfortable chair in front of a monitor in a soundproof room. The cap with attached optodes and electrodes is placed on the participant's scalp, so that the optodes are covering the motor cortex (C3) on the left hemisphere according to the International 10-20 system for electrode placement [33]. The signal acquisition softwares are initiated to get a live feed of the data measurement. The optodes and electrodes are adjusted until the noise is minimal by moving the hair to the side under the holes for optodes if needed, and by applying more water to the electrodes. When a clear signal is visible, a band is fastened around the participant's head to ensure that the optodes are kept in place during the experiment.

Trial block

The subjects is presented with six sequences of six random task trials plus one "no movement" trial at the start of each sequence, which gives a total of 36 evenly distributed task trials (6 hand, 6 foot and 6 no movement) plus 6 additional no movement trials. Each trial consists of a 5 s baseline period, where the subject is asked to sit as still as possible, a 15 s period where the subject has to perform the task, and a random silent resting period between 15 and 25 s to ensure that the signal returns to baseline before the next trial, see figure 2.7 on the next page.

The running stimulus script will present the visual cues, with instructions, to the participant according to the randomly selected task. The instruction is either:

- "Tap your fingers", where the participant will perform a tapping motion with the fingers, but try to not move any other part of the body.
- "Move your toes", where the subject will "crunch the toes" so that the movement is isolated to the feet and is not affecting the legs and upper body.
- "Do not move" , where the participant will keep still.

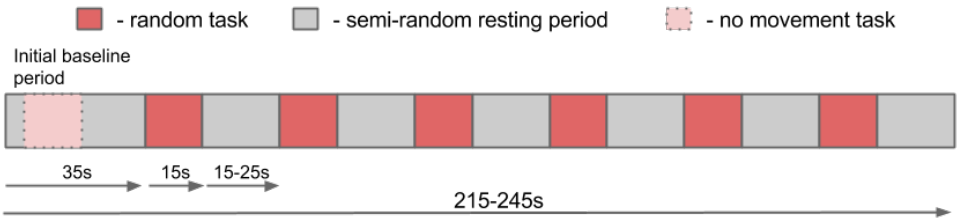

Figure 2.7: Diagram showing one sequence of the experiment trial block. Each sequence starts with an initial resting period to ensure a stable baseline, and the first no movement trial (pink) is recorded in this period. After baseline is established, random task trials of 15 s each (red) will commence, followed by a semi-random resting period (grey). The reason for a semi-random resting period is to eliminate response which can be caused by expectancy.

- During the resting period the visual instruction is "Rest".

A screen showing the visual instructions of the task is placed in front of the participant. EEG measurements are subjected to significant noise as a result of eye movement and eye blinks so to minimize that effect the subjects are asked to keep their eyes focused on a dot in the middle of the screen in front of them.

After each sequence the participant is able to take a moment to relax, have a drink of water, re-position their seat, etc. They are told to signal when they are ready for the next sequence, this is done so that the participant can feel more at ease and in control of the situation.

Online block

The online block consists of a small game which the participant can play until they no longer wish to. The objective of this game is to fill four circles by tapping the fingers during a recording period. The classifier trained in the preceding block is applied to the recorded data and will try to determine the intention of the participant. If the classifier predicts movement a circle is filled, if the classifier predicts no movement all the circles are blanked out and the participant must start over. The purpose of this block is just a proof of concept that online fNIRS is possible with integration to the Field Trip buffer system. This block was later omitted, reasons for this is discussed in chapter 4 on page 59.

2.6 Data analysis procedures

The data from the experiments are preprocessed and analyzed separately to plot the average brain activity for all subjects during the different movement tasks, this is done by converting the raw fNIRS and EEG data into hemodynamic changes and spectral densities respectively. This is done to show whether the brain signals exhibit patterns which are expected: blood oxygen level dependent response (BOLD) for fNIRS and sensorimotor rhythms (SMR) for EEG. This will thereby show that the basis for calculating the performance of each modality is sound. The performance is then calculated using a linear logistic regression classifier and compared, using a Wilcoxon rank sum test to determine significance. The center of gravity (CoG), i.e. the location where the brain activity originates, is then calculated by weighing each channel location by the relative strength of the response for that channel.

All analyses are done post hoc in Matlab, using tools and functions developed at the Donders Inst., see Appendices F on page 137, in addition to functions and scripts written by the author of this thesis, see Appendices E on page 101.

2.6.1 fNIRS data processing and analysis

The raw fNIRS data consists of 16 channels of optical density values which are converted into relative hemoglobin changes using the modified Beer-Lambert law. The bad channels are identified and removed based on a robust variance/mean computation, see Appendix F.3 on page 142. The beginning and end of the fNIRS data stream is also removed, because it contains movement artifacts from when the cap is adjusted and taken off. The remaining data is filtered as a whole with a low pass FFT-filter at 0.35Hz to remove general noise from light absorption due to hair follicles, skull thickness etc. (>100Hz) and artifacts like the heart pulse (approx. 1Hz). The data is further high pass filtered at 0.01Hz to remove slow drifts. The data stream is then sliced into trials based on the events registered during the experiment. The data used for classification is further sliced into three second segments of the trial ranging from +3 s to 18 s, this is to give the classifier training more trials and to prevent overfitting. All further processing is for illustrative purposes, the classifications are based on the data up until this point. The trials are de-trended by subtracting the 0-mean and linear trends, see Appendix F.2 on page 139. After this a 5 second baseline average is subtracted from each channel before the channels are averaged. The bad trials are removed using the same function as for identifying the bad channels. The average of all trials for each condition and each subject is calculated before calculating and plotting the grand average BOLD response. The average for each subject is normalized by calculating and dividing by the Euclidean distance of the data vector,

this is done to account for the variability among subjects. See figure 2.8 for a flowchart of the fNIRS data analysis.

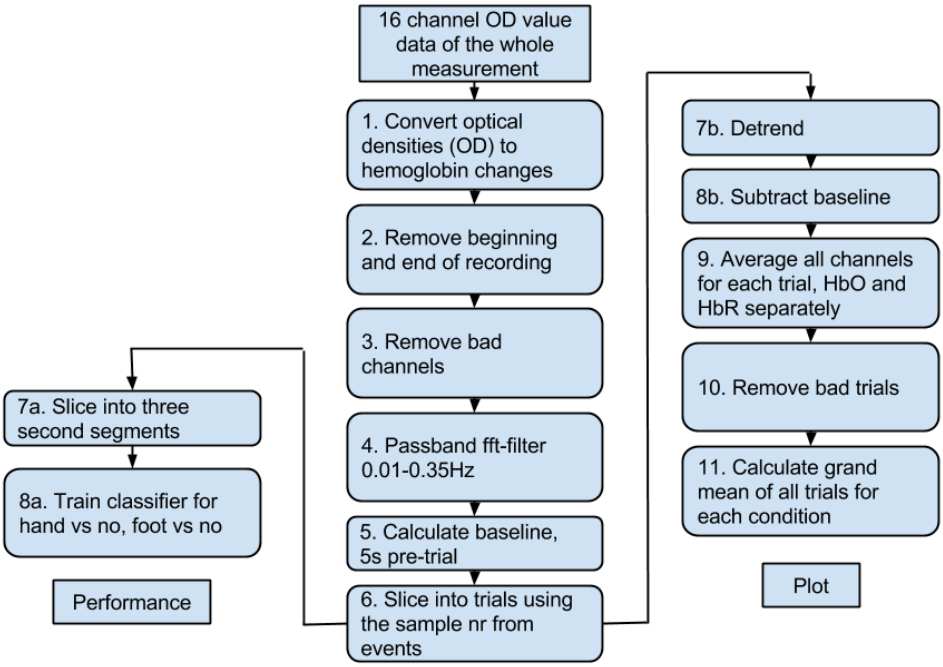

Figure 2.8: Flowchart showing the analysis pipeline for the fNIRS data ending in plot (fig. 1.7 on page 18) and performance (tab. 3.1 on page 51).

2.6.2 EEG data processing and analysis

The event related de-synchronization (ERD) is a change in the power spectrum of the signal recorded with EEG from the motor cortex, which occur during movement. The spectral density of the data recorded during movement will therefore be noticeably different than the spectral density of the baseline data (no movement). This difference is a measure of how large the brain activity is for each channel, and is used to plot where the brain activity is located.

Firstly, the 32 channel EEG data is de-trended and the bad channels are identified and removed from further analysis using the same functions as for the fNIRS data analysis. Then a spatial filter is applied to remove the common average noise among the electrodes. The bad trials are removed from further analysis by the same procedure as for channels. A Welch filter is applied to convert the signals to power spectrum densities. The frequencies of interest are sub-selected and the area under receiver operating curve (AUC) is calculated. The receiver operating curve is the

rate of true positives (sensitivity) as a function of the rate of false positives (fall-out). The AUC is computed by calculating the area under this curve. The AUC is a measure of discrimination between two data sets (in this case hand or foot movement vs no movement) and is plotted to show the discrimination between movement task and no movement for each electrode. In other words, if the discrimination is high there is a large response recorded in that area. The data is further used to train a linear logistic regression classifier, same procedure as for the fNIRS analysis procedure. The analysis procedure for EEG data is presented as a flow chart in figure 2.9.

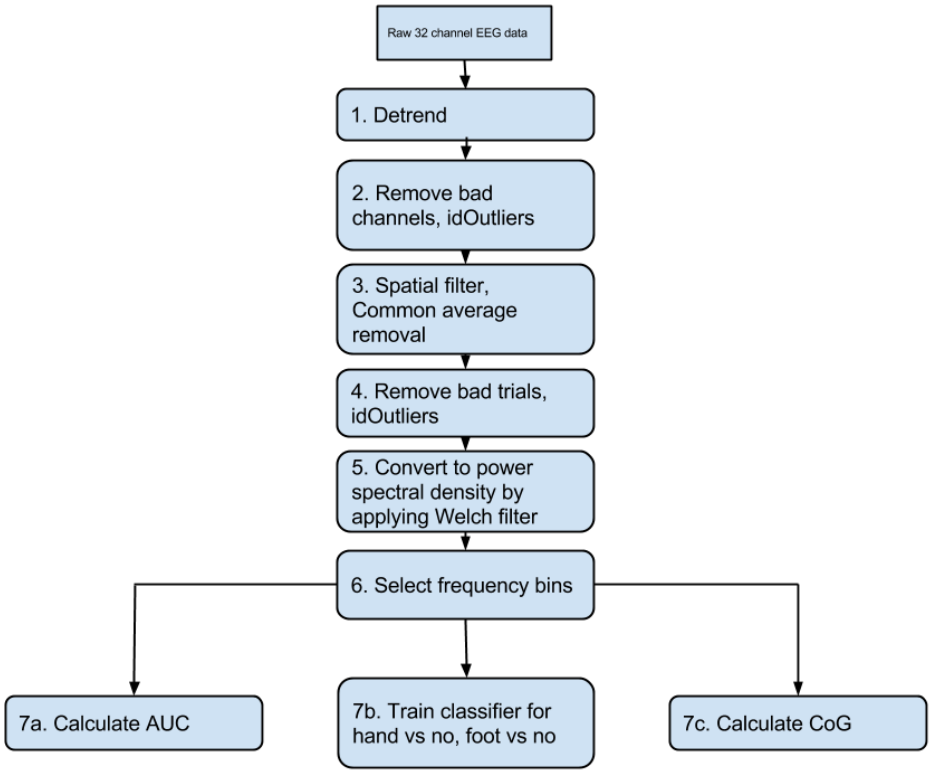

Figure 2.9: Flowchart showing the analysis pipeline of EEG data ending in plot (fig. 3.4 on page 49, fig 3.2 on page 47) and performance (tab. 3.1 on page 51).

2.6.3 Classifier

To assess the performance of the two modalities the data recorded in the trial block, and the classes associated with it, is fed to a classifier training algorithm (Appendix F.4 on page 145). This algorithm uses a linear logistic regression model and tries to relate the data to the known output, i.e. classes. Because biological data has a high degree of variation this algorithm uses a 10-fold cross validation, meaning that it separates the data into 10 subsets and uses 9 to train the classifier which is tested on the remaining subset. This is done consecutively for all the subsets and the optimal regularisation strength is then selected. This gives a measure of performance based on the percentage of true positive classifications the algorithm achieves during its testing phase, where 0.5 is pure chance and 1.0 is perfect discrimination between classes. The classification analysis is separated into hand vs no movement and foot vs no movement and calculated for EEG and fNIRS separately.

2.6.4 Center of Gravity

fNIRS. To calculate the center of gravity (CoG) for fNIRS, each channel location is weighted by the mean hemodynamic response for that channel. This is the same procedure used by Koenraadt et al. [45]. The X_i represents the x y coordinate of each channel, a_i represents the mean hemodynamic response for each channel. The X_{CoG} is calculated for both HbO and HbR separately. The hemodynamic response for HbR is negative, so a_i is calculated from the absolute value.

$$X_{CoG} = \sum a_i X_i / \sum a_i \tag{2.1}$$

EEG. To calculate the CoG for EEG the same principle of weighing channels by their mean response follows, the difference being that the event related de-synchronization (ERD) is the measure of response. Each channel location is weighted by the relative ERD for each channel which is a measure for the strength of the response. This is done by subtracting the average power across all frequencies in the no movement condition for each channel, b_i, from the average in the movement condition, a_i, and dividing by b_i. This fractional reduction in power during movement is < 1 for ERD and > 1 for ERS. The positive channels are then weighted by $1 - relERD$.

$$relERD = (a_i - b_i)/b_i \tag{2.2}$$

$$cW = 1 - relERD \tag{2.3}$$

$$X_{CoG} = \sum X_i cW_i / \sum cW_i \; for \; X_{ERD_i} > 0 \tag{2.4}$$

The participant performs the hand movement task with *both* hands, and the response will therefore be located in the motor cortices of both brain hemispheres and the CoG for EEG will have two locations of origin. The weight of the left hand response will draw the CoG towards the center. The fNIRS is only measured on the left hemisphere, however, so to compare the two the CoG for EEG, hand movement, is calculated using only the electrodes on the left hemisphere. For the foot movement task the electrodes from both hemispheres are used, since the foot movement CoG for EEG is expected to be around the vertex (most central point, Cz in the 10-20 system) and it will only be used to calculate the correlation between ΔCoG and classification rate.

Chapter 3

Results

16 participants signed up for this study, one was excluded due to not meeting the criteria for participation, and 3 did not show up at the scheduled time. Experiments were conducted on the remaining 12 subjects (7 female) aged from 22 - 60 (mean $30 \pm 10.3SD$), at Radboud University in Nijmegen, the Netherlands. The participants were paid 25 Euro to participate, and they all gave their freely informed consent before participation as per regulations. No adverse effects were observed during the experiments.

All the results are produced according to the analysis procedures described in section 2.6 on page 40. The data behind these results are from subject 3 to 12, the data from the first two subjects have been excluded due to hardware issues during the experiment, resulting in only fNIRS data with no EEG data for comparison. The results are discussed further in chapter 4 on page 59. The figures presented in this section show patterns which are expected for both EEG and fNIRS.

3.1 BOLD response

The grand average hemodynamic response for each task, obtained by averaging over all trials and subjects is presented in fig 3.1 on the following page. The trial duration, i.e. the duration of stimuli, is from 0 - 15 seconds and is marked with yellow. The grey fields represent one standard deviation above and below the mean oxygenated (HbO) and de-oxygenated (HbR) hemoglobin response respectively.

When the trial begins, the consumption of oxygen in the motor cortex is increased, resulting in a decrease of de-oxygenated hemoglobin and an increase of oxygenated hemoglobin, as the blood vessels expand to accommodate the increased demand for oxygen to the cells in the activated area. The BOLD response takes approx. 7 seconds to reach max and min level of HbO and HbR respectively, and is expected to maintain approximately maximum amplitude until stimulus ends. Both hand

movement and no movement exhibit the patterns which are expected. The foot movement response, however, returns to baseline approx. 7 seconds before the stimulus ends. Reasons for this is discussed further in the next chapter.

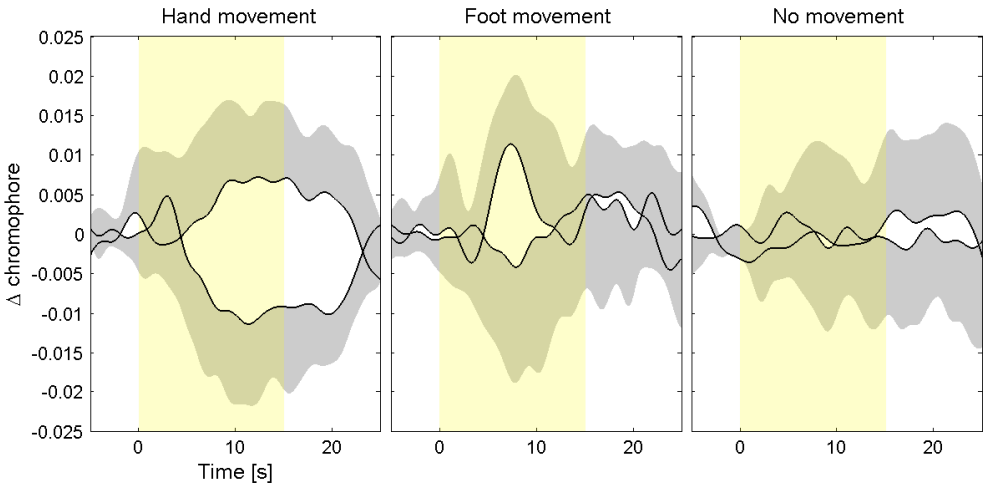

Figure 3.1: Total grand average of the BOLD response for the three movement conditions, hand movement, foot movement and no movement. The data has been normalized to account for the variability among subjects. The duration of stimulus is from 0 - 15 s, marked with yellow. The grey fields represents one standard deviation above the HbO and below the HbR mean response respectively. The hand and no movement plots show the expected patterns in the hemodynamic response. The foot movement response returns to baseline after the initial rise approx. 7 seconds earlier than expected.

3.2 Sensorimotor rhythmic response

The area under the receiver operating curve (AUC) is a measure of discrimination between movement and no movement tasks in the power spectrum. In other words, an AUC value towards 1.0 means that there is a large difference in power for a certain frequency. The grand average AUC plots for each electrode, averaged over all the subjects are presented in figure 3.2 on the next page and 3.4 on page 49 for hand vs no movement and foot vs no movement respectively. The event related de-synchronization (ERD) is a decrease in power in the mu (8 - 12 Hz) and beta (18 - 30 Hz) bands of the electro-physiological brain signal, which means that when there is a stronger AUC, there is an ERD: an indicator of cortical activity in the motor cortex. Grand average spectral densities for

each electrode are presented in figure 3.3 on the next page and figure 3.5 on page 50, for hand and foot movement response respectively.

As seen in figure 3.2, there is clear activity around C3 and C4, where the location of hand movement cortical activity is expected to be. The foot movement response is generally weaker than for hand movement, possibly because the source is located deeper within the brain. However, it is largely situated around Cz, which is expected. Note that the response for hand movement is larger over C4, i.e. the opposite side to where the fNIRS optodes are located. These plots are showing that the sensorimotor rhythms exhibit the patterns which are expected for cortical activity of hand and foot movement

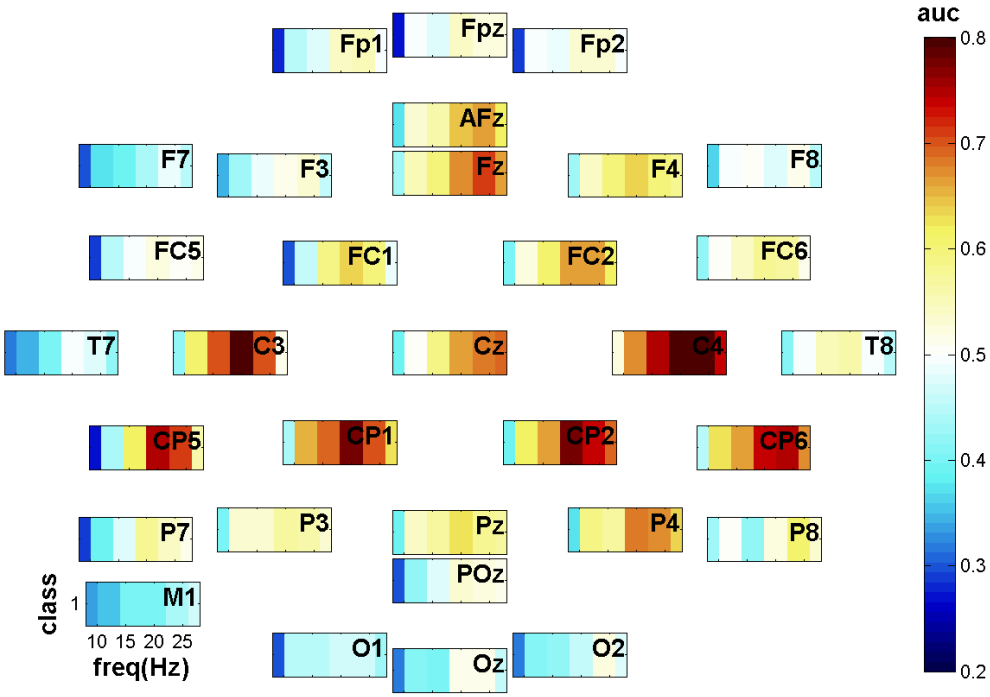

Figure 3.2: Grand average of area under the receiver operating curve (AUC) for hand movement condition for each electrode. A high discrimination between classes (towards red) is showing that the cortical activity is localized around C3 and C4, the areas associated with hand movement. An AUC value of 0.5 means no discernible discrimination, i.e. pure chance. This plot shows patterns that are expected for hand movement cortical activity. Note that there is a larger response around C4 on the right hemisphere which is the opposite side of where the fNIRS optodes are placed.

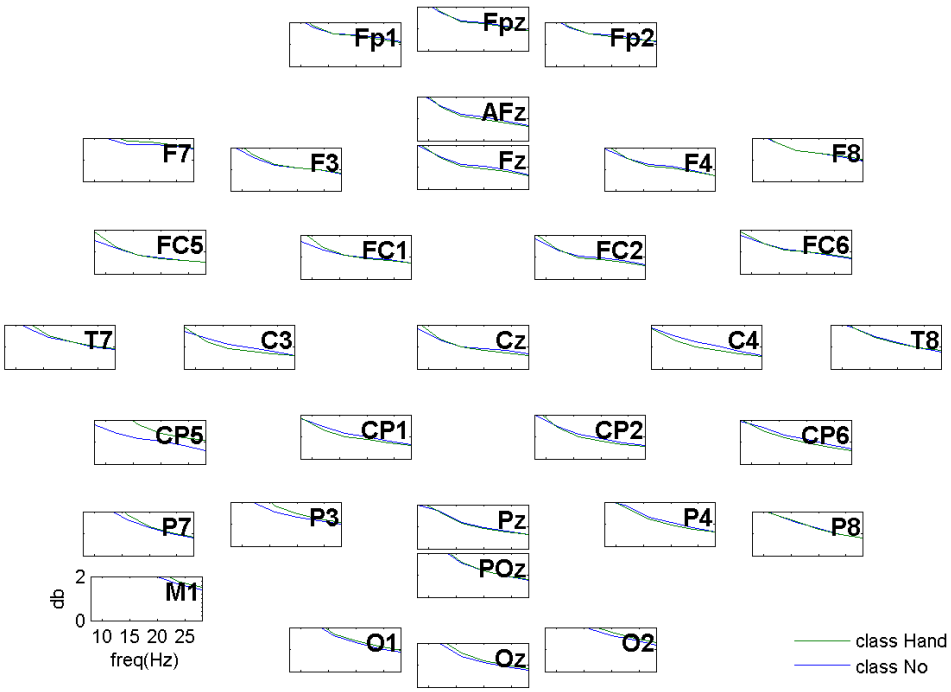

Figure 3.3: Grand average spectral densities for each electrode, hand movement condition. An ERD is the reduction in power for the movement condition vs the no movement condition. A clear decrease in power can be seen around C3 and C4.

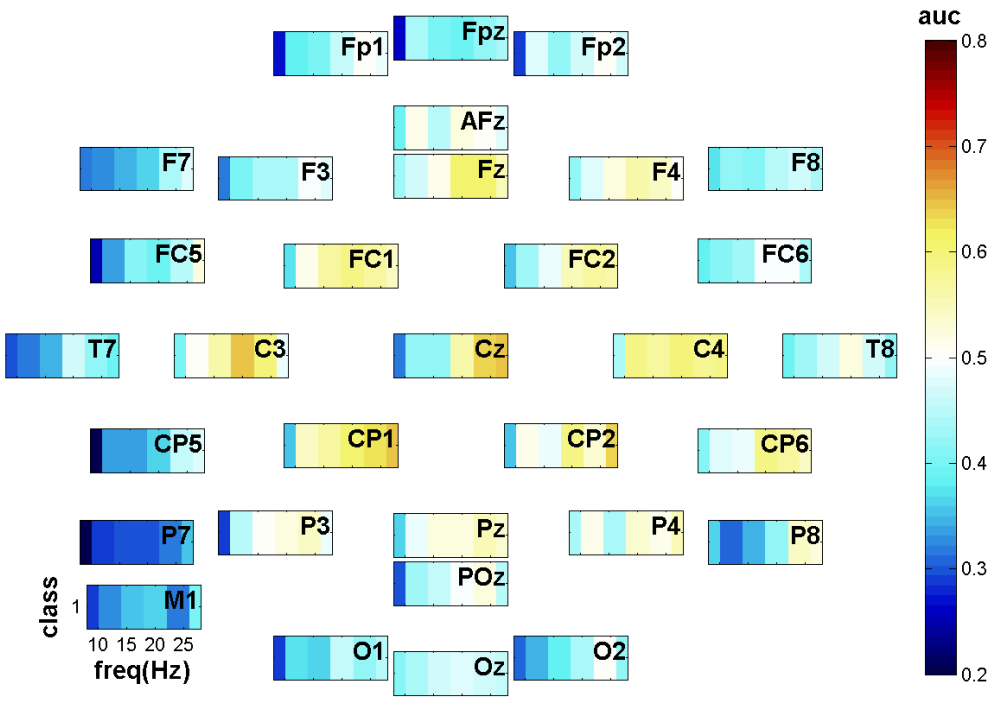

Figure 3.4: Grand average of the area under the ROC curve for each electrode, foot movement task. A high discrimination (towards red) for frequencies around 18-30Hz is a typical indicator of cortical activity. The activity is localized around Cz. This plot show the patterns which are expected for foot movement cortical activity.

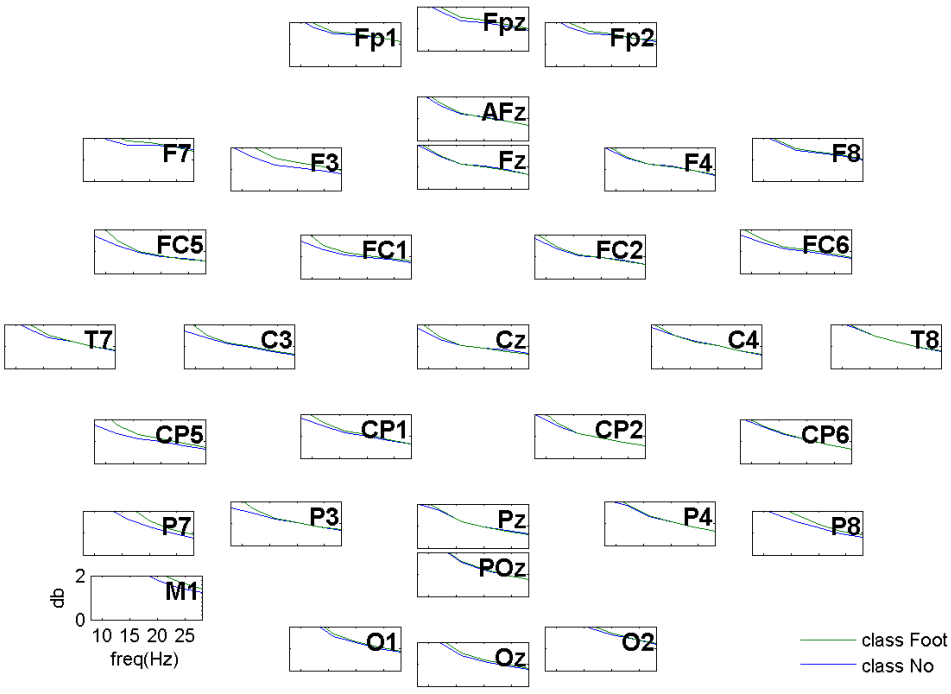

Figure 3.5: Grand average spectral densities for each electrode, foot movement condition. An ERD is the reduction in power for the movement condition in regards to the no movement condition. The decrease in power is weaker than for hand movement, but can be seen in Cz. The source is located deeper within the brain and might explain why this is so.

3.3 Classification rates

Calculating the classification rate is based on the ability to discriminate between the individual movement tasks and the no movement task. Classification rates for each subject and both modalities and tasks are presented in table 3.1. Both modalities are able to discriminate between no movement and movement (hand and foot) with significance. The average performance of fNIRS and EEG for hand movement task is 0.77 and 0.86 respectively and for the foot movement task the performance is 0.70 and 0.89. Due to the characteristics of the classification rates, this being that they are bound between 0 and 1 and that they tend to be non-gaussian, a Wilcoxon rank-sum test was chosen to determine the significance [52] of differences. Performing the test reveals a significant difference between EEG and fNIRS in the foot movement task ($p = 0.013$), but the difference in hand movement task did not reach significance ($p = 0.14$).

Subject	fNIRS hand	fNIRS foot	EEG hand	EEG foot
S3	0.78	0.68	0.67	0.96
S4	0.82	0.72	0.92	1.00
S5	0.57	0.50	1.00	0.96
S6	0.85	0.73	0.62	0.71
S7	0.80	0.72	1.00	0.66
S8	0.65	0.71	0.83	0.96
S9	0.77	0.51	1.00	0.83
S10	0.94	0.80	0.56	0.91
S11	0.70	0.93	1.00	1.00
S12	0.83	0.74	0.96	0.87
Mean	0.77	0.70	0.86	0.89
SD	0.11	0.12	0.17	0.12

Table 3.1: Classification rates for each subject. Classification rates are based on training the data with a 10-fold cross validating linear logistic regression algorithm, as explained in section 2.6.3 on page 43. The numbers are a measure of performance, where 1.0 is a perfect discrimination between classes and 0.5 is pure chance, i.e. the classifier cannot predict the outcome. The average performance of EEG is significantly higher than fNIRS when detecting foot movement, but the difference between average performance when detecting hand movement did not reach significance.

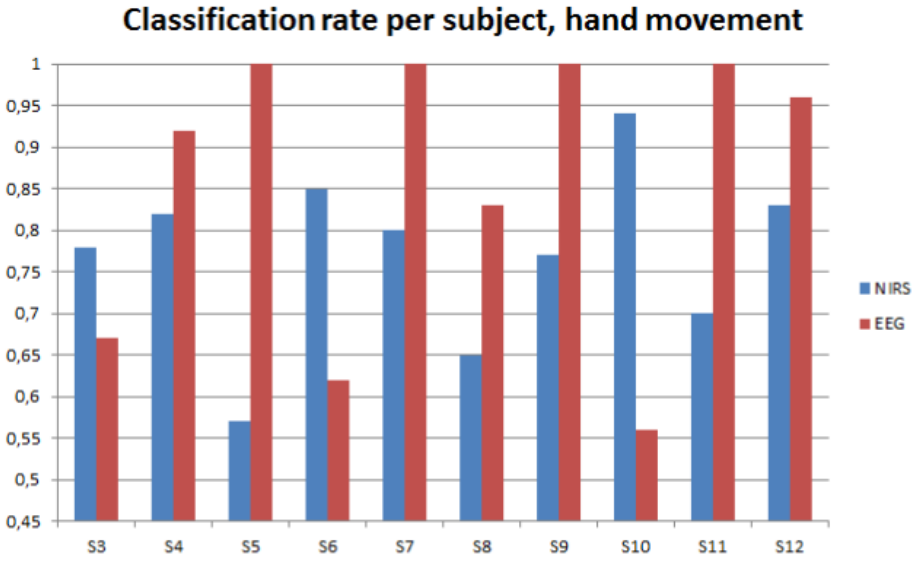

(a) Classification rates for each subject, hand movement task.

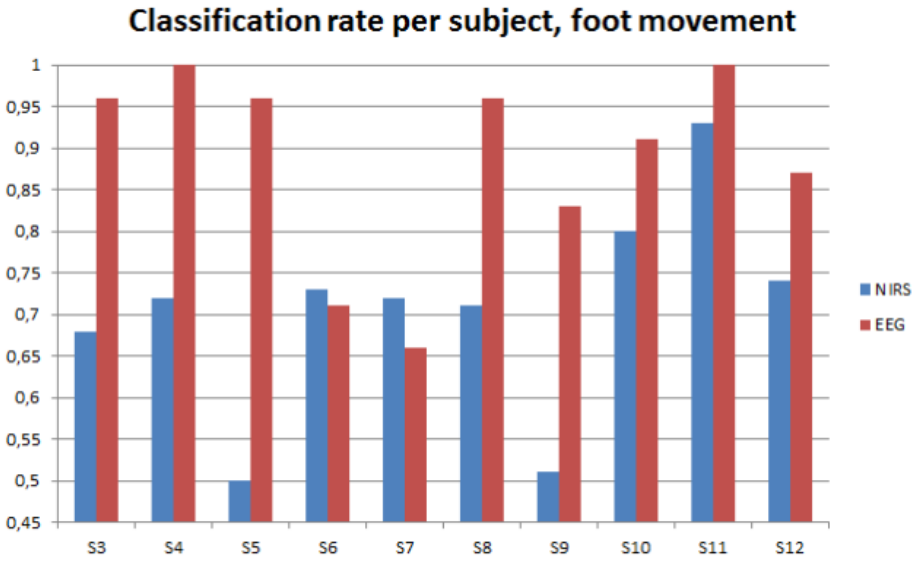

(b) Classification rates for each subject, foot movement task.

Figure 3.6: Classification rates for each subject, hand and foot movement task. These diagrams range from 0.45 to 1.0, because 0.5 is, essentially, the lowest possible score and means that the classifier can only guess the intention of the user. Subject S5 and S9 had no significant classification rate for fNIRS, foot movement. Subject S5 scored low for both hand and foot movement with fNIRS.

3.4 Task discrimination using fNIRS

To produce evidence on whether a system using fNIRS is able to discriminate between the center of gravity (CoG) for hand and foot movement, each channel location is weighed by the mean response for that channel. The cap is placed on the subject's head according to the standards for electrode placement. This ensures that the optodes are placed in approximately the same location, minimizing the variability among subjects.

The results are presented in table 3.2, and the average is plotted in figure 3.7. This plot represents the fNIRS area of coverage, which is an area of 8 x 4.4 cm centered over C3, as previously explained. The x-axis is mediolateral direction and the y-axis is anteroposterior. The grey and black circles represent the transmitters and receivers that are placed on the scalp, respectively. The diamonds represent hand movement, and the squares represent foot movement. The foot movement CoGs are located more lateral than hand movement, although no significant difference between hand and foot movement was found when performing a student's t-test.

	Hand HbO		Hand HbR		Foot HbO		Foot HbR	
subject	X	Y	X	Y	X	Y	X	Y
S3	3.68	1.78	3.99	1.84	3.76	1.55	3.88	1.13
S4	5.62	1.96	2.80	2.32	3.94	1.55	4.08	1.64
S5	3.81	1.52	4.12	2.27	4.59	1.42	2.95	2.10
S6	3.90	1.32	4.03	1.62	3.89	1.17	1.57	2.84
S7	5.27	1.55	3.29	2.53	2.99	2.49	4.34	2.05
S8	4.61	1.69	3.82	2.20	4.68	1.76	4.26	2.11
S9	3.63	1.51	2.07	2.40	2.31	2.38	2.09	2.36
S10	5.43	1.97	5.42	1.91	5.55	2.03	5.48	1.88
S11	5.15	1.99	4.39	1.76	4.78	1.93	5.48	2.32
S12	3.43	1.97	3.90	1.99	3.34	1.59	3.13	2.54
Mean	4.45	1.73	3.78	2.08	3.98	1.79	3.73	2.10
SD	0.81	0.23	0.86	0.29	0.91	0.40	1.23	0.45

Table 3.2: Coordinates for the center of gravity for each subject, fNIRS, hand and foot movement. The numbers are centimeters from the lower left optode. The center point (C3), is located at $X, Y = [4, 2.2]cm$, see figure 3.7 on the next page. No significant difference between hand and foot movement, for either oxygenated (HbO) or de-oxygenated (HbR) hemoglobin, was found.

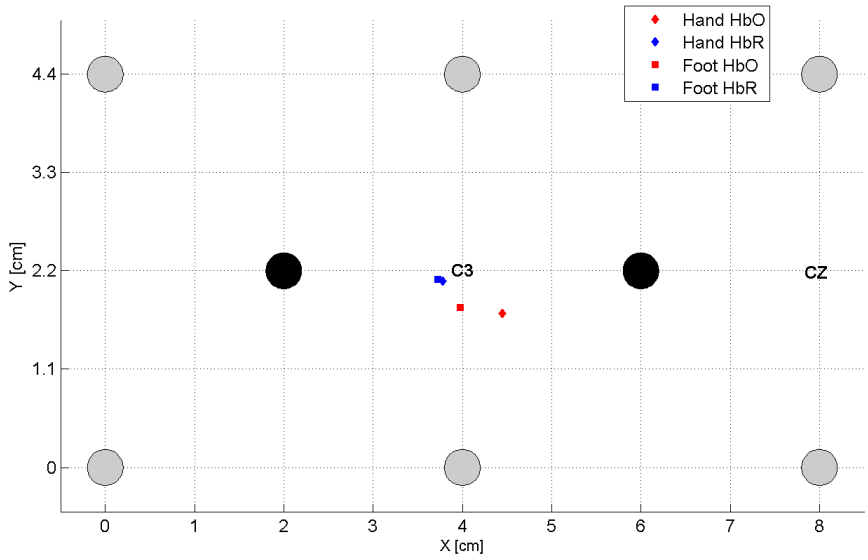

Figure 3.7: Center of gravity for hand and foot movement measured by fNIRS, diamonds and squares represent hand and foot movement respectively. Red and blue represents HbO and HbR respectively. The grey and black circles represent the location of the transmitters and receivers respectively. No significant difference between location for hand and foot movement was found, see table 3.2 on the previous page.

3.5 Difference in CoG (Δ*CoG*)

The difference in average CoG for the two modalities, hand and foot movement task, is shown in figure 3.8 and figure 3.9 on the next page. The CoG for EEG, hand movement task, is calculated using the data from electrodes located on the left hemisphere only, this is because the subjects were instructed to move *both* hands during the trial. Moving both hands will produce a response on each hemisphere, as seen in figure 3.2 on page 47, so to compare EEG with fNIRS, which is only recording on the left hemisphere, the electrodes on the median line and right hemisphere is removed from the analysis. Foot movement cause only a single CoG for EEG so in this case both hemispheres are used for analysis.

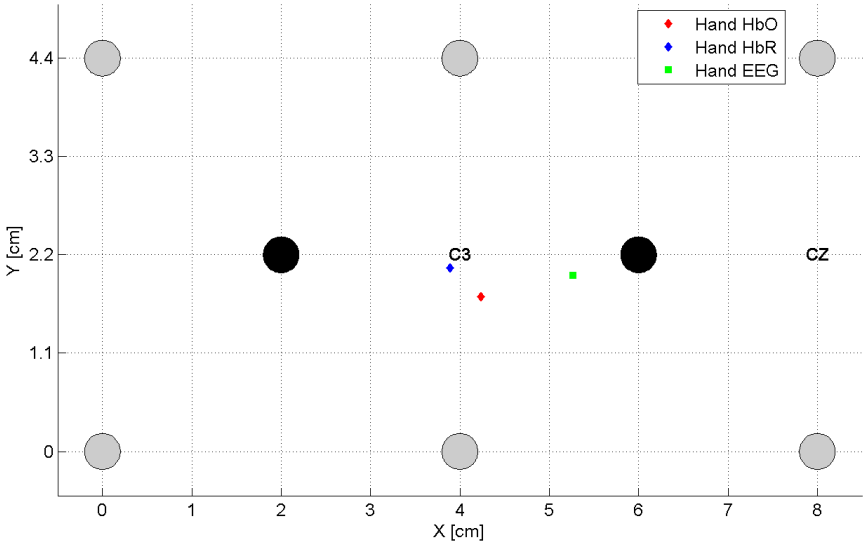

Figure 3.8: Grand average CoG, hand movement task, for EEG and fNIRS plotted on the area covering the left hemisphere motor cortex. The grey and black circles represent fNIRS transmitters and receivers. The red and blue diamond represent the CoG for fNIRS, HbO and HbR. The green square represent the CoG for EEG. This plot show that all CoGs are located around C3, where hand movement response is expected to be.

The CoGs presented in figure 3.8 is located where they are expected to be. However, the foot movement CoGs measured with fNIRS, presented in figure 3.9 on the following page, is located more laterally than expected. To see if the *difference* in CoG (Δ*CoG*) affects the performance of fNIRS, the correlation between Δ*CoG* and performance for fNIRS is calculated. Subject S4 was excluded from these analyses due to no relative ERD in the

EEG i.e. no data for comparing the two modalities.

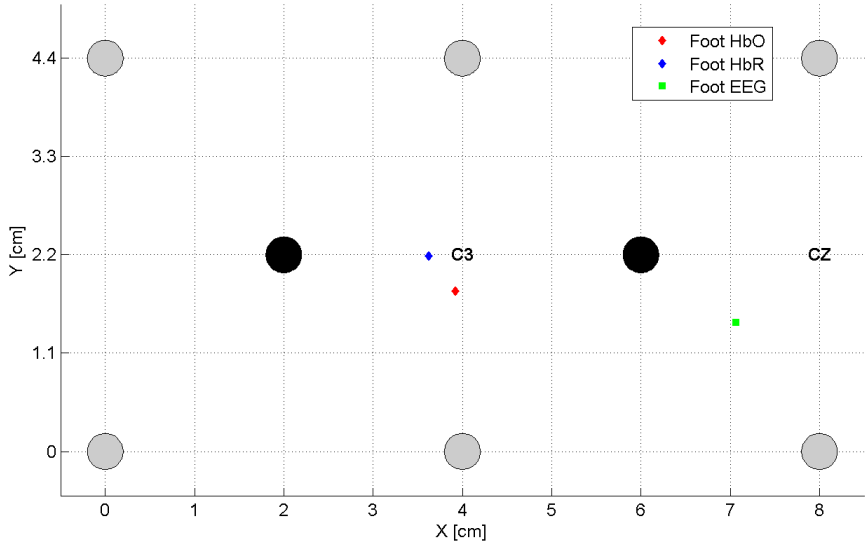

Figure 3.9: Grand average CoG, foot movement task, for EEG and fNIRS plotted on the area covering the left hemisphere motor cortex. The grey and black circles represent fNIRS transmitters and receivers. The red and blue diamond represent the CoG for fNIRS, HbO and HbR. The green square represent the CoG for EEG. The location for foot movement in the motor cortex is in the central sulcus a couple of centimeters down, and the CoG for both modalities are therefore expected to be close to the vertex (Cz). This plot shows that the CoG for EEG is located approximately where it is expected to be, but the CoGs for fNIRS is more lateral than expected, i.e. they should be closer to Cz.

The correlations between the ΔCoG and the fNIRS classification rates, which is a measure of how reliably the system can detect movement, were calculated, and the results are presented in figure 3.10 on the next page. No significant correlation between the ΔCoG and performance was found.

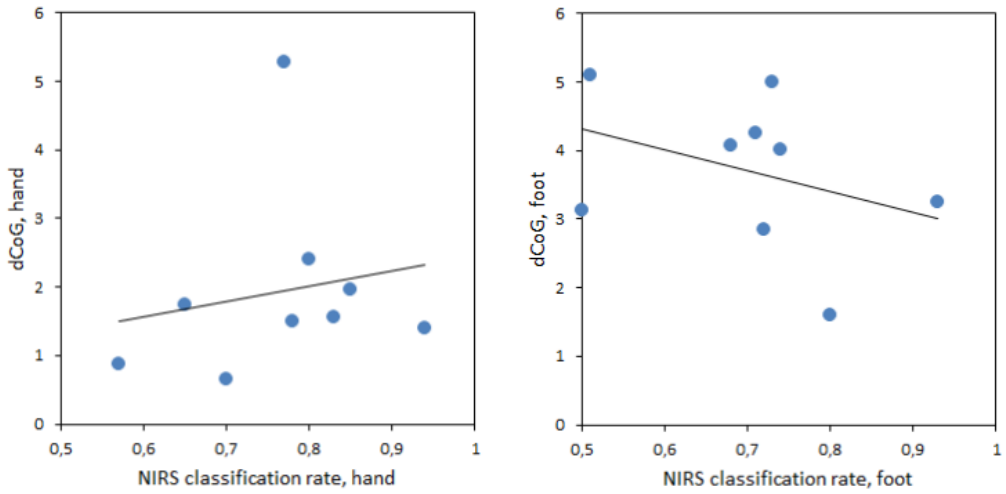

Figure 3.10: Left: Correlation between ΔCoG and classification rate for fNIRS, hand movement ($r = 0.18, p = 0.65$). Right: Correlation between ΔCoG and classification rate for fNIRS, foot movement ($r = -0.36, p = 0.35$). No significant correlation between ΔCoG and the classification rates were found.

Chapter 4

Discussion

Observations

During the experiment the results gathered with a post hoc analysis did not show any intelligible results, and a debugging of the whole system was necessary. No error in the data recording pipeline was found, but several small errors in the signal processing procedure were. Additionally, it was discovered that the instructions given to the participant were somewhat misinterpreted, and resulted in the participant moving during the initial resting period where the first no movement trial of each sequence was recorded. This was corrected by simply removing the first trial of each sequence for all subjects in the analysis. Because of these errors, the online block which was planned was not executed for any of the participants. This block was only meant as a proof of concept for the use of fNIRS online, and therefore not critical for answering the research questions.

A moderate anti-correlation ($r = -0.59, p = 0.09$) between classification rates, i.e. performance, for hand movement for the two modalities was observed, suggesting that the two modalities might be mutually exclusive in this study. This is presented in figure 4.1.

It was also observed that the subjects with darker hair color had noisier fNIRS signals than the subjects with blond hair, although this resulted in more of the channels being removed for the dark hair subjects during the analysis procedure, the bold response was not affected by this. This is merely a subjective observation, but might be interesting for future studies to give more evidence on the robustness of fNIRS.

Primary objective

The primary objective of this study was to determine if using fNIRS yields a higher performance rate when detecting movement of the hands and feet than EEG using a 10 fold linear regression classification training on the measured data. From the results in section 3.3 on page 51 the classification rates for hand movement, both EEG and fNIRS, are on par with findings

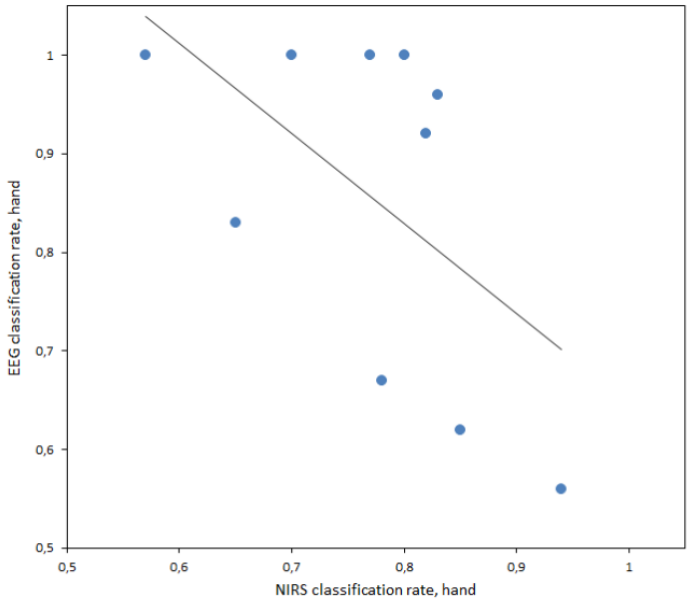

Figure 4.1: Correlation between classification rates for both modalities, hand movement task ($r = -0.59$, $p = 0.09$), showing a moderate, yet significant, anti-correlation.

from similar studies (Blokland et al.[28], Fazli et al.[35]). Considering that the cap was a prototype and that the subjects were not extensively selected, these classification rates are relatively high. However, comparing the two modalities to each other reveals that the EEG has a higher classification rate than fNIRS at detecting both hand and foot movement, although not statistically significant for hand movement ($P = 0.14$).

An anti-correlation between performance rates when detecting hand movement was observed, see figure 4.1, which suggests that the two modalities are mutually exclusive in this particular setup, i.e. when one modality performs well the other does not. This further suggests that the connection between electrode/optode and the scalp can only be optimal for one of the modalities at a time. Figure 3.2 on page 47 also reveals that the hand movement response, recorded with EEG, is stronger on the right hemisphere opposite to where the fNIRS optodes were placed. These observations suggest that the combined optode/electrode setup used in this study, can not measure the response reliably simultaneously.

Observation 1. *AUC plot showing less response on left hemisphere, see fig 3.2 on page 47.*

Possible explanation: *EEG does not detect cortical activity as well where it is combined with fNIRS.*

Observation 2. *The performance when detecting hand movement for EEG and fNIRS anti-correlates.*

Possible explanation: *The optode/electrode setup makes the system mutually exclusive for EEG and fNIRS.*

Conclusion: *The combined optode/electrode setup, used in this study, does not detect movement in the same area reliably.*

Secondary objective

The secondary objective was to determine if a system using fNIRS is able to discriminate between hand and foot movement. As can be seen in figure 3.1 on page 46, the hemodynamic response to foot movement task drops to baseline after the initial rise, where the hand movement task settles at max. amplitude throughout the duration of stimulus. This might indicate that fNIRS is not in fact measuring the foot movement, but rather a propagating effect caused by the surge of oxygenated blood through the cortex as the foot center, which is located deeper in the brain, is activated. The location of foot movement CoG, as seen in figure 3.7 on page 54, might also be an indicator of this, since it is located more lateral than hand movement when it was expected to be more medial, because the physiological location for foot movement cortical activity is in the central sulcus (close to the vertex), see figure 1.5 on page 13.

A study on mice conducted by Sheth et al.[53] found that the hemodynamic response starts to propagate after 2-3s and continues for several seconds, the cerebral blood volume changes propagate retrograde into feeding arterioles and the oxygenation changes anterograde into draining veins. Another study conducted by Chen et al.[54] states that the propagation of vasodilation is independent of direction of blood flow and has a decay phase that has a uniform spatial dependence. The propagation occurs rapidly in directions away from center, and the return to baseline is first observed in peripheral regions, last at the center of parenchyma (region of activation). Based on the facts stated in these studies, I will argue the possibility of one out of two different, probable scenarios, although further studies are needed to verify this:

1. The foot center is first activated and the hemodynamic response propagates upwards to the area that fNIRS detects. If this is true the signal will show up as a response and then return to baseline sooner than at the center of parenchyma. The center and peripheral regions reach peak response at approximately the same time, but the return to baseline starts first in the peripheral regions, see diagram in figure 4.2 on the next page.

2. The measured hemodynamic response is actually a measurement of residual movement in the upper body as the subject starts the task. The diagram in 4.3 on page 63 represents this scenario. When the subject settles to a stable movement rhythm the upper body

parenchymas will stop being active and the measured response will return to baseline earlier than expected. If this is true, the fNIRS channels are not able to target the foot movement parenchyma in this setup.

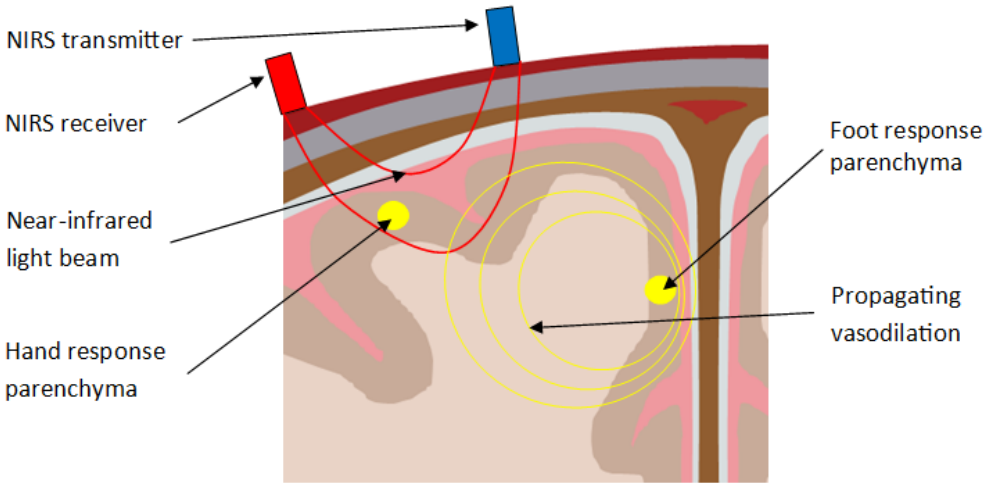

Figure 4.2: Diagram showing a possible propagation of vasodilation through the tissue during foot movement. The foot movement parenchyma (response origin) is located in the central sulcus. As stimulus progresses, the hemodynamic response propagates outwards and may be detected by the fNIRS channel targeting the hand movement parenchyma. When the stimulus ends the vasodialtion will first subside at the farther region from the parenchyma which might explain the short response for foot movement in figure 3.1 on page 46.

EEG has a significantly higher performance rate than fNIRS at detecting foot movement, which infers that EEG is more reliable. If scenario 1 is true, i.e. fNIRS is in fact targeting the correct area, then I can conclude that EEG has a higher performance rate than fNIRS at detecting foot movement. If scenario 2 is true, i.e. the fNIRS optodes are not targeting the foot movement area but rather measuring residual upper body movement, then this will further argue the importance of the optode setup, meaning more optodes are needed to ensure proper cortical coverage.

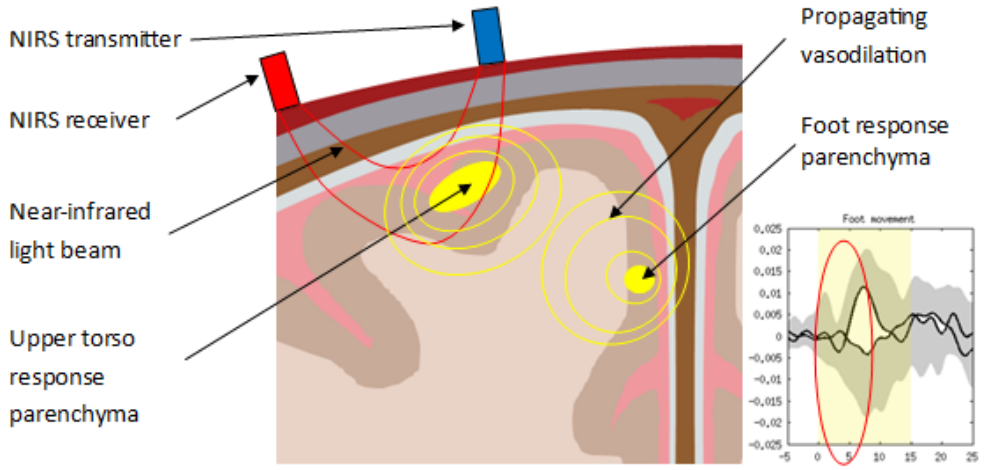

(a) Hemodynamic response propagation from 0 - 7 s.

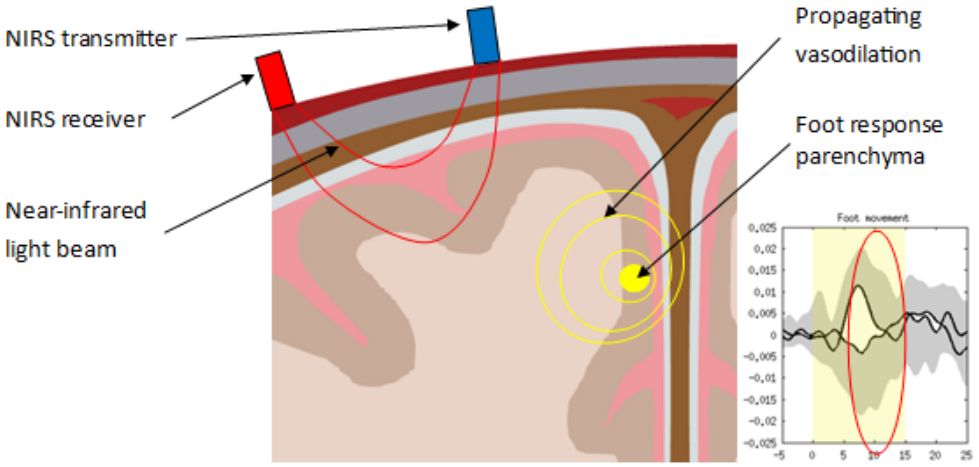

(b) Hemodynamic response propagation from 8 - 15 s.

Figure 4.3: Diagram showing a possible propagation of vasodilation during foot movement stimulation. At the start of the stimulus cue there might be residual movement in the upper body and arms. Once the subject stabilizes, this residual movement may be reduced, meaning that the response which is measured is not produced by the foot movement parenchyma, but rather residual upper body movement, and therefore will subside earlier than expected.

Observation 1. *The fNIRS CoG for foot movement was measured more lateral than the CoG for hand movement.*

Possible expl.: *The fNIRS might be measuring something else than foot movement.*

Observation 2: *The hemodynamic response propagates through tissue.*

Possible expl. A: *The measurement is of actual foot movement, see fig 4.2 on page 62.*

Possible expl. B: *The measurement is of residual upper body movement, see fig 4.3 on the preceding page.*

Observation 3. *EEG has significantly higher performance rate at detecting foot movement than fNIRS.*

Conclusion: *If explanation A is true, the system is targeting the correct area and EEG has a significantly higher performance rate. If explanation B is true, the optode setup is not targeting the correct area.*

Tertiary objective

The third objective, as stated in section 1.5 on page 23, was to determine if the difference in location of center of gravity (CoG) for fNIRS and EEG correlates with the classification rate for fNIRS. As seen in figure 3.10 on page 57, no significant correlation between the ΔCoG and fNIRS classification rate was found for either movement task. This means the CoG for EEG falls within the fNIRS area of coverage. If the true CoG would be outside the area of fNIRS coverage the classification rate for fNIRS would be 0.5 (lowest possible) for that measurement, and the correlation would show an "all or nothing" characteristic, in other words, some kind of hemodynamic response is measured within the fNIRS area of coverage. Whether this response is true to the type of movement task, can not be determined by this analysis.

Observation 1. *No significant correlation between difference in CoG and fNIRS performance.*

Conclusion: *Some kind of hemodynamic response is measured within the fNIRS area of coverage.*

Sources of error

The cap that was used was a prototype which was modified with styrofoam and glue. This, of course, was not optimal and might have led to the optodes and electrodes not being in as close contact with the scalp as they require, suggesting one reason for the lack of significant answers. Another possible reasons for this lack of significance might also be misinterpretations of the instructions given to the participants. If the participant were to move a few seconds before a new trial, the baseline recording would be contaminated with movement response because the hemodynamic response is quite slow. Although the participants were monitored during the experiments, and corrected if this was observed, a small portion of the recorded trials were probably affected by movement contamination. The classification rates, which are calculated from un-baselined data, is not affected by this, but it may, however, have led to more of the trials being removed later in the analysis procedure, and thereby increasing the variance. For future fNIRS studies I will suggest that this must be taken in close consideration, and that measures must be taken to ensure a contaminate free baseline. This can be done by increasing the baseline period, and giving more strict instructions to the participant.

Chapter 5

Summary of findings

The main aim of this study is to determine whether or not fNIRS may be considered a feasible alternative to EEG in an intraoperative awareness monitoring system, based on the modalities' performance at detecting hand and foot movement, in addition to meeting the criteria for clinical feasibility: a minimal generic electrode/optode montage that works for all patients, and takes a minimal amount of time to set up; a false positive rate not exceeding one per two hours operating time, and a time to detect awareness not exceeding 2.5 min.

Regarding the false positive rate and time to detection, the online block that was scheduled was not executed due to issues with the signal processing during the experiments. I deemed it necessary to perform a debugging of the system to ensure that the recorded data was not compromised, and because I was pressed for time the online block was omitted. This block was meant more as a proof of concept, and answering the proposed hypotheses had a higher priority.

BCI systems that combine fNIRS and EEG have shown promise when it comes to increased performance [28, 35], and it might also be a method to use in order to solve the problem of BCI illiteracy. However, in an application where setup time and ease of use is essential, such as an intraoperative awareness monitor, this increased performance has to be substantial in order to outweigh the disadvantage of a prolonged or too complex setup.

The first objective was to determine which modality had the best performance rate at detecting hand and foot movement. Although no definite conclusions regarding hand movement can be drawn, the observations made in this objective indicates that the combined EEG-fNIRS setup cannot reliably measure the responses simultaneously. This, in turn, means that the fNIRS optode placement cannot rely on the 10-20 framework for electrode placement. One possible action to ensure that the optode placement targets the correct area is to perform a testing block before the actual measurement, and adjust the optode placement to where the response is strongest. This would mean an increased setup time which

is an argument against the use of fNIRS in an intraoperative awareness monitor where setup time is essential for its feasibility.

For the second objective, which was to determine if fNIRS has the ability to discriminate between hand and foot movement, the observations made indicates that the optodes may not target the correct area. If the optodes are in fact targeting the correct area, then I can conclude that EEG has a significantly higher performance rate than fNIRS at detecting foot movement. However, if the optodes are not targeting the correct area, a larger number of optodes are needed to ensure that the measurement is correct. This will increase both the setup time and complexity if this paradigm were to be implemented in an intraoperative awareness monitor.

In any case, the setup is affected, either by prolonging the time it takes to ensure a reliable signal, or by adding to the complexity of the electrode/optode montage, see deduction tree in figure 5.1 on the next page. I will argue, based on these observations, that functional near-infrared spectroscopy (fNIRS) is not a feasible alternative to electroencephalography (EEG) as measurement technology in an intraoperative awareness monitoring system, although further research is needed to verify this argument.

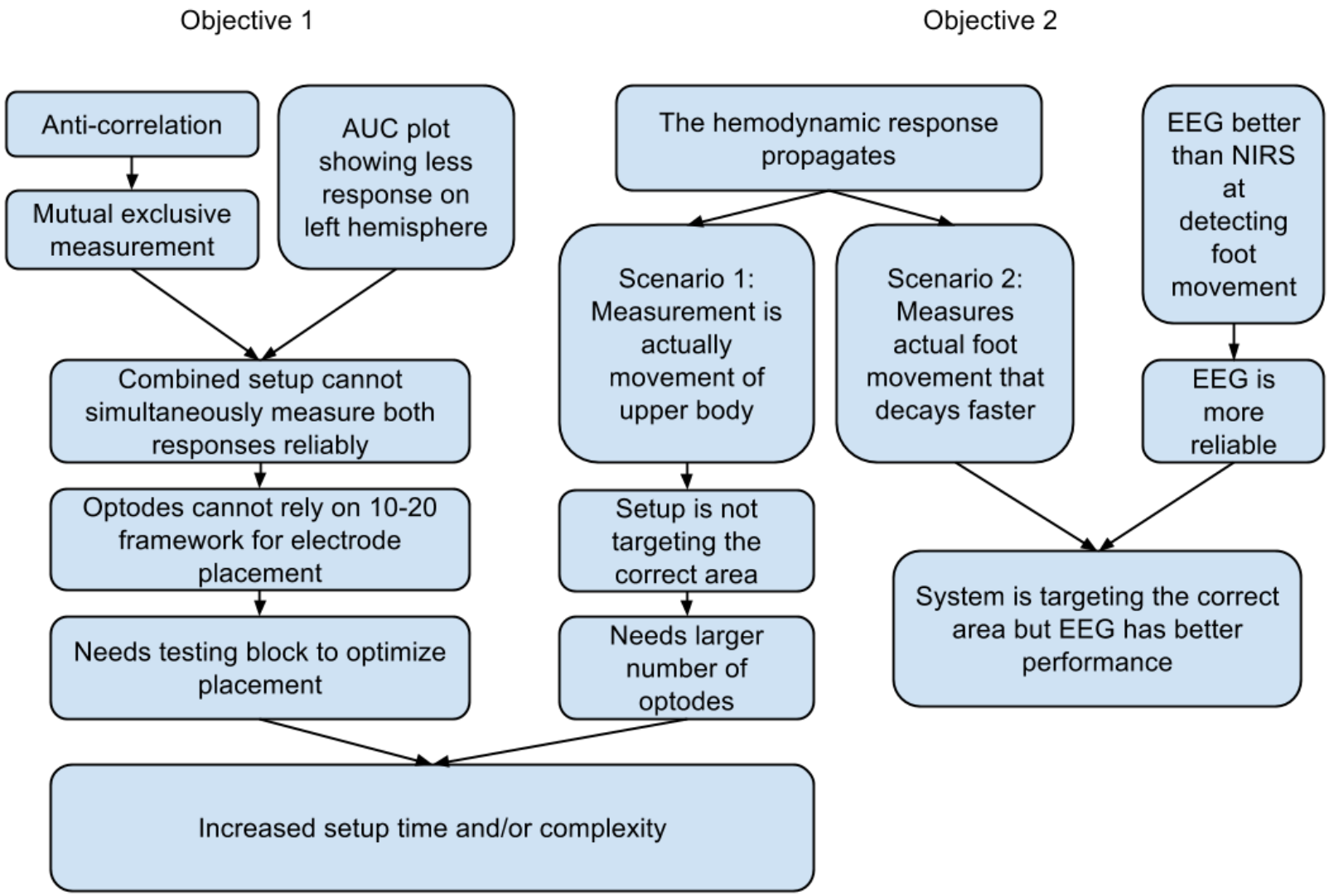

Figure 5.1: Deductions made from observations in objectives 1 and 2.

Bibliography

[1] R. D. Miller and M. C. Pardo, eds. *Basics of Anesthesia, 6th Edn.* Elsevier Inc., USA, 2011.

[2] C. Langton Hewer. 'The Stages And Signs of Genral Anaesthesia'. In: *The British Medical Journal* 2 (1937), pp. 274–276. DOI: 10.1136/bmj.2.3996.274.

[3] Peter S. Sebel et al. 'The Incidence of Awareness During Anesthesia: A Multicenter United States Study'. In: *Anesthesia and Analgesia* 99.3 (2004), pp. 833–839. DOI: 10.1213/01.ANE.0000130261.90896.6C. eprint: http://www.anesthesia-analgesia.org/content/99/3/833.full.pdf+html. URL: http://www.anesthesia-analgesia.org/content/99/3/833.abstract.

[4] Mohamed M. Ghoneim et al. 'Awareness During Anesthesia: Risk Factors, Causes and Sequelae: A Review of Reported Cases in the Literature'. In: *Anesthesia and Analgesia* 108.2 (2009), pp. 527–535. DOI: 10.1213/ane.0b013e318193c634. eprint: http://www.anesthesia-analgesia.org/content/108/2/527.full.pdf+html. URL: http://www.anesthesia-analgesia.org/content/108/2/527.abstract.

[5] C. L. Errando et al. 'Awareness with recall during general anaesthesia: a prospective observational evaluation of 4001 patients'. In: *British Journal of Anaesthesia* 101.2 (2008), pp. 178–185. DOI: 10.1093/bja/aen144. eprint: http://bja.oxfordjournals.org/content/101/2/178.full.pdf+html. URL: http://bja.oxfordjournals.org/content/101/2/178.abstract.

[6] Yvonne M. Blokland et al. 'Towards a Novel Monitor of Intraoperative Awareness: Selecting Paradigm Settings for a Movement-Based Brain-Computer Interface'. In: *PLoS ONE* 7.9 (Sept. 2012), e44336. DOI: 10.1371/journal.pone.0044336. URL: http://dx.doi.org/10.1371%2Fjournal.pone.0044336.

[7] George A. Mashour et al. 'Assessment of intraoperative awareness with explicit recall: a comparison of 2 methods.' In: *Anesthesia and analgesia* 116.4 (Apr. 2013), pp. 889–91. ISSN: 1526-7598. DOI: 10.

1213/ANE.0b013e318281e9ad. URL: http://www.ncbi.nlm.nih.gov/pubmed/23460567.

[8] Jackie Andrade and Catherine Deeprose. 'Unconscious memory formation during anaesthesia'. In: *Best Practice & Research Clinical Anaesthesiology* 21.3 (Sept. 2007), pp. 385–401. ISSN: 15216896. DOI: 10.1016/j.bpa.2007.04.006. URL: http://www.sciencedirect.com/science/article/pii/S1521689607000390.

[9] Rolf H. Sandin et al. 'Awareness during anaesthesia: a prospective case study'. In: *The Lancet* 355.9205 (2000), pp. 707 –711. ISSN: 0140-6736. DOI: http://dx.doi.org/10.1016/S0140-6736(99)11010-9. URL: http://www.sciencedirect.com/science/article/pii/S0140673699110109.

[10] J E Osterman et al. 'Awareness under anesthesia and the development of posttraumatic stress disorder.' In: *General hospital psychiatry* 23.4 (2001), pp. 198–204. ISSN: 0163-8343. URL: http://www.ncbi.nlm.nih.gov/pubmed/11543846.

[11] Sally E. Rampersad and Michael F. Mulroy. 'A case of awareness despite an "adequate depth of anesthesia" as indicated by a Bispectral Index monitor.' In: *Anesthesia and analgesia* 100.5 (May 2005), 1363–4, table of contents. ISSN: 0003-2999. DOI: 10.1213/01.ANE.0000148121.84560.8D. URL: http://www.ncbi.nlm.nih.gov/pubmed/15845686.

[12] J. Bruhn, T. W. Bouillon and S. L. Shafer. 'Electromyographic activity falsely elevates the bispectral index.' In: *Anesthesiology* 92.5 (May 2000), pp. 1485–7. ISSN: 0003-3022. URL: http://www.ncbi.nlm.nih.gov/pubmed/10781298.

[13] Michael Avidan et al. 'Anesthesia Awareness and the Bispectral Index'. In: *The New England Journal of Medicine* 358.11 (2008), pp. 1097–1108.

[14] A. Ekman, L. Brudin and R. Sandin. 'A comparison of bispectral index and rapidly extracted auditory evoked potentials index responses to noxious stimulation during sevoflurane anesthesia.' In: *Anesthesia and analgesia* 99.4 (Oct. 2004), pp. 1141–6. ISSN: 0003-2999. DOI: 10.1213/01.ANE.0000130618.99860.48. URL: http://www.ncbi.nlm.nih.gov/pubmed/15385365.

[15] Sascha Kreuer et al. 'A-line, bispectral index, and estimated effect-site concentrations: a prediction of clinical end-points of anesthesia.' In: *Anesthesia and analgesia* 102.4 (Apr. 2006), pp. 1141–6. ISSN: 1526-7598. DOI: 10.1213/01.ane.0000202385.96653.32. URL: http://www.ncbi.nlm.nih.gov/pubmed/16551913.

[16] Sascha Kreuer. 'Comparison of Alaris AEP index and bispectral index during propofol-remifentanil anaesthesia'. In: *British Journal of Anaesthesia* 91.3 (Sept. 2003), pp. 336–340. ISSN: 0007-0912. DOI: 10.1093/bja/aeg189. URL: http://bja.oxfordjournals.org/lookup/doi/10.1093/bja/aeg189.

[17] Stefan von Delius et al. 'Auditory evoked potentials compared with bispectral index for monitoring of midazolam and propofol sedation during colonoscopy.' In: *The American journal of gastroenterology* 104.2 (Feb. 2009), pp. 318–25. ISSN: 1572-0241. DOI: 10.1038/ajg.2008.73. URL: http://www.ncbi.nlm.nih.gov/pubmed/19190608.

[18] Jonathan R. Wolpaw and Elizabeth Winter Wolpaw, eds. *Brain-Computer Interfaces: Principles and Practice*. Oxford University Press, Inc., 2012.

[19] Marcel van Gerven et al. 'The brain-computer interface cycle.' In: *Journal of neural engineering* 6.4 (Aug. 2009), p. 041001. ISSN: 1741-2552. DOI: 10.1088/1741-2560/6/4/041001. URL: http://www.ncbi.nlm.nih.gov/pubmed/19622847.

[20] Gernot R Müller-putz and Gert Pfurtscheller. 'Control of an Electrical Prosthesis With an SSVEP-Based BCI'. In: *IEEE Transactions on Biomedical Engineering* 55.1 (2008), pp. 361–364.

[21] Brice Rebsamen et al. 'Controlling a Wheelchair Indoors Using Thought'. In: *Intelligent Systems, IEEE* 22.2 (2007), pp. 18–24.

[22] Tom Carlson and Jose del R. Millan. 'Brain-Controlled Wheelchairs'. In: *Robotics Automation Magazine, IEEE* 20.1 (2013), pp. 65–73.

[23] L. A. Farwell and E. Donchin. 'Talking off the top of your head: toward a mental prosthesis utilizing event-related brain potentials.' In: *Electroencephalography and clinical neurophysiology* 70.6 (Dec. 1988), pp. 510–23. ISSN: 0013-4694. URL: http://www.ncbi.nlm.nih.gov/pubmed/2461285.

[24] A. Belitski, J. Farquhar and P. Desain. 'P300 audio-visual speller.' In: *Journal of neural engineering* 8.2 (Apr. 2011), p. 025022. ISSN: 1741-2552. DOI: 10.1088/1741-2560/8/2/025022. URL: http://www.ncbi.nlm.nih.gov/pubmed/21436523.

[25] Shirley M. Coyle, Tomás E Ward and Charles M Markham. 'Brain-computer interface using a simplified functional near-infrared spectroscopy system.' In: *Journal of neural engineering* 4.3 (Sept. 2007), pp. 219–26. ISSN: 1741-2560. DOI: 10.1088/1741-2560/4/3/007. URL: http://www.ncbi.nlm.nih.gov/pubmed/17873424.

[26] Jerry J. Shih, Dean J. Krusienski and Jonathan R. Wolpaw. 'Brain-computer interfaces in medicine.' In: *Mayo Clinic proceedings* 87.3 (Mar. 2012), pp. 268–79. ISSN: 1942-5546. DOI: 10.1016/j.mayocp.2011.12.008. URL: http://www.pubmedcentral.nih.gov/articlerender.fcgi?artid=3497935\&tool=pmcentrez\&rendertype=abstract.

[27] Koen Koenraadt. 'Shedding light on corticol control of movement'. PhD thesis. Radboud University,Nijmegen,Holland, 2014.

[28] Yvonne Blokland et al. 'Combined EEG-fNIRS Decoding of Motor Attempt and Imagery for Brain Switch Control: An Offline Study in Patients With Tetraplegia.' In: *IEEE transactions on neural systems and rehabilitation engineering : a publication of the IEEE Engineering in Medicine and Biology Society* 22.2 (Mar. 2014), pp. 222–229. ISSN: 1558-0210. DOI: 10.1109/TNSRE.2013.2292995. URL: http://www.ncbi.nlm.nih.gov/pubmed/24608682.

[29] Rolf B. Saager, Nicole L. Telleri and Andrew J. Berger. 'Two-detector Corrected Near Infrared Spectroscopy (C-NIRS) detects hemodynamic activation responses more robustly than single-detector NIRS.' In: *NeuroImage* 55.4 (Apr. 2011), pp. 1679–85. ISSN: 1095-9572. DOI: 10.1016/j.neuroimage.2011.01.043. URL: http://www.ncbi.nlm.nih.gov/pubmed/21256223.

[30] Christopher M. Bishop, ed. *Pattern Recognition and Machine Learning*. Springer Science+Business Media, LCC, 2006.

[31] Emanuel Donchin and Michael G. H. Coles. 'Is the P300 component a manifestation of context updating?' In: *Behavioral and Brain Sciences* 11 (03 Sept. 1988), pp. 357–374. ISSN: 1469-1825. DOI: 10.1017/S0140525X00058027. URL: http://journals.cambridge.org/article_S0140525X00058027.

[32] Wilder Penfield and Theodor Rasmussen. *The cerebral cortex of man; a clinical study of localization of function*. Oxford, England: Macmillan, 1950.

[33] H. H. Jasper. 'The ten twenty electrode system of the international federation'. In: *Electroencephalography and clinical neurophysiology* 10 (1958), p. 371.

[34] Marco Ferrari and Valentina Quaresima. 'A brief review on the history of human functional near-infrared spectroscopy (fNIRS) development and fields of application'. In: *NeuroImage* 63.2 (2012), pp. 921 –935. ISSN: 1053-8119. DOI: http://dx.doi.org/10.1016/j.neuroimage.2012.03.049. URL: http://www.sciencedirect.com/science/article/pii/S1053811912003308.

[35] Siamac Fazli et al. 'Enhanced performance by a hybrid NIRS-EEG brain computer interface.' In: *NeuroImage* 59.1 (Jan. 2012), pp. 519–29. ISSN: 1095-9572. DOI: 10.1016/j.neuroimage.2011.07.084. URL: http://www.ncbi.nlm.nih.gov/pubmed/21840399.

[36] P. T. Fox and M. E. Raichle. 'Focal physiological uncoupling of cerebral blood flow and oxidative metabolism during somatosensory stimulation in human subjects'. In: *Proceedings of the National Academy of Sciences* 83.4 (1986), pp. 1140–1144. eprint: http://www.pnas.org/content/83/4/1140.full.pdf+html. URL: http://www.pnas.org/content/83/4/1140.abstract.

[37] Stèphane Perrey. 'Non-invasive NIR spectroscopy of human brain function during exercise'. In: *Methods* 45.4 (2008), pp. 289 –299. ISSN: 1046-2023. DOI: http://dx.doi.org/10.1016/j.ymeth.2008.04.005. URL: http://www.sciencedirect.com/science/article/pii/S1046202308000777.

[38] Shirley Coyle et al. 'On the suitability of near-infrared (NIR) systems for next-generation brain–computer interfaces'. In: *Physiological Measurement* 25.4 (Aug. 2004), pp. 815–822. ISSN: 0967-3334. DOI: 10.1088/0967-3334/25/4/003. URL: http://stacks.iop.org/0967-3334/25/i=4/a=003?key=crossref.2b3bec58c1fb74ea68c7e4e57a6ac10d.

[39] Daniel Richard Leff et al. 'Assessment of the cerebral cortex during motor task behaviours in adults: A systematic review of functional near infrared spectroscopy (fNIRS) studies'. In: *NeuroImage* 54.4 (2011), pp. 2922 –2936. ISSN: 1053-8119. DOI: http://dx.doi.org/10.1016/j.neuroimage.2010.10.058. URL: http://www.sciencedirect.com/science/article/pii/S1053811910013510.

[40] Peter Rolfe. 'IN VIVO NEAR-INFRARED SPECTROSCOPY'. In: *Annu. Rev. Biomed. Eng. 2000.* 02 (2000), pp. 715–754.

[41] A. Duncan et al. 'Measurement of cranial optical path length as a function of age using phase resolved near infrared spectroscopy.' In: *Pediatric research* 39.5 (May 1996), pp. 889–94. ISSN: 0031-3998. DOI: 10.1203/00006450-199605000-00025. URL: http://www.ncbi.nlm.nih.gov/pubmed/8726247.

[42] M. Cope and David T. Delpy. 'System for long-term measurement of cerebral blood and tissue oxygenation on newborn infants by near infra-red transillumination'. In: *Med. & Biol. Eng. & Comput.* 26 (1988), pp. 289–294.

[43] Carmen Vidaurre and Benjamin Blankertz. 'Towards a cure for BCI illiteracy.' In: *Brain topography* 23.2 (June 2010), pp. 194–8. ISSN: 1573-6792. DOI: 10.1007/s10548-009-0121-6. URL: http://www.

pubmedcentral.nih.gov/articlerender.fcgi?artid=2874052\&tool=pmcentrez\&rendertype=abstract.

[44] Tiago Falk et al. 'IMPROVING THE PERFORMANCE OF NIRS-BASED BRAIN-COMPUTER INTERFACES IN THE PRESENCE OF BACKGROUND AUDITORY DISTRACTIONS Institute of Biomaterials and Biomedical Engineering University of Toronto , Toronto , Canada'. In: *IEEE transactions on neural systems and rehabilitation engineering : a publication of the IEEE Engineering in Medicine and Biology Society* (2010), pp. 517–520.

[45] K. L. M. Koenraadt et al. 'Multi-channel NIRS of the primary motor cortex to discriminate hand from foot activity'. In: *Journal of Neural Engineering* 9.4 (Aug. 2012), 046010 (7pp). ISSN: 1741-2552. DOI: 10.1088/1741-2560/9/4/046010. URL: http://www.ncbi.nlm.nih.gov/pubmed/22763344.

[46] Petter Laake and Bjørn R. Olsen. *Forskning i medisin og biofag*. Gyldendal Akademisk, 2008.

[47] MATLAB. *version 7.12.0 (R2011a)*. Natick, Massachusetts: The MathWorks Inc., 2011.

[48] Robert Oostenveld et al. 'FieldTrip: Open source software for advanced analysis of MEG, EEG, and invasive electrophysiological data.' In: *Computational intelligence and neuroscience* 2011 (Jan. 2011), pp. 1–9. ISSN: 1687-5273. DOI: 10.1155/2011/156869. URL: http://www.pubmedcentral.nih.gov/articlerender.fcgi?artid=3021840\&tool=pmcentrez\&rendertype=abstract.

[49] David H. Brainard. 'The Psychophysics Toolbox'. In: *Spatial Vision* 10.4 (1997), pp. 433–436. URL: http://booksandjournals.brillonline.com/content/journals/10.1163/156856897x00357.

[50] Denis G. Pelli. 'The VideoToolbox software for visual psychophysics: transforming numbers into movies'. In: *Spatial Vision* 10.4 (1997), pp. 437–442. URL: http://booksandjournals.brillonline.com/content/journals/10.1163/156856897x00366.

[51] Mario Kleiner et al. 'What's new in Psychtoolbox-3'. In: *Perception* 36.14 (2007), pp. 1–1.

[52] Janez Demsar. 'Statistical Comparisons of Classifiers over Multiple Data Sets'. In: *Journal of Machine Learning Research* 7 (2006), pp. 1–30.

[53] Sameer A. Sheth et al. 'Spatiotemporal evolution of functional hemodynamic changes and their relationship to neuronal activity.' In: *Journal of cerebral blood flow and metabolism : official journal of the International Society of Cerebral Blood Flow and Metabolism* 25.7 (July 2005), pp. 830–841. ISSN: 0271-678X. DOI: 10.1038/sj.jcbfm.9600091. URL: http://www.ncbi.nlm.nih.gov/pubmed/15744249.

[54] Brenda R. Chen et al. 'High-speed vascular dynamics of the hemodynamic response'. In: *NeuroImage* 54.2 (Jan. 2011), pp. 1021–1030. ISSN: 1095-9572. DOI: 10.1016/j.neuroimage.2010.09.036. URL: http://www.pubmedcentral.nih.gov/articlerender.fcgi?artid=3018836\&tool=pmcentrez\&rendertype=abstract.

Appendices

Appendix A

Declaration of Conformity for Oxymon MKIII

Artinis Medical Systems B.V.

Declaration of Conformity

CE Marking

We, Artinis Medical Systems b.v.
St. Walburg 4, 6671 AS Zetten, Nederland

declare under our sole responsibility that the product: *Oxymon MKIII*
to which this declaration relates is in conformity with the following harmonised standards:

Directives:	LVD 73/23/EEC EMC 89/336/EEC
Product Safety Standard:	EN61010-1:1993/A2:1995
Laser Safety Standard:	EN60825-1:1994
EMC Susceptibility Standard:	EN50082-1
EMC Emissions Standard:	EN50081-2, EN55011 Class A Conducted emissions EN500081-2, EN55011 Class B Radiated emissions

The Oxymon MKIII is to be used as investigational tool only.

R.van der Burght
General manager

Place Zetten

Date: August 23, 2007

Artinis Medical Systems B.V.
St Walburg 4, 6671 AS Zetten, The Netherlands
Tel: +31 (0)488 422 710, **Fax:** +31 (0)488 422 829
Bank account ABN-AMRO 62.54.45.651
Chamber of commerce Arnhem 09127900 0000
http://www.artinis.com

Appendix B

Oxymon MKIII information leaflet

OXYMON *Mk III*

Optical Imaging made easy and affordable

Introduction

All cells in all organs of the body have a constant but variable need for oxygen. However the body stores for oxygen are minimal. So a constant and adequate supply of oxygen to the tissues through the circulation is essential. In critical situations therefore monitoring a subject's local tissue oxygenation can be of life-saving value. This information can be obtained with the Oxymon which utilizes the technique of near infrared spectroscopy.

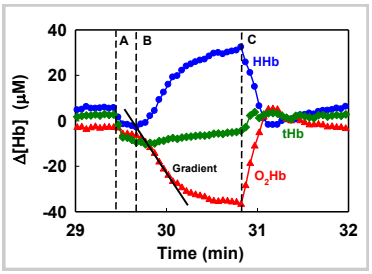

Example of measurement on muscle, where an exercise period (A) is followed by an occlusion (B-C) from which the local oxygen consumption (mVO_2) is determined from the gradient of the oxyhemoglobin (O_2Hb) signal.

Applications

Main applications are found while monitoring brain and/ or muscle tissue:

- Researching patients in the operating theatre or in intensive care units where the oxygen supply to the brain might become critical.
- Neonatal research.
- Researching a hampered blood supply to the limbs, e.g. as seen in peripheral vascular disease.
- Monitoring of regional muscle oxygenation in sports medicine or during rehabilitation training.
- Measuring regional flow, volume and saturation.
- Functional brain monitoring, e.g. measuring the response of brain oxygenation to a sensory stimulus.
- Fast optical signal.

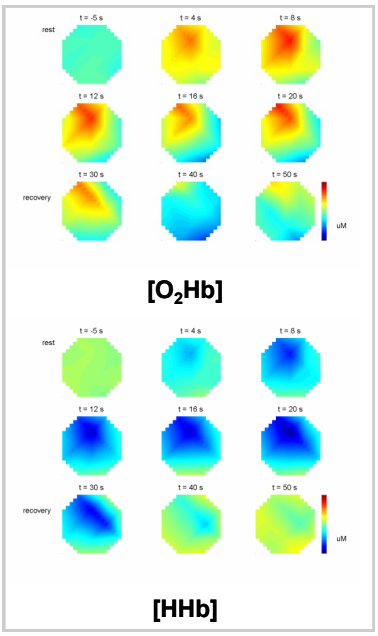

Example of a functional NIRS tracing using a 12 channel setup. The optodes are placed over the left motor cortex, while the subject performs a finger tapping task with his right hand during 20 seconds, starting at t = 0 s. An increase in blood flow is observed over the motor cortex.

Principle

Near infrared spectroscopy (NIRS), the technique on which the Oxymon is based, relies mainly on two characteristics of human tissue. Firstly, the relative transparency of tissue for light in the NIR range, and secondly to the oxygenation dependent absorbance of hemoglobin. Using the Oxymon, being based on this principle, it becomes possible to monitor your subject:

- Non-invasively.
- Easily transportable, bedside measurements.
- With continuous recording and feedback.
- Without the need of a special infrastructure.
- Without specially trained personnel.
- Affordable and no disposables needed.

Company Information

ARTINIS MEDICAL SYSTEMS BV
Einsteinweg 17
6662 PW Elst
The Netherlands

Tel: +31 481 350980
Fax: +31 481 350269
Mail: askforinfo@artinis.com

artinis
medical systems

The Oxymon is a scientifically sound and user friendly instrument. The Oxymon is designed as a plug-and-play instrument. This means that you can start with one or two channels, and gradually extend the number of channels according to your needs. Data collected with the superior analysis software, Oxysoft, included with the Oxymon are stored on a separate PC, easily accessible for analysis, backup and export. Important are the options for customized hardware and software, like NMR compatible probes and fast sampling. Furthermore we can offer superior user support.

Multi Channel Oxymon Mk III system

Technical specifications

Technology	Continuous wave near infrared spectroscopy using modified Lambert-Beer Law
Measures	Changes in oxy- and deoxyhemoglobin and optionally regional tissue saturation index (TSI) using spatially resolved spectroscopy
Operating system	Windows XP, Vista or 7, with at least USB 1.1
Channels	Between 1 and 96, depending on configuration and splitting of fibers. Maximum configuration is 2 x 4 cabinets with 8 transmitter/8 receiver. Minimum is one cabinet with one transmitter/one receiver
Light source	Temperature stabilized pulsed laser sources (Class I according to IEC- 60825-1, safety of lasers)
Wavelengths	Standard nominal 765 and 855 nm, others possible
Detector(s)	Temperature stabilized and cooled avalanche photo diode with ambient light protection
Sampling time	From 0.1 Hz to 50 Hz (up to 250 Hz optional)
Noise	~0.001 standard deviation in optical density at a total of ~6 optical densities at 10Hz measurement frequency
Storage	Real-time, unlimited data storage
External inputs	Optional are 8 additional analog data inputs at 50 Hz (up to 250 Hz optional), +/- 4 Volt
Optode fibers	Standard 3 meter, lengths up to 10 meter available
Optode holders	Standard with multiple distances for muscle or head, multi-channel generally customer specific
Optode distance	Depending on application. Frontal head with brain device up to 6 cm possible with arterial pulsation still visible. For fNIRS 3 - 4 cm is recommended.
Upgrades	The instrument can easily be upgraded
Power	Auto sensing 110-240V, approx. 40 Watt
Dimensions	Weight 7 to 8 kg, WxDxH: 37x30x9 cm
Environment	Operating temp. ~10-27 ºC, both source and detector temperature stabilized, altitude 0-5750 m
Interference	With NMR compatible fibers the instrument can be used inside the MRI. EEG/ECG does not interfere the optical signal

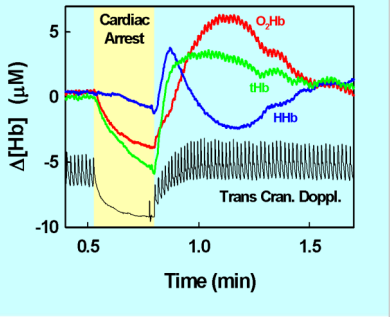

Simultaneous NIRS and trans cranial Doppler registration of a patient during an elective cardiac arrest. Optodes were placed on the frontal side of the head, with a distance of 5.5 cm.

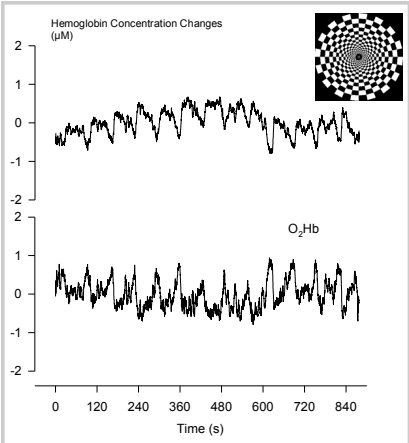

This is an unfiltered tracing of the oxygenation changes in the left visual cortex of one subject, while watching 13 blocks of a flickering checkerboard on a computer screen (see inlet in right upper corner). Each block lasts 20 seconds.

References

>> Mehagnoul-Schipper DJ, van der Kallen B, Colier WNJM et. al. Simultaneous measurements of cerebral oxygenation changes during brain activation by NIRS and fMRI in healthy young and elderly subjects. *Human Brain Mapping* 2002. 16: 14-23.

>> Colier WNJM, Quaresima V, Wenzel R, van der Sluijs MC, Oeseburg B, Ferrari M, Villringer A. Hemodynamic changes detected simultaneously in both occipital areas by functional near infrared spectroscopy. *Vision Res.* 2001; 41:97-102.

>> Colier WNJM, Binkhorst RA, Hopman MT and Oeseburg B. Cerebral and circulatory haemodynamics before vasovagal syncope induced by orthostatic stress. *Clin Physiol.* 1997; 17(1): 83-94.

>> van Beekvelt MC, Colier WNJM, Wevers RA, van Engelen B. Performance of near-infrared spectroscopy in measuring local oxygen consumption and blood flow in skeletal muscle. *J Appl Physiol* 2001. 90: 511-519.

>> van Beekvelt MC, van Engelen BG, Wevers RA, Colier WNJM. Quantitative near-infrared spectroscopy discriminates between mitochondrial myopathies and normal muscle. *Ann Neurol.* 1999;46:667 -70.

>> Quaresima V, Colier WNJM, van der Sluijs M, Ferrari M. Nonuniform quadriceps O2 consumption revealed by multipoint measurements. *Biochem Biophys Res Comm* 2001; 285(4): 1034-39.

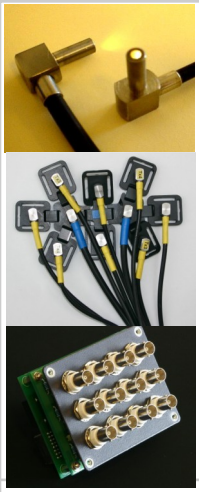

Being a small flexible company with more than 16 years of experience in near infrared spectroscopy we are aware of the special needs of scientists. Custom made additions to the Oxymon, or support with setting up your research can all be arranged.

Rev 1104

artinis

Appendix C

WMA Declaration of Helsinki - Ethical Principles for Medical Research Involving Human Subjects

C.1 INTRODUCTION

1. The World Medical Association (WMA) has developed the Declaration of Helsinki as a statement of ethical principles for medical research involving human subjects, including research on identifiable human material and data. The Declaration is intended to be read as a whole and each of its constituent paragraphs should not be applied without consideration of all other relevant paragraphs.

2. Although the Declaration is addressed primarily to physicians, the WMA encourages other participants in medical research involving human subjects to adopt these principles.

3. It is the duty of the physician to promote and safeguard the health of patients, including those who are involved in medical research. The physician's knowledge and conscience are dedicated to the fulfilment of this duty.

4. The Declaration of Geneva of the WMA binds the physician with the words, "The health of my patient will be my first consideration", and the International Code of Medical Ethics declares that, "A physician shall act in the patient's best interest when providing medical care."

5. Medical progress is based on research that ultimately must include studies involving human subjects. Populations that are underrepresented in medical research should be provided appropriate access to participation in research.

6. In medical research involving human subjects, the well-being of the individual research subject must take precedence over all other interests.

7. The primary purpose of medical research involving human subjects is to understand the causes, development and effects of diseases and improve preventive, diagnostic and therapeutic interventions (methods, procedures and treatments). Even the best current interventions must be evaluated continually through research for their safety, effectiveness, efficiency, accessibility and quality.

8. In medical practice and in medical research, most interventions involve risks and burdens.

9. Medical research is subject to ethical standards that promote respect for all human subjects and protect their health and rights. Some research populations are particularly vulnerable and need special protection. These include those who cannot give or refuse consent for themselves and those who may be vulnerable to coercion or undue influence.

10. Physicians should consider the ethical, legal and regulatory norms and standards for research involving human subjects in their own countries as well as applicable international norms and standards. No national or international ethical, legal or regulatory requirement should reduce or eliminate any of the protections for research subjects set forth in this Declaration.

C.2 PRINCIPLES FOR ALL MEDICAL RESEARCH

11. It is the duty of physicians who participate in medical research to protect the life, health, dignity, integrity, right to self-determination, privacy, and confidentiality of personal information of research subjects.

12. Medical research involving human subjects must conform to generally accepted scientific principles, be based on a thorough knowledge of the scientific literature, other relevant sources of information, and adequate laboratory and, as appropriate, animal experimentation. The welfare of animals used for research must be respected.

13. Appropriate caution must be exercised in the conduct of medical research that may harm the environment.

14. The design and performance of each research study involving human subjects must be clearly described in a research protocol. The protocol should contain a statement of the ethical considerations involved and should indicate how the principles in this Declaration have been addressed. The protocol should include information regarding funding, sponsors, institutional affiliations, other potential conflicts of interest, incentives for subjects and provisions for treating and/or compensating subjects who are harmed as a consequence of participation in the research study. The protocol should describe arrangements for post-study access by study subjects to interventions identified as beneficial in the study or access to other appropriate care or benefits.

15. The research protocol must be submitted for consideration, comment, guidance and approval to a research ethics committee before the study begins. This committee must be independent of the researcher, the sponsor and any other undue influence. It must take into consideration the laws and regulations of the country or countries in which the research is to be performed as well as applicable international norms and standards but these must not be allowed to reduce or eliminate any of the protections for research subjects set forth in this Declaration. The committee must have the right to monitor ongoing studies. The researcher must provide monitoring information to the committee, especially information about any serious adverse events. No change to the protocol may be made without consideration and approval by the committee.

16. Medical research involving human subjects must be conducted only by individuals with the appropriate scientific training and qualifications. Research on patients or healthy volunteers requires the supervision of a competent and appropriately qualified physician or other health care professional. The responsibility for the protection of research subjects must always rest with the physician or other health care professional and never the research subjects, even though they have given consent.

17. Medical research involving a disadvantaged or vulnerable population or community is only justified if the research is responsive to the health needs and priorities of this population or community and if there is a reasonable likelihood that this population or community stands to benefit from the results of the research.

18. Every medical research study involving human subjects must be preceded by careful assessment of predictable risks and burdens to the individuals and communities involved in the research in comparison with foreseeable benefits to them and to other individuals or

communities affected by the condition under investigation.

19. Every clinical trial must be registered in a publicly accessible database before recruitment of the first subject.

20. Physicians may not participate in a research study involving human subjects unless they are confident that the risks involved have been adequately assessed and can be satisfactorily managed. Physicians must immediately stop a study when the risks are found to outweigh the potential benefits or when there is conclusive proof of positive and beneficial results.

21. Medical research involving human subjects may only be conducted if the importance of the objective outweighs the inherent risks and burdens to the research subjects.

22. Participation by competent individuals as subjects in medical research must be voluntary. Although it may be appropriate to consult family members or community leaders, no competent individual may be enrolled in a research study unless he or she freely agrees.

23. Every precaution must be taken to protect the privacy of research subjects and the confidentiality of their personal information and to minimize the impact of the study on their physical, mental and social integrity.

24. In medical research involving competent human subjects, each potential subject must be adequately informed of the aims, methods, sources of funding, any possible conflicts of interest, institutional affiliations of the researcher, the anticipated benefits and potential risks of the study and the discomfort it may entail, and any other relevant aspects of the study. The potential subject must be informed of the right to refuse to participate in the study or to withdraw consent to participate at any time without reprisal. Special attention should be given to the specific information needs of individual potential subjects as well as to the methods used to deliver the information. After ensuring that the potential subject has understood the information, the physician or another appropriately qualified individual must then seek the potential subject's freely-given informed consent, preferably in writing. If the consent cannot be expressed in writing, the non-written consent must be formally documented and witnessed.

25. For medical research using identifiable human material or data, physicians must normally seek consent for the collection, analysis, storage and/or reuse. There may be situations where consent would be impossible or impractical to obtain for such research or would

pose a threat to the validity of the research. In such situations the research may be done only after consideration and approval of a research ethics committee.

26. When seeking informed consent for participation in a research study the physician should be particularly cautious if the potential subject is in a dependent relationship with the physician or may consent under duress. In such situations the informed consent should be sought by an appropriately qualified individual who is completely independent of this relationship.

27. For a potential research subject who is incompetent, the physician must seek informed consent from the legally authorized representative. These individuals must not be included in a research study that has no likelihood of benefit for them unless it is intended to promote the health of the population represented by the potential subject, the research cannot instead be performed with competent persons, and the research entails only minimal risk and minimal burden.

28. When a potential research subject who is deemed incompetent is able to give assent to decisions about participation in research, the physician must seek that assent in addition to the consent of the legally authorized representative. The potential subject's dissent should be respected.

29. Research involving subjects who are physically or mentally incapable of giving consent, for example, unconscious patients, may be done only if the physical or mental condition that prevents giving informed consent is a necessary characteristic of the research population. In such circumstances the physician should seek informed consent from the legally authorized representative. If no such representative is available and if the research cannot be delayed, the study may proceed without informed consent provided that the specific reasons for involving subjects with a condition that renders them unable to give informed consent have been stated in the research protocol and the study has been approved by a research ethics committee. Consent to remain in the research should be obtained as soon as possible from the subject or a legally authorized representative.

30. Authors, editors and publishers all have ethical obligations with regard to the publication of the results of research. Authors have a duty to make publicly available the results of their research on human subjects and are accountable for the completeness and accuracy of their reports. They should adhere to accepted guidelines for ethical reporting. Negative and inconclusive as well as positive results should be published or otherwise made publicly available.

Sources of funding, institutional affiliations and conflicts of interest should be declared in the publication. Reports of research not in accordance with the principles of this Declaration should not be accepted for publication.

C.3 ADDITIONAL PRINCIPLES FOR MEDICAL RESEARCH COMBINED WITH MEDICAL CARE

31. The physician may combine medical research with medical care only to the extent that the research is justified by its potential preventive, diagnostic or therapeutic value and if the physician has good reason to believe that participation in the research study will not adversely affect the health of the patients who serve as research subjects.

32. The benefits, risks, burdens and effectiveness of a new intervention must be tested against those of the best current proven intervention, except in the following circumstances:

    The use of placebo, or no treatment, is acceptable in studies where no current proven intervention exists; or

    Where for compelling and scientifically sound methodological reasons the use of placebo is necessary to determine the efficacy or safety of an intervention and the patients who receive placebo or no treatment will not be subject to any risk of serious or irreversible harm. Extreme care must be taken to avoid abuse of this option.

33. At the conclusion of the study, patients entered into the study are entitled to be informed about the outcome of the study and to share any benefits that result from it, for example, access to interventions identified as beneficial in the study or to other appropriate care or benefits.

34. The physician must fully inform the patient which aspects of the care are related to the research. The refusal of a patient to participate in a study or the patient's decision to withdraw from the study must never interfere with the patient-physician relationship.

35. In the treatment of a patient, where proven interventions do not exist or have been ineffective, the physician, after seeking expert advice, with informed consent from the patient or a legally authorized representative, may use an unproven intervention if in the physician's judgement it offers hope of saving life, re-establishing health or alleviating suffering. Where possible, this

intervention should be made the object of research, designed to evaluate its safety and efficacy. In all cases, new information should be recorded and, where appropriate, made publicly available.

Appendix D

Informed consent form and fact sheet

Donders Institute
for Brain, Cognition and Behaviour

Donders Centre for Cognition

STUDY-SPECIFIC INFORMED CONSENT FORM
For participation in:*

☐ Behavioural ☐ EEG ☐ Sled ☐ Robot

***tick the applicable box(es)**

To be filled out by the PARTICIPANT prior to the start of the experiment:

I confirm that:

- I was satisfactorily informed about the study both verbally and in writing, by means of the general information brochure and additional study specific information brochure(s) (versions 1.6, November 2013), as well as about the study itself by the researcher concerned.
- I have had the opportunity to put forward questions regarding the study and that these questions have been answered satisfactorily
- I have carefully considered my participation in the experiment.
- I participate of my own free will.

I agree that:

- My data will be acquired and stored for scientific purposes as mentioned in the general information brochure.
- My experimental and coded data will be shared with others for strict scientific reasons
- I will be informed by a designated expert about any information which is of clinical relevance to me

I understand that:

- I have the right to withdraw from the experiment at any time without having to give a reason.
- My privacy is protected according to Dutch law.
- My consent will be sought every time I participate in a new experiment.

I give my consent to take part in this experiment:

Name:……. Date of birth:……..... (dd/mm/yy)

Signature:.....Date and place:……...

To be filled out by the RESEARCHER prior to the start of the experiment:
The undersigned declares that the person named above has been informed both in writing and in person about the experiment. He /she guarantees subjects' privacy protection according to Dutch law.

Name:……..PI group:……

Name experiment:……..

Signature:..... ……..Date and place:……

Donders Institute
for Brain, Cognition and Behaviour

Donders Centre for Cognition

SCREENING FORM *
Version 1.6

To be filled out by the PARTICIPANT prior to the start of the experiment

	Please answer the following questions first	**Yes**	**No**
-	Do you suffer from a neurological or psychiatric disease?		
-	Do you take psychoactive medication/substances such as antidepressants, antiepileptics,antipsychotics or hard drugs?		
-	Are you pregnant or do you think you are?		
-	Do you suffer from claustrophobia?		
-	Are you younger than 18 years?		

If you answered "Yes" to one of the above questions, you may not be able to participate in the experiment.

Name:

Date of birth:

Signature: Date:

** This form is only to be used for research with people of 18 years or older, who are of sound mind and judgement. The person involved has to give his or her consent personally.*

P.T.O

SCREENING FORM
Version 1.6

To be filled out completely by the RESEARCHER after the experiment

Name : PI group :

Experiment name:

Reported incidental findings:

Incidental findings YES/ NO

If YES, please describe:

Reported adverse events:

Adverse Events YES/ NO

If YES, please describe:

Participation in science experiment

“fNIRS as an alternative to EEG in detection of intra-operative awareness”

Fact sheet

What the study entails

A cap with several sensors imbedded will be placed on your head, these sensors will measure the oxygen consumption and electrical signals in parts of your brain as the experiment goes on. You will be asked to sit in a chair and follow instruction that will be given on a monitor in front of you. After each block and sequence you will get a short break to adjust your position, drink water, etc. The whole experiment consists of three parts and is detailed below.

Part one, cap fitting

- The first part is to set up the experiment and ensure that the signals are as strong and clear as possible.
- This may take up to 30 minutes.

Part two, movement experiment

- This part is a movement based experiment where your task is to either tap your fingers, tap your feet or sit relaxed and do nothing during a cue on the screen.
- This part consists of six sequences of seven trials each, after each sequence you will be given time to get ready for the next, have a drink of water, etc.
- This part will take about 40 minutes

Part three, online feedback

- After the experiment there is a online feedback part where you get to control a simple computer game. The mission in this game is tap your fingers or feet during a cue and light up four circles in a row.

Possible advantages and disadvantages

The advantage for you is to partake in new science that may prevent patients from being awake and paralyzed during surgery, and thereby help to prevent possible psychological harm to people. There is no expected risk in participating, the equipment that is used is safe for use on human subjects and the experiment does not entail any discomfort. The collected data will be saved to a safe location and will be anonymized so that it can not be traced back to you and thereby not pose any risk to your integrity.

What happens to the collected data and information?

The data and information about you will only be used as described in this fact sheet. All data and information will be processed without the use of your name, personal number or other identifiable information.

Voluntary participation

Your participation is completely voluntary. You may at any time, and without any obligation to give a reason, withdraw from the experiment. Withdrawal from the experiment will have no consequence for you. If you wish to partake you must give your informed consent by signing the agreement form on the next page. If you have signed this form and later wish to withdraw your consent, you may do so without any consequence. If you have any questions or wish to withdraw contact Magnus Reinsfelt Krogh at mlkrogh (at) student.matnat.uio.no

Criteria for participation

The participant:

- has to be between 18 and 60 years of age.
- has to have normal health, hearing and vision. Corrected vision is permitted.
- has to be willing to perform the tasks mentioned above.
- has to be willing to give his/her informed consent.
- can not have or have had neurological damage or disease that may propose a risk to the result or to the participant.

Information about the results of this study

You as a participant have the right to get information about the results and outcome of this study. Since this study is part of a master thesis the results will be made publicly available when the thesis is graded. Barring any unforeseen incidents that may delay this thesis it will be made available at duo.uio.no fall 2014.

Appendix E

MATLAB scripts and functions written by the author

E.1 Oxymon to Field Trip script

```
function []=buffer_nirs(host,port,varargin);
% feed data from Artinis Oxymon to fieldtrip buffer
% Magnus Krogh
% based on signal proxy script developed at Donders Inst.
%
% []=buffer_nirs(host,port,varargin);
%
% Inputs:
%  host - [str] hostname on which the buffer server is running (localhost)
%  port - [int] port number on which to contact the server     (1972)
% Options:
%  fsample - [int] data sample rate                            (250)
%  nCh     - [int] number of channels                           (24)
%  blockSize- [int] number of samples to send at a time to buffer (1)
%  Cnames   - {str} cell array of strings with the channel names in ([])
%               if empty, channel names are 'rand01', 'rand02', etc
%  stimEventRate - [int] rate in samples at which stimulated 'stimulus'  (100)
%                   events are generated
%  queueEventRate - [int] rate (in samples) at which simulated 'queue'   (500)
%                   events are generated
%  keyboardEvents - [bool] do we listen for keyboard events and generate (1)
%                   'keyboard' events from them?
%  verb           - [int] verbosity level.  If <0 then rate in samples to print
status info (0)
if ( nargin<2 || isempty(port) ) port=1972; end;
if ( nargin<1 || isempty(host) ) host='localhost'; end;
mdir=fileparts(mfilename('fullpath'));
addpath(fullfile(mdir,'buffer'));

opts=struct('fsample',250,'nCh',24,'blockSize',1,'Cnames',[],'stimEventRate',0,
'queueEventRate',0,'keyboardEvents',false,'verb',0);
opts=parseOpts(opts,varargin);
if ( isempty(opts.Cnames) )
  opts.Cnames={'AD1' 'AD2' 'AD3' 'AD4' 'AD5' 'AD6' 'AD7' 'AD8' 'OD1' 'OD2' 'OD3'
  'OD4' 'OD5' 'OD6' 'OD7' 'OD8' 'OD9' 'OD10' 'OD11' 'OD12' 'OD13' 'OD14' 'OD15'
  'OD16'};
  for i=numel(opts.Cnames)+1:opts.nCh; opts.Cnames{i}=sprintf('rand%02d',i); end;
end

% N.B. from ft_fuffer/src/message.h: double -> ft type ID 10
hdr=struct('fsample',opts.fsample,'channel_names',{opts.Cnames},'nchans',opts.nCh,
'nsamples',0,'nsamplespre',0,'ntrials',1,'nevents',0,'data_type',10);
buffer('put_hdr',hdr,host,port);
dat=struct('nchans',hdr.nchans,'nsamples',opts.blockSize,'data_type',hdr.data_type,
'buf',[]);
simevt=struct('type','stimulus','value',0,'sample',[],'offset',0,'duration',0);
keyevt=struct('type','keyboard','value',0,'sample',[],'offset',0,'duration',0);
fsample =opts.fsample;
blockSize=opts.blockSize;
```

```
nsamp=0; nblk=0; nevents=0;
tic;stopwatch=toc;
% key listener
if ( opts.keyboardEvents )
  figure(1);set(gcf,'name','Press key here to generate events','menubar','none',
  'toolbar','none');
  set(gcf,'keypressfcn',@keyListener);
end


%open tmp file
[filen,path]=uigetfile('*.oxy3.tmp','Select .oxy3.tmp file');
fid=fopen(fullfile(path,filen),'r+');

clc;
fread(fid,4); %get rid of header
while( true );
  nblk=nblk+1;
  nsamp=nsamp+blockSize;

  loc=ftell(fid); %get current byte location
  fseek(fid,0,1); %move to end of file
  eof=ftell(fid); %save end location
  fseek(fid,loc,-1); %move back to current location

  if((eof-loc)>52)

    %feed one line to buffer
    OD=fread(fid,16,'int16'); %this is the actual OD values
    AD=fread(fid,8,'int16'); %this is the actual AD values
    onS=fread(fid,4); %sample information and events

    dat.buf(1:numel(AD),:)=(-AD/8000)+4.096; %adjust data, scaling factors and
    offset has been calculated
    dat.buf(numel(AD)+1:numel(AD)+numel(OD))=(OD/4000);
    buffer('put_dat',dat,host,port);
    disp(dat.buf(9:14)'); %just to show that it is running
  else
    pause(.002);
  end

  if ( opts.verb~=0 )
    if ( opts.verb>0 || (opts.verb<0 && mod(nblk,ceil(-opts.verb/blockSize))==0) )
      fprintf('%d %d %d %f (blk,samp,event,sec)\r',nblk,nsamp,nevents,toc-stopwatch
      );
    end
  end
  if ( opts.stimEventRate>0 && mod(nblk,ceil(opts.stimEventRate/blockSize))==0 )
      % insert simulated events also
```

```
      nevents=nevents+1;
      simevt.value=ceil(rand(1)*2);simevt.sample=nsamp;
      buffer('put_evt',simevt,host,port);
  end
  if ( opts.queueEventRate>0 && mod(nblk,ceil(opts.queueEventRate/blockSize))==0 )
      % insert simulated events also
      nevents=nevents+1;
      simevt.value=sprintf('queue.%d',ceil(rand(1)*2));
      simevt.sample=nsamp;
      buffer('put_evt',simevt,host,port);
  end
  if ( opts.keyboardEvents )
      h=get(gcf,'userData');
      if ( ~isempty(h) )
          keyevt.value=h; set(gcf,'userData',[]); keyevt.sample=nsamp;
          buffer('put_evt',keyevt,host,port);
          fprintf('\nkey=%s\n',h);
      end
  end
end
return;
function []=keyListener(src,ev)
set(src,'userData',ev.Character);

%-------------
function testCase();
% start buffer server
buffer('tcpserver',struct(),'localhost',1972);
buffer_signalproxy('localhost',1972);
% now try reading data from it...
hdr=buffer('get_hdr',[],'localhost');
dat=buffer('get_dat',[],'localhost');

% generate data without making any events
buffer_signalproxy([],[],'stimEventRate',0,'queueEventRate',0,'verb',-100)
```

E.2 Analysis control script

```
%% Control script for signal processing of EEG and NIRS data
%  Magnus L. R. Krogh
%

%% INITIALIZE PATHS %%%%%%%%%%%%%%%%%%%%%%%%%%%%%%%%%%%%%%%%%%%%%%%%%%%%%%%%
if ( exist('initPaths','file') )
    initPaths;
else
    run ~/buffer_bci/utilities/initPaths;
end
%%

Rx1=1; Rx2=2; Tx1=[1,2]; Tx2=[3,4]; Tx3=[5,6]; Tx4=[7,8];
%% OPTIONS %%%%%%%%%%%%%%%%%%%%%%%%%%%%%%%%%%%%%%%%%%%%%%%%%%%%%%%%%%%%%%%%
names={'all'};                      % names of subjects in the raw data file
types={ 'offl' 'smr' };             % types of analysis

rawdatafile='SsmrData.mat';         % select raw data struct
procdatafile='SProc.mat';           % select file name for processed data


filterband=[.0145 .015 .35 .355];   % band pass filter specs
badChanTresh=1.4;                   % bad channel threshold
badTrTresh=.9;                      % bad trial threshold
trLength=[-10 35];                  % start and end of trial window
baseEvents=7;                       % for removal of the first no movement trial

visual=1;                           % show figures
totalgr=0;                          % plot total grand average
savefig=0;                          % save figures
savedat=1;                          % save data

% save option info for annotating figures
info={strcat('badCh: ',num2str(badChanTresh)) strcat('badTr:',num2str(badTrTresh))
...
    strcat('filt:',num2str(filterband(2)),'-',num2str(filterband(3)))};

%% START %%%%%%%%%%%%%%%%%%%%%%%%%%%%%%%%%%%%%%%%%%%%%%%%%%%%%%%%%%%%%%%%%%
fprintf('Loading data...\n')
load(strcat('~/workspace/analysisData/',rawdatafile));

if(strcmp(names{1},'all')) names=fieldnames(raw); end % loop through all subjects

names([1 2])=[]; %exclude the first two subjects, no EEG data

%loop through types of analysis
for j=1:numel(types)
    type=types{j};
    %loop through subjects
```

```
for i=1:numel(names)
    close all

    clear subject subtraction config data devents state xmlInfo OD
    subject=names{i};
    fprintf('Processing subject %s type %s\n',names{i},type);

    switch type
        case 'offl' % offline NIRS analysis
            config=raw.(subject).bold.info.config;      % extract optode config
            devents=raw.(subject).bold.devents;         % extract event info
            xmlInfo=raw.(subject).xmlInfo;              % extract xml info
            template=raw.(subject).bold.info.template;  % extract optode
            template
            OD=raw.(subject).OD;                        % extract raw data

            mkpreproc;                                  % run analysis script


        case 'smr' % offline EEG analysis

            if (isempty(fieldnames(raw.(subject).(type))))
                fprintf('No smr data, continue to next\n');
                continue
            end

            capFile='cap_tmsi_mk';          % file containing EEG electrode
            location
            thresh=[.0 .1 .2 5];            % bad trial threshold
            badchThresh=1e-4;               % bad channel threshold
            overridechnms=1;                % override channel names

            data=raw.(subject).(type).data;         % extract raw data
            devents=raw.(subject).(type).devents;   % extract event info
            state=raw.(subject).(type).state;       % extract header info

            %remove first no movement trial
            devents(1:7:end)=[];
            data(1:7:end)=[];

            cond=[devents.value];

            %remove baseline data
            for k=1:numel(data)
                data(k).buf(:,1:5*state.hdr.fsample)=[];
            end

            % run analysis of EEG data, hand movement vs no movement
            [C3smrclsfr,C3smrRes]=buffer_train_ersp_clsfr(data(cond==1|cond==3
```

```
                ),...
                    devents(cond==1|cond==3),state.hdr,...
                    'spatialfilter','car','freqband',[6 10 26 30],'badchrm',1,...
                    'badtrrm',1,'objFn','lr_cg','compKernel',0,'dim',3,'capFile',
                    capFile,...
                    'overridechnms',overridechnms,'visualize',visual,'cog',1);

                % run analysis of EEG data, foot movement vs no movement
                [C2smrclsfr,C2smrRes]=buffer_train_ersp_clsfr(data(cond==1|cond==2
                ),...
                    devents(cond==1|cond==2),state.hdr,...
                    'spatialfilter','car','freqband',[6 10 26 30],'badchrm',1,...
                    'badtrrm',1,'objFn','lr_cg','compKernel',0,'dim',3,'capFile',
                    capFile,...
                    'overridechnms',overridechnms,'visualize',visual,'cog',1);

                if(savefig || savedat)
                    mksave;     % save figures and data
                end

        end
         message = sprintf('Click the OK button to continue');
         uiwait(msgbox(message));
    end
end

if(totalgr) totalgrand; end

fprintf('Finished\n');
```

E.3 fNIRS specific analysis script

```
%% Control script for analysing NIRS data
% Magnus L. R. Krogh

clear grand med chanAvg avg procdat c1datC2 c1datC3

% channel names and positions
chNames={'Rx1-Tx1' 'Rx1-Tx2' 'Rx1-Tx3' 'Rx1-Tx4'...
         'Rx2-Tx1' 'Rx2-Tx2' 'Rx2-Tx3' 'Rx2-Tx4'};
chPos=[5 5 7 7 3 3 1 1;3.3 1.1 3.3 1.1 3.3 1.1 3.3 1.1];

%% DATA PROCESSING %%%%%%%%%%%%%%%%%%%%%%%%%%%%%%%%%%%%%%%%%%%%%%%%%%%%%%%%%%%%
fprintf('Processing NIRS data, %d trials ...\n', numel(data));
onl.xmlInfo=xmlInfo;
onl.xmlInfo.nbSamples=25/onl.xmlInfo.SampleTime;
cond=[devents.value];
switch type
    case 'bold' % for processing online data, not used
        [classdat,O2Hb,HHb]=preproc(data,onl.xmlInfo,'template',template,...
        'badChanTresh',badChanTresh,'filterband',filterband);
    case 'offl' % processing offline data
        [classdat,O2Hb,HHb,badCh]=preprocOffl(OD,devents,xmlInfo,'template',...
        template,'badChanTresh',badChanTresh,'filterband',filterband,...
        'trLength',trLength,'baseEv',baseEvents,'seqBase',seqBase);
end
cond(1:baseEvents:end)=[];  % remove first no movement events
chNames(badCh)=[];          % remove bad channel names
chPos(:,badCh)=[];          % remove bad channel position


%% DATA AVERAGING %%%%%%%%%%%%%%%%%%%%%%%%%%%%%%%%%%%%%%%%%%%%%%%%%%%%%%%%%%%%
% average of all channels for each trial (1 x nS x nTr)
avg={mean(O2Hb,1) mean(HHb,1) cond};

% remove bad trials
if(~isempty(badTrTresh))
    fprintf('4. Removing bad trials, ');
    badTr=false(1,numel(cond));

    idO=idOutliers(avg{1},3,badTrTresh);
    badTr=idO;

    avg{1}(:,:,badTr)=[];
    avg{2}(:,:,badTr)=[];
    avg{3}(badTr)=[];
    cond(badTr)=0;
    fprintf('%d trials removed\n',sum(badTr));
end

% calculate median, grand average and channel average
```

```
med=    {median(O2Hb(:,:,~badTr))...
         median(HHb(:,:,~badTr))...
         avg{3}};

grand= {mean(avg{1}(:,:,avg{3}==1),3)... % no movement, O2Hb
         mean(avg{2}(:,:,avg{3}==1),3)... % no movement, HHb
         mean(avg{1}(:,:,avg{3}==2),3)... % foot movement, O2Hb
         mean(avg{2}(:,:,avg{3}==2),3)... % foot movement, HHb
         mean(avg{1}(:,:,avg{3}==3),3)... % hand movement, O2Hb
         mean(avg{2}(:,:,avg{3}==3),3)};  % hand movement, HHb

chanAvgO=cat(3,mean(O2Hb(:,:,avg{3}==1),3),...
               mean(O2Hb(:,:,avg{3}==2),3),...
               mean(O2Hb(:,:,avg{3}==3),3));

chanAvgH=cat(3,mean(HHb(:,:,avg{3}==1),3),...
               mean(HHb(:,:,avg{3}==2),3),...
               mean(HHb(:,:,avg{3}==3),3));

fprintf('5. Training classifier.\n');
st=onl.xmlInfo.SampleTime; % sample time

%% CLASSIFIER TRAINING %%%%%%%%%%%%%%%%%%%%%%%%%%%%%%%%%%%%%%%%%%%%%%%%%%%%%%%%
%% hand movement classifier %%%%%
% concatenate data for classification
cldatC3=cat(3,classdat(:,:,cond==1),classdat(:,:,cond==3));

%cut away pre- and post trial
cldatC3(:,1:(-trLength(1)+3)/st,:)=[];
cldatC3(:,end-((trLength(2)-18)/st)+1:end,:)=[];

%split into 3s segments
cldatC3=reshape(cldatC3,size(cldatC3,1),size(cldatC3,2)/5,size(cldatC3,3)*5);
labels=[-ones(1,sum(cond==1)*5) ones(1,sum(cond==3)*5)];  % class labels

% train classifier
[C3clsfr, C3res]=cvtrainLinearClassifier(cldatC3,labels);

% extract optimal classification
C3clfrate=C3res.tstbin(:,:,C3res.opt.Ci);
fprintf('\n\nClassification rate: %6.2f\n',C3clfrate);


%% foot movement classifier %%%%%%
clear labels
% concatenate data for classification
cldatC2=cat(3,classdat(:,:,cond==1),classdat(:,:,cond==2));

%cut away pre- and post task
```

```
cldatC2(:,1:(-trLength(1)+3)/st,:)=[];
cldatC2(:,end-((trLength(2)-18)/st)+1:end,:)=[];

%split into 3s segments
cldatC2=reshape(cldatC2,size(cldatC2,1),size(cldatC2,2)/5,size(cldatC2,3)*5);
labels=[-ones(1,sum(cond==1)*5) ones(1,sum(cond==2)*5)]; % class labels

% train classifier
[C2clsfr, C2res]=cvtrainLinearClassifier(cldatC2,labels,[],10);

% extract optimal classification
C2clfrate=C2res.tstbin(:,:,C2res.opt.Ci);
fprintf('\n\nClassification rate: %6.2f\n',C2clfrate);


%% PLOTTING
if(visual) mkplot; end

%% SAVING
if(savefig || savedat) mksave; end
```

E.4 fNIRS specific analysis preprocessing function

```
function [unproc,O2Hb,HHb,badCh] = preprocOffl(OD,devents,xmlInfo,varargin)
% Function for processing and analysing NIRS signals
% Magnus L. R. Krogh
%
% Inputs:
%  dat          - (struct) dataset from field trip buffer
%  marks        - (1 x nMarks) sample number markers
%
% Outputs:
%  unproc       - unbaselined data for the classifier
%  O2Hb         - processed oxygenated hemoglobin data
%  HHb          - processed deoxygenated hemoglobin data
%  badCh        - bad channel identification
%
% Options:
%  template     - [subtemplate, Rx, Tx] template used recording NIRS
%  filterband   - [highpass lowpass] filter frequency band ([0.01 0.35])
%  baseline     - (int) seconds of baseline (5)
%  badChanThresh  - [tresh] remove bad channels, no removal if empty
%  trLength     - [start end] length of trial in seconds
%  baseEv       - (int) remove the first trail in each sequence
%  detrend      - (bool) detrend data

Rx1=1; Rx2=2; Tx1=[1,2]; Tx2=[3,4]; Tx3=[5,6]; Tx4=[7,8];

opts=struct('template',...
    [1 Rx1 Tx1;...
    2 Rx1 Tx2;...
    3 Rx1 Tx3;...
    4 Rx1 Tx4;...
    5 Rx2 Tx1;...
    6 Rx2 Tx2;...
    7 Rx2 Tx3;...
    8 Rx2 Tx4],...
    'filterband',[0.0001 0.01 .35 .355],'baseline',5,'badChanTresh',[],...
    'filt',[],'trLength',[-5 20],'baseEv',7,'detrend',1);

% merge input options with default
[opts,varargin]=parseOpts(opts,varargin);
template=opts.template;
filterband=opts.filterband;
baseline=opts.baseline;
badChanTresh=opts.badChanTresh;
trLength=opts.trLength;
baseEv=opts.baseEv;
detr=opts.detrend;

% variables
st=xmlInfo.SampleTime;                          % sample time
```

```
trDur=trLength(2)-trLength(1);                % trial duration
marks=[devents.sample];                       % event markers
baseMarks=marks(1:baseEv:end);                % markers for first trail in each
sequence
marks(1:baseEv:end)=[];;                      % remove first markers in each sequence
nT=numel(marks);                              % number of trials
marks=marks+((trLength(1)+baseline)/st);      % move markers to fit trial duration

% convert optical density to hemoglobin changes
fprintf('1. Converting to hemoglobin changes\n');
for l=1:size(template,1)
    [q,tmpO(l,:),tmpH(l,:)]=single_ch(OD,xmlInfo,1,template(l,2),template(l,3:4));
end

% remove start and end of data stream
tmpO(:,marks(end)+(trDur/st)+2:end)=[];
tmpH(:,marks(end)+(trDur/st)+2:end)=[];

badCh=false(8,1); % set bad channel identification to false

% remove bad channels
if(~isempty(badChanTresh))
    fprintf('2. Removing bad channels, ');
    idO=idOutliers(tmpO,1,badChanTresh); % identify bad channels
    badCh=idO;
    tmpO(badCh,:)=[];
    tmpH(badCh,:)=[];
    fprintf('%d channels removed\n',sum(badCh));
end

% filter data stream
if(~isempty(filterband))
    fs=250;
    len=size(tmpO,2);
    filt=mkFilter(filterband,floor(len/2),fs/len);
    tmpO=fftfilter(tmpO,filt,[],2);
    tmpH=fftfilter(tmpH,filt,[],2);
end

% slice into trials
for i=1:nT
    O2Hb(:,:,i)=tmpO(:,marks(i)+1:marks(i)+trDur/st);
    HHb(:,:,i)=tmpH(:,marks(i)+1:marks(i)+trDur/st);
end

% return unbaselined data for the classifier
unproc=cat(1,O2Hb,HHb);

% detrend data, only if trial window is symmetrical around BOLD response
```

```
if(detr && trDur>44)
    fprintf('3. Detrending\n');
    O2Hb=detrend(O2Hb,2);
    HHb=detrend(HHb,2);
end

%subtract baseline
O2Hb=bsxfun(@minus,O2Hb,mean(O2Hb(:,(-trLength(1)-baseline)/st+1:...
    -trLength(1)/st,:),2));
HHb=bsxfun(@minus,HHb,mean(HHb(:,(-trLength(1)-baseline)/st+1:...
    -trLength(1)/st,:),2));
end
```

E.5 fNIRS CoG analysis script

```
%% Script for calculating and plotting CoG for NIRS
% Magnus L. R. Krogh

% load data
procdatafile='SProc.mat';
load(strcat('~/workspace/analysisData/',procdat));

% variables
trLength=[-10 35];  % length of trial window
st=0.004;           % sampling time
visual=1;           % visualize output

names=fieldnames(mk); % extract subject names (S1, S2, S3 ...)

for i=1:numel(names) % loop through subjects
    clear x y a3H a2H a3O a3H
    subj=names{i};
    chAvgO=mk.(subj).offl.chanAvgO.OHb; % channel average, O2Hb (ch x data x cond)
    chAvgH=mk.(subj).offl.chanAvgO.HHb; % channel average, HHb (ch x data x cond)
    x=mk.(subj).offl.chPos(1,:)';       % channel position
    y=mk.(subj).offl.chPos(2,:)';       % channel position

    % calculate CoG
    a3O=abs(mean(chAvgO(:,-trLength(1)/st:(-trLength(1)+15)/st,3),2));
    a2O=abs(mean(chAvgO(:,-trLength(1)/st:(-trLength(1)+15)/st,2),2));
    a3H=abs(mean(chAvgH(:,-trLength(1)/st:(-trLength(1)+15)/st,3),2));
    a2H=abs(mean(chAvgH(:,-trLength(1)/st:(-trLength(1)+15)/st,2),2));
    cog(:,:,i)=[sum(x.*a3O)/sum(a3O) sum(y.*a3O)/sum(a3O);...   % hand O2Hb
                sum(x.*a3H)/sum(a3H) sum(y.*a3H)/sum(a3H);...   % hand HHb
                sum(x.*a2O)/sum(a2O) sum(y.*a2O)/sum(a2O);...   % foot O2Hb
                sum(x.*a2H)/sum(a2H) sum(y.*a2H)/sum(a2H)];     % foot HHb

    % save CoG
    mk.(subj).offl.cog=cog(:,:,i);
end

%% plot CoG
if(visual)

    cog=mean(cog,3); % average CoG for all subjects

    figure(1);
    suptitle('Center of gravity for hand and foot movement');
    scatter(cog(1,1),cog(1,2),'fill','d','r');
    axis equal;
    axis([-.5 8.5 -.5 5]);
    set(gca,'YTick',[0 1.1 2.2 3.3 4.4]);
    grid on;
    hold on;
```

```
    scatter(cog(2,1),cog(2,2),'fill','d','b');
    hold on;
    scatter(cog(3,1),cog(3,2),'fill','S','r');
    hold on;
    scatter(cog(4,1),cog(4,2),'fill','S','b');
    l=legend('Hand O2','Hand H','Foot O2','Foot H');
    legend(l,'boxoff');
    xlabel('X [cm]');
    ylabel('Y [cm]');


    % visualize optode placement locations
    r=.2;
    px=[0 4 8 0 4 8]; py=[0 0 0 4.4 4.4 4.4];
    hold on;
    rectangle('Position',[2-r 2.2-r r*2 r*2],'Curvature',1,'FaceColor',[0 0 0]);
    hold on;
    rectangle('Position',[6-r 2.2-r r*2 r*2],'Curvature',1,'FaceColor',[0 0 0]);
    text(8,2.2,'CZ','VerticalAlignment','Middle','HorizontalAlignment','Center');
    text(4,2.2,'C3','VerticalAlignment','Middle','HorizontalAlignment','Center');
    for i=1:6
        hold on;
        rectangle('Position',[px(i)-r py(i)-r r*2 r*2],'Curvature',1,...
            'FaceColor',[0.8 0.8 0.8]);
    end
end
```

E.6 BOLD grand average plot script

```
%% Script for plotting total grand average over all subjects, NIRS
% Magnus L. R. Krogh

% load processed data file and run
names=fieldnames(mk);

type='offl';
trLength=[-5 25];
st=0.004;



% load averages
for i=1:numel(names)
    c1.O2Hb(i,:)=mk.(names{i}).(type).grand{1};
    c1.HHb(i,:)=mk.(names{i}).(type).grand{2};
    c2.O2Hb(i,:)=mk.(names{i}).(type).grand{3};
    c2.HHb(i,:)=mk.(names{i}).(type).grand{4};
    c3.O2Hb(i,:)=mk.(names{i}).(type).grand{5};
    c3.HHb(i,:)=mk.(names{i}).(type).grand{6};

    C3clfr(i)=mk.(names{i}).(type).clsfr.C3.clfrate;
    C2clfr(i)=mk.(names{i}).(type).clsfr.C2.clfrate;
end

C3rate=mean(C3clfr);
C2rate=mean(C2clfr);

sD=[(10+trLength(1))/st+1  (10+trLength(2))/st];

% grand average
c1.grand.O2Hb=mean(c1.O2Hb(:,sD(1):sD(2)));
c1.grand.HHb=mean(c1.HHb(:,sD(1):sD(2)));
c2.grand.O2Hb=mean(c2.O2Hb(:,sD(1):sD(2)));
c2.grand.HHb=mean(c2.HHb(:,sD(1):sD(2)));
c3.grand.O2Hb=mean(c3.O2Hb(:,sD(1):sD(2)));
c3.grand.HHb=mean(c3.HHb(:,sD(1):sD(2)));

%% plot
st=0.004;
t=trLength(1)+st:st:trLength(2);
scale=[trLength -.5 .5];

tx=[t,fliplr(t)];


% Margin of error, one standard deviation
c1ErrO2=std(c1.O2Hb(:,sD(1):sD(2)));
c1ErrHb=std(c1.HHb(:,sD(1):sD(2)));
```

```
c2ErrO2=std(c2.O2Hb(:,sD(1):sD(2)));
c2ErrHb=std(c2.HHb(:,sD(1):sD(2)));
c3ErrO2=std(c3.O2Hb(:,sD(1):sD(2)));
c3ErrHb=std(c3.HHb(:,sD(1):sD(2)));

Y1=[c1.grand.O2Hb,fliplr(c1.grand.O2Hb+c1ErrO2)];
Y2=[c2.grand.O2Hb,fliplr(c2.grand.O2Hb+c2ErrO2)];
Y3=[c1.grand.HHb-c1ErrHb,fliplr(c1.grand.HHb)];
Y4=[c2.grand.HHb-c2ErrHb,fliplr(c2.grand.HHb)];
Y5=[c3.grand.O2Hb,fliplr(c3.grand.O2Hb+c3ErrO2)];
Y6=[c3.grand.HHb-c3ErrHb,fliplr(c3.grand.HHb)];

% total grand
str1=strcat('Clfrate: ',num2str(C3rate));
str2=strcat('Clfrate: ',num2str(C2rate));

h8=figure(6);
clf; set(h8, 'PaperUnits','centimeters','PaperPosition', [0 0 21 7]);
subplot(1,3,1);
fill(tx,Y5,'b',tx,Y6,'g');
hold on;
plot(t,c3.grand.O2Hb,'k','LineWidth',2);
hold on;
plot(t,c3.grand.HHb,'k','LineWidth',2);
axis(scale);
title('Hand movement');
xlabel('Time [s]');
ylabel('\Delta chromophore');
yL = get(gca,'YLim');

subplot(1,3,2);
fill(tx,Y2,'b',tx,Y4,'g');
hold on;
plot(t,c2.grand.O2Hb,'k','LineWidth',2);
hold on;
plot(t,c2.grand.HHb,'k','LineWidth',2);
axis(scale);
title('Foot movement');

subplot(1,3,3);
fill(tx,Y1,'b',tx,Y3,'g');
hold on;
plot(t,c1.grand.O2Hb,'k','LineWidth',2);
hold on;
plot(t,c1.grand.HHb,'k','LineWidth',2);
axis(scale);
title('No movement');
```

```
%save
dir='~/workspace/archive/analysis/';
stamp=datestr(clock,'yymmdd-HHMM-');
saveas(h8,strcat(dir,stamp,'S-totGrand'),'png');
```

E.7 Analysis saving script

```
%% Script for saving processed data in directory structure
% Magnus L. R. Krogh

dir=strcat('~/workspace/archive/analysis/'); % directory for saving

% check if directory exists, if not create it
if (exist(dir,'dir')==0)
    fprintf('Creating directory %s\n',dir);
    mkdir(dir);
end

%load save stucture if it exists, if not create it
if(exist(strcat('~/workspace/analysisData/',procdatafile))==2)
    load(strcat('~/workspace/analysisData/',procdatafile));
else
    mk=struct();
    save(strcat('~/workspace/analysisData/',procdatafile),'mk');
end

%% save data to struct
if(savedat)
    switch type
        case 'offl'
            fprintf('Saving to structure\n');
            mk.(subject).(type).grand=grand;
            mk.(subject).(type).median=med;
            mk.(subject).(type).chanAvgO=struct('OHb',chanAvgO,'HHb',chanAvgH);
            mk.(subject).(type).chNames=chNames;
            mk.(subject).(type).chPos=chPos;
            mk.(subject).(type).clsfr.C3=struct('clfrate',C3clfrate,...
                'clsfr',C3clsfr,'res',C3res);
            mk.(subject).(type).clsfr.C2=struct('clfrate',C2clfrate,...
                'clsfr',C2clsfr,'res',C2res);
            save(strcat('~/workspace/analysisData/',procdatafile),'mk','-append');

        case 'smr'
            fprintf('Saving...\n');
            mk.(subject).(type)=struct('capfile',capFile,...
                'thresh',thresh,'badchThresh',badchThresh,'overridechnms',...
                overridechnms,'C2smrclsfr',C2smrclsfr,'C2smrRes',...
                C2smrRes,'C3smrclsfr',C3smrclsfr,'C3smrRes',C3smrRes);
            save(strcat('~/workspace/analysisData/',procdatafile),'mk','-append');
    end
end

%% save figures to archive
if(savefig)
    stamp=datestr(clock,'yymmdd-HHMM-');
    fprintf('Saving figures to: %s \n', dir);
```

```
    switch type
        case 'offl'
            saveas(h1,strcat(dir,stamp,subject,'-grand'),'jpg');
            saveas(h5,strcat(dir,stamp,subject,'-avg'),'jpg');
            saveas(h6,strcat(dir,stamp,subject,'-med'),'jpg');
            saveas(h7,strcat(dir,stamp,subject,'-chan'),'jpg');

        case 'smr'
            h3=figure(1);
            h4=figure(2);
            saveas(h3,strcat(dir,'ERSP',stamp),'fig');
            saveas(h3,strcat(dir,stamp,subject,'-ERSP'),'jpg');
            saveas(h4,strcat(dir,'AUC',stamp),'fig');
            saveas(h4,strcat(dir,stamp,subject,'-AUC'),'jpg');
    end
end
```

E.8 Experiment stimulus script

```
%% Script for visual stimuli and sending events during experiments
% Magnus L. R. Krogh

%% INITIALIZE PATHS
if ( exist('initPaths','file') )
    initPaths;
else
    run ~/buffer_bci/utilities/initPaths;
end
addpath(genpath('~/BCI_code/external_toolboxes/Psychtoolbox/'));
clc;

%% OPEN CONNECTION TO BUFFER
buffhost='localhost';buffport=1973;
global ft_buff; ft_buff=struct('host',buffhost,'port',buffport);
hdr=[];
% wait for the buffer to contain valid data
while ( isempty(hdr) || ~isstruct(hdr) || (hdr.nchans==0) )
    try
        hdr=buffer('get_hdr',[],buffhost,buffport);
    catch
        hdr=[];
        fprintf('Invalid header info... waiting.\n');
    end;
    pause(1);
end;

% set the real-time-clock to use
initgetwTime();
initsleepSec();

%% BLOCK 1 BOLD/SMR  %%%%%%%%%%%%%%%%%%%%%%%%%%%%%%%%%%%%%%%%%%%%%%%%%%%%%%%%%%%%
%% INITIALIZE VARIABLES
nSeq=6;                         % number of sequences
nEpoch=6;                       % number of trials per sequence (+1 no movement)
screen=1;                       % select monitor for visual stimulus, 1-monitor
0-main

nCond=3;                        % number of conditions (hand, foot, no)
cueDuration=15;                 % cue duration (seconds)
epochDuration=1;
baseDuration=5;                 % baseline duration (seconds)
restDuration=[15 20];           % semi-random rest duration between values
startRest=60;                   % initial resting period at start of sequence
stimSeq=zeros(3,nSeq,nEpoch);   % initialize stimulus sequence variable


% psychtoolbox window variables for the visual stimulus
black=0;
```

```
white=255;
grey=150;
red=[255 10 10];

Screen('Preference','SkipSyncTests', 1); % skip syncing since it's not important
[wPtr,wrect]=Screen('OpenWindow', screen, black);    % full screen monitor
Screen(wPtr,'TextFont' ,'Calibri');                  % set font
Screen('TextSize', wPtr, 24);                        % set font size

circle=[wrect(3)/2-20 wrect(4)/2-20 wrect(3)/2+20 wrect(4)/2+20]; % make cirle
line=(.55:.04:1)*wrect(4);      % lines for where the text will appear


%% START VISUAL STIMULUS %%%%%%%%%%%%%%%%%%%%%%%%%%%%%%%%%%%%%%%%%%%%%%%%%%%%%%%%
Screen('FillOval',wPtr,grey,circle);
Screen('DrawText', wPtr, 'Please keep your eyes on the dot during the trials.'...
    ,wrect(3)*0.24 ,line(1) ,white);
Screen('DrawText', wPtr, 'Say when you are ready to start the experiment.'...
    ,wrect(3)*0.24 ,line(2) ,white);
Screen('Flip',wPtr);
%%

waitforbuttonpress;
if(nCond<3)
    %make random stimulus sequence
    stimTemp=zeros(nSeq*nEpoch,1);
    stimSeqFull=mkStimSeqRand(nEpoch*nSeq,(nEpoch+1)*nSeq/nCond);
    for sti=1:(nEpoch+1)*nSeq/nCond
        stimTemp=stimTemp|stimSeqFull(:,sti);
    end
    stimSeq=reshape(stimTemp,nEpoch,nSeq);
else
    for i=1:nEpoch
        stimSeq(:,:,i)=mkStimSeqRand(nCond,nSeq);
    end
end
%%


for si=1:nSeq % loop through sequences
    Screen('FillOval',wPtr,red,circle);
    Screen('DrawText', wPtr, 'Do not move' ,wrect(3)*0.43 ,line(1) ,white);
    Screen('Flip',wPtr);
    sleepSec(15);

    % send event with condition 1 (no movement) to both buffers
    sendEvent('smr.epoch',1);                        % NIRS data buffer
    sendEvent('smr.epoch',1,-1,0,0,buffhost,1972);   % EEG data buffer
```

```
    sleepSec(cueDuration+11); % wait

    for ei=1:nEpoch % loop through trials
        cond=find(stimSeq(:,si,ei)>0);
        fprintf('Seq nr: %d, Trial nr: %d, Stimcode: %d\n', si, ei, cond);

        % send event with random condition to both buffers
        sendEvent('smr.epoch',cond);
        sendEvent('smr.epoch',cond,-1,0,0,buffhost,1972);

        % baseline cue
        Screen('FillOval',wPtr,grey,circle);
        Screen('DrawText', wPtr, 'Do not move' ,wrect(3)*0.425 ,line(1) ,white);
        Screen('Flip',wPtr);
        sleepSec(baseDuration);

        % movement condition cue
        if (cond==3) %movement condition hand
            Screen('FillOval',wPtr,red,circle);
            Screen('DrawText', wPtr, 'Tap your fingers' ,wrect(3)*0.41 ,line(1) ,
            white);
            Screen('Flip',wPtr);
            sleepSec(cueDuration);
            Screen('FillOval',wPtr,grey,circle);
            Screen('DrawText', wPtr, 'Rest' ,wrect(3)*0.475 ,line(1) ,white);
            Screen('Flip',wPtr);
            sleepSec(randi(restDuration,1,1));

        elseif (cond==2) % movement condition feet
            Screen('FillOval',wPtr,red,circle);
            Screen('DrawText', wPtr, 'Move your toes',wrect(3)*0.425,line(1),white);
            Screen('Flip',wPtr);
            sleepSec(cueDuration);
            Screen('FillOval',wPtr,grey,circle);
            Screen('DrawText', wPtr, 'Rest' ,wrect(3)*0.475 ,line(1) ,white);
            Screen('Flip',wPtr);
            sleepSec(randi(restDuration,1,1));

        else % no movement
            Screen('FillOval',wPtr,red,circle);
            Screen('DrawText', wPtr, 'Do not move' ,wrect(3)*0.425 ,line(1) ,white);
            Screen('Flip',wPtr);
            sleepSec(cueDuration);
            Screen('FillOval',wPtr,grey,circle);
            Screen('DrawText', wPtr, 'Rest' ,wrect(3)*0.475 ,line(1) ,white);
            Screen('Flip',wPtr);
            sleepSec(5);
        end
    end
```

```
    if(si<nSeq) % break between sequences
        Screen('FillOval',wPtr,grey,circle);
        Screen('DrawText',wPtr,...
            'Say when you are ready to start the next sequence.',...
            wrect(3)*0.24 ,line(1) ,white);
        Screen('Flip',wPtr);
        waitforbuttonpress;
    end
end

% send event ending data recording
sendEvent('smr.recording', 'end');
sendEvent('smr.recording','end',-1,0,0,buffhost,1972);

Screen('DrawText', wPtr, 'Thank you very much for participating.',...
    wrect(3)*0.2 ,line(5) ,white);
Screen('Flip',wPtr);
waitforbuttonpress;
sca;
```

E.9 Experiment signal processing script

```
%% NIRS signal processing script which saves measured data online
% Magnus L. R. Krogh


%% INITIALIZE PATHS
if ( exist('initPaths','file') )
    initPaths;
else
    run ~/buffer_bci/utilities/initPaths;
end

%% OPEN CONNECTION TO BUFFER
buffhost='localhost';buffport=1973;
global ft_buff; ft_buff=struct('host',buffhost,'port',buffport);
% wait for the buffer to return valid header information
hdr=[];
while ( isempty(hdr) || ~isstruct(hdr) || (hdr.nchans==0) )
    try
        hdr=buffer('get_hdr',[],buffhost,buffport);
    catch
        hdr=[];
        fprintf('Invalid header info... waiting.\n');
    end;
    pause(1);
end;
% set the real-time-clock to use
initgetwTime();
initsleepSec();

%% INITIALIZE SAVE STRUCTURE
if(~exist('subject','var'))
    subject=input('Enter subject name\n','s');
end
fprintf('Starting signal processing script on subject %s\n',subject);
datadir=strcat('~/workspace/data/',subject,'/');

% test if directory exists, if not create it
if(exist(datadir)==0)
    mkdir(datadir);
end

%% VARIABLES
b1_ms=25000;        % duration of recording from each event (ms)
b1name='BOLDdata';  % name of saved data structure
%%

%% BLOCK 1 (BOLD)
fprintf('Start recording block 1 ...\n');
```

```
% data recording function, waits for events to start recording
[b1data,b1devents,b1state]=buffer_waitData(buffhost,buffport,[],'startSet',...
    {'smr.epoch'},'trlen_ms',b1_ms,'exitSet',{'smr.recording' 'end'});

% remove last "end recording" event
mi=matchEvents(b1devents,'smr.recording','end'); b1devents(mi)=[]; b1data(mi)=[];

% save data
fprintf('Saving %d epochs to : %s\n',numel(b1devents),strcat(datadir,b1name));
save(strcat(datadir,b1name),'b1data','b1devents','b1state');
%%
```

```
%% EEG signal processing script which saves measured data online
% Magnus L. R. Krogh


%% INITIALIZE PATHS
if ( exist('initPaths','file') )
    initPaths;
else
    run ~/buffer_bci/utilities/initPaths;
end

%% OPEN CONNECTION TO BUFFER
buffhost='localhost';buffport=1972;
global ft_buff; ft_buff=struct('host',buffhost,'port',buffport);
% wait for the buffer to return valid header information
hdr=[];
while ( isempty(hdr) || ~isstruct(hdr) || (hdr.nchans==0) )
    try
        hdr=buffer('get_hdr',[],buffhost,buffport);
    catch
        hdr=[];
        fprintf('Invalid header info... waiting.\n');
    end;
    pause(1);
end;
% set the real-time-clock to use
initgetwTime();
initsleepSec();

%% INITIALIZE SAVE STRUCTURE
if(~exist('subject','var'))
    subject=input('Enter subject name\n','s');
end
fprintf('Starting signal processing script on subject %s\n',subject);
datadir=strcat('~/workspace/data/',subject,'/');

% test if directory exists, if not create it
if(exist(datadir)==0)
    mkdir(datadir);
end

%% VARIABLES
b1_ms=10000;        % duration of recording from each event (ms)
b1name='SMRdata';   % name of saved data structure
%%

%% BLOCK 1 (smr)
fprintf('Start recording block 1 ...\n');
```

```
% data recording function, waits for events to start recording
[b1data,b1devents,b1state]=buffer_waitData(buffhost,buffport,[],'startSet',...
    {'smr.epoch'},'trlen_ms',b1_ms,'exitSet',{'smr.recording' 'end'});

% remove last "end recording" event
mi=matchEvents(b1devents,'smr.recording','end'); b1devents(mi)=[]; b1data(mi)=[];

% save data
fprintf('Saving %d epochs to : %s\n',numel(b1devents),strcat(datadir,b1name));
save(strcat(datadir,b1name),'b1data','b1devents','b1state');
%%
```

Appendix F

MATLAB scripts and functions developed at Donders Inst.

These scripts and functions are released under the GNU General Public License for open source software by Dr. Jason Farquhar. These tools can be found at `www.github.com/jadref/buffer_bci`.

F.1 Shell script to start buffer

startBuffer.sh

```
#!/bin/bash
buffdir=`dirname $0`
bciroot=~/output
subject='test';
if [ $# -gt 0 ]; then subject=$1; fi
session=`date +%y%m%d`
if [ $# -gt 1 ]; then session=$2; fi
block=`date +%h%m`_$$
if [ $# -gt 2 ]; then block=$2; fi
outdir=$bciroot/$subject/$session/$block/raw_buffer
logfile=$bciroot/$subject/$session/$block.log
echo outdir: $outdir
echo logfile : $logfile
mkdir -p $bciroot/$subject/$session/$block
touch $logfile
if [ `uname -s` == 'Linux' ]; then
   buffexe=$buffdir'/buffer/bin/saving_buffer_glx32';
   if [ -r $buffdir/recording ]; then
    buffexe=$buffdir'/recording';
   fi
   if [ -r $buffdir/buffer/bin/glnx86/recording ]; then
     buffexe=$buffdir'/buffer/bin/glnx86/recording';
   fi
   if [ -r $buffdir/buffer/glnx86/recording ]; then
     buffexe=$buffdir'/buffer/glnx86/recording';
   fi
else # Mac
   buffexe=$buffdir'/buffer/bin/saving_buffer';
   if [ -r $buffdir/buffer/bin/maci/recording ]; then
     buffexe=$buffdir'/buffer/bin/maci/recording'
   fi
   if [ -r $buffdir/buffer/maci/recording ]; then
     buffexe=$buffdir'/buffer/maci/recording'
   fi
fi
$buffexe $outdir > $logfile
```

F.2 Detrend functions

```
function [X,dtm]=detrend(X,dim,order,wght,MAXEL)
% Linearly de-trend input, i.e. 0-mean and linear trends subtracted
%
% [X,dtm]=detrend(X,[dim,order,wght,MAXEL])
%
% Inputs:
%  X      -- n-d input matrix
%  dim    -- dimension of X to detrend along
%  order  -- [int] order of detrending {1,2} (1)
%  wght   -- [size(X,dim),1] weighting matrix for the points in X(dim)
%  MAXEL  -- max-size before we start chunking for memory savings
% Outputs:
%  X      -- detrended X
%  dtm    -- linear matrix used to detrend X
if ( nargin < 2 || isempty(dim) ) dim=find(size(X)>1,1,'first'); end;
if ( dim < 0 ) dim=ndims(X)+dim+1; end;
if ( nargin < 3 || isempty(order) ) order=1; end;
if ( nargin < 4 || isempty(wght) ) wght=1; end; wght=wght(:);
if ( nargin < 5 || isempty(MAXEL) ) MAXEL=2e6; end;

if ( order > 2 || order < 1) error('Only 1/2nd order currently'); end;

% Compute a linear detrending matrix
xb  = [(1:size(X,dim))'-size(X,dim) ones(size(X,dim),1)]; % orthogonal target's to
regress with
xbw = repop(xb,'.*',wght); % include weighting effect
dtm = inv([ xbw(:,1:end-1)'*xb(:,1:end-1) xbw(:,1:end-1)'*xb(:,end);
            xbw(:,end)'*xb(:,1:end-1)     xbw(:,end)'*xb(:,end)])*xbw';

szX=size(X);
[idx,chkStrides,nchks]=nextChunk([],szX,dim,MAXEL);
while ( ~isempty(idx) )
   Xch = X(idx{:});
   if ( order==2 )
      chidx={};for d=1:ndims(Xch); chidx{d}=1:size(Xch,d); end;
      Xch(chidx{1:dim-1},2:end,chidx{dim+1:end}) = diff(Xch,order-1,dim);
      Xch(chidx{1:dim-1},1    ,chidx{dim+1:end}) = Xch(chidx{1:dim-1},2,chidx{dim+1
      :end}); % BODGE
   end

   % comp scale and bias
   ab  = tprod(double(Xch),[1:dim-1 -dim dim+1:ndims(X)],dtm,[dim -dim],'n');
   % comp linear trend
   Xest= tprod(xb,[dim -dim],ab,[1:dim-1 -dim dim+1:ndims(X)],'n');
   Xch = Xch-Xest; % remove linear trend

   if( order==2 ) Xch=cumsum(Xch,dim); end
   X(idx{:})=Xch;
```

```
   idx=nextChunk(idx,szX,chkStrides);
end

return;

%--------------------------------------------------------------------------
function testCase()
f=cumsum(randn(1000,100)); dim=1;

clf; plot(f(:,1),'b'); hold on;

ff=detrend(f,1); % normal

ff=detrend(f,1,[],[1 zeros(1,size(f,1)-2) 1]); % weighted

ff=detrend(f,1,[],[1 ones(1,size(f,1)-2)*5e-2 1]); % weighted

ff=detrend(f,1,[],[],2000); % chunked

ff=detrend(f,1,[],mkFilter(size(f,1),[300 500])); % weighted

plot(ff(:,1),linecol());
```

F.3 ID outliers functions

```
function [badInd,feat,threshs,stdfeat,mufeat]=idOutliers(X,dim,thresh,feat,maxIter,
verb)
% identify outlining elements in a matrix using robust variance/mean computation
%
% [badInd,feat,threshs,stdfeat,mufeat]=idOutliers(X,dim,thresh,feat,maxIter,verb)
%
% Inputs:
%  X      -- [n-d] data to identify outling elements of
%  dim    -- dimension(s) along which to look for outlying elements
%  thresh -- [2x1] threshold in data-std-deviations std-deviations to test to remove
%            1st element is threshold above (3), 2nd is threshold below (-inf)
%  idx    -- [Nx1] or [size(X,dim) bool] sub-set of indicies along dim to consider
%  maxIter-- [int] number of times round the remove+re-compute var loop (6)
%  feat   -- [str] which feature type to use {'mu','var'}  ('var')
%  summary-- additional descriptive info

if(nargin<2 || isempty(dim) )    dim=1;       end;
if(nargin<3 || isempty(thresh) ) thresh=3.5; end;
if(nargin<4 || isempty(feat)   ) feat='var'; end;
if(nargin<5 || isempty(maxIter)) maxIter=3;  end;
if(nargin<6 || isempty(verb) )   verb=0;     end;

szX=size(X);

% compute stds over this dim
rdims = setdiff(1:ndims(X),dim);
[stds mus]=mvar(X,rdims);
stds  = sqrt(abs(stds));
if ( prod(szX(rdims))==1 ) stds=mus; end; % deal with vector inputs

if ( strcmp(feat,'var') )   feat=stds;  % outlying variance
elseif (strcmp(feat,'mu') ) feat=mus;   % outlying mean
elseif ( isnumeric(feat) && isequal(size(feat),szX(dim)) )
   feat=feat;                           % outlying given feature value
else error('Unrecognised feature type: %s',feat);
end

badInd=false(size(feat));
threshs=[];
for iter=1:maxIter;
   % compute variance of std over this dim for the good points
   mufeat(iter)  = median(feat(~badInd));
   stdfeat(iter) = std(feat(~badInd));
   % plot(feat);hold on;plot([0;numel(feat)],[1;1]*[mufeat mufeat+stdfeat
   mufeat-stdfeat mufeat+thresh*stdfeat]);
   % remove anything too far from the mean std,std
   threshs(1,iter)=mufeat(iter)+thresh(1)*stdfeat(iter);
   badIndi = (feat > threshs(1,iter));
   if( numel(thresh)>1 ) % lower test
```

```
      threshs(2,iter)=mufeat(iter)-thresh(2)*stdfeat(iter);
      badIndi = badIndi | (feat < threshs(2,iter));
   end
   if ( sum(badIndi|badInd) == sum(badInd) ) break; end; % no new pts added
   %if(verb>0)fprintf('%d) %d removed =
   %d',iter,sum(badIndi-badInd),sum(badInd)); end;
   badInd = badInd | badIndi;
end
return;
%-------------------------------------------------------------
function testCase()
X=randn(1000,1);
oI=randn(size(X))>1; X(oI)=X(oI)*5;
bad=idOutliers(X);
```

F.4 Classifier training functions

```
function [clsfr,res]=buffer_train_ersp_clsfr(X,Y,hdr,varargin);
opts=struct('capFile','1010','overridechnms',0);
[opts,varargin]=parseOpts(opts,varargin);
if ( nargin<3 ) error('Insufficient arguments'); end;
% extract the data - from field begining with trainingData
if ( iscell(X) )
  if ( isnumeric(X{1}) )
    X=cat(3,X{:});
  else
    error('Unrecognised data format!');
  end
elseif ( isstruct(X) )
  X=cat(3,X.buf);
end
X=single(X);
if ( isstruct(Y) ) Y=cat(1,Y.value); end; % convert event struct into labels

fs=[];
if ( isstruct(hdr) )
  if ( isfield(hdr,'channel_names') ) chNames=hdr.channel_names; end;
  if ( isfield(hdr,'fsample') ) fs=hdr.fsample; end;
elseif ( iscell(hdr) && isstr(hdr{1}) )
  chNames=hdr;
end

% get position info and identify the eeg channels
di = addPosInfo(chNames,opts.capFile,opts.overridechnms); % get 3d-coords
ch_pos=cat(2,di.extra.pos3d); ch_names=di.vals; % extract pos and channels names
iseeg=[di.extra.iseeg];

% call the actual function which does the classifier training
[clsfr,res]=train_ersp_clsfr(X,Y,'ch_names',ch_names,'ch_pos',ch_pos,'fs',fs,
'badCh',~iseeg,varargin{:});
return;
```

```
function [clsfr,res]=train_ersp_clsfr(X,Y,varargin)
% train a simple ERSP (spectral power) classifer
%
% [clsfr]=train_ersp_clsfr(X,Y,...)
%
% Inputs:
%  X          - [ ch x time x epoch ] data set
%  Y          - [ nEpoch x 1 ] set of data class labels
% Options:  (specify as 'name',value pairs, e.g. train_ersp_clsfr(X,Y,'fs',10);
%  ch_pos     - [3 x nCh] 3-d co-ordinates of the data electrodes
%               OR
%               {str} cell array of strings which label each channel in *1010 system*
%  fs         - sampling rate of the data
%  timeband   - [2 x 1] band of times to use for classification, all if empty ([])
%  freqband   - [2 x 1] or [3 x 1] or [4 x 1] band of frequencies to use
%               EMPTY for *NO* spectral filter
%  width_ms   - [float] width in millisecs for the windows in the welch spectrum
(250)
%               estimation.
%               N.B. the output frequency resolution = 1000/width_ms, so 4Hz with
250ms
%  spatialfilter -- [str] one of 'slap','car','none'  ('slap')
%  badchrm    - [bool] do we do bad channel removal    (1)
%  badchthresh - [float] threshold in std-dev units to id channel as bad (3.5)
%  badtrrm    - [bool] do we do bad trial removal      (1)
%  badtrthresh - [float] threshold in std-dev units to id trial as bad (3)
%  detrend    - [bool] do we detrend the data          (1)
%  visualize - [int] visualize the data
%               0 - don't visualize
%               1 - visualize, but don't wait
%               2 - visualize, and wait for user before continuing
%  verb       - [int] verbosity level
%  ch_names   - {str} cell array of strings which label each channel
%  class_names - {str} names for each of the classes in Y in *increasing* order ([])
% Outputs:
%  clsfr   - [struct] structure contining the stuff necessary to apply the trained
classifier
%  res     - [struct] detailed results for each fold
opts=struct('fs',[],'timeband',[],'freqband',[],'width_ms',250,'windowType',
'hanning','aveType','amp',...
            'detrend',1,'spatialfilter','slap',...
            'badchrm',1,'badchthresh',3.1,'badchscale',2,...
            'badtrrm',1,'badtrthresh',3,'badtrscale',2,...
            'ch_pos',[],'ch_names',[],'verb',0,'capFile','1010','visualize',1,...
            'badCh',[],'nFold',10,'class_names',[],'cog',0);
[opts,varargin]=parseOpts(opts,varargin);

% get the sampling rate
if ( isempty(opts.fs) ) error('Sampling rate not specified!'); end;
```

```
di=[]; ch_pos  =opts.ch_pos; ch_names=opts.ch_names;
if ( iscell(ch_pos) && isstr(ch_pos{1}) ) ch_names=ch_pos; ch_pos=[]; end;
if ( isempty(ch_pos) && ~isempty(ch_names) ) % convert names to positions
  di = addPosInfo(ch_names,opts.capFile); % get 3d-coords
  ch_pos=cat(2,di.extra.pos3d); ch_names=di.vals; % extract pos and channels names
end

%1) Detrend
if ( opts.detrend )
  fprintf('1) Detrend\n');
  X=detrend(X,2); % detrend over time
end

%2) Bad channel identification & removal
isbadch=[]; chthresh=[];
if ( opts.badchrm || ~isempty(opts.badCh) )
  fprintf('2) bad channel removal, ');
  isbadch = false(size(X,1),1);
  if ( ~isempty(opts.badCh) )
      isbadch(opts.badCh)=true;
      goodCh=find(~isbadch);
      if ( opts.badchrm )
          [isbad2,chstds,chthresh]=idOutliers(X(goodCh,:,:),1,opts.badchthresh);
          isbadch(goodCh(isbad2))=true;
      end
  elseif ( opts.badchrm ) [isbadch,chstds,chthresh]=idOutliers(X,1,opts.badchthresh
  );
  end;
  X=X(~isbadch,:,:);
  if ( ~isempty(ch_names) ) % update the channel info
    ch_pos  =ch_pos(:,~isbadch(1:numel(ch_names)));
    ch_names=ch_names(~isbadch(1:numel(ch_names)));
  end
  fprintf('%d ch removed\n',sum(isbadch));
end

%3) Spatial filter/re-reference
R=[];
if ( size(X,1)> 5 ) % only spatial filter if enough channels
  switch lower( opts.spatialfilter )
   case 'slap';
    fprintf('3) Slap\n');
    if ( ~isempty(ch_pos) )
      R=sphericalSplineInterpolate(ch_pos,ch_pos,[],[],'slap');%pre-compute the
      SLAP filter we'll use
    else
      warning('Cant compute SLAP without channel positions!');
    end
   case 'car';
```

```
    fprintf('3) CAR\n');
    R=eye(size(X,1))-(1./size(X,1));
   case {'whiten','wht'};
    fprintf('3) whiten\n');
    R=whiten(X,1,1,0,0,1); % symetric whiten
   case 'none';
   otherwise; warning(sprintf('Unrecog spatial filter type: %s. Ignored!',opts.
   spatialfilter ));
  end
end
if ( ~isempty(R) ) % apply the spatial filter
  X=tprod(X,[-1 2 3],R,[1 -1]);
end

%2.2) time range selection
timeIdx=[];
if ( ~isempty(opts.timeband) )
  timeIdx = opts.timeband * fs; % convert to sample indices
  timeIdx = max(min(timeIdx,size(X,2)),1); % ensure valid range
  X    = X(:,timeIdx(1):timeIdx(2),:);
end

%2.5) Bad trial removal
if ( opts.badtrrm )
  fprintf('2) bad trial removal');
  [isbadtr,trstds,trthresh]=idOutliers(X,3,opts.badtrthresh);
  X=X(:,:,~isbadtr);
  Y=Y(~isbadtr);
  fprintf(' %d tr removed\n',sum(isbadtr));
end;

%4) welch to convert to power spectral density
fprintf('4) Welch\n');
[X,wopts,winFn]=welchpsd(X,2,'width_ms',opts.width_ms,'windowType',opts.windowType,
'fs',opts.fs,...
                         'aveType',opts.aveType,'detrend',1);
freqs=0:(1000/opts.width_ms):opts.fs; % position of the frequency bins

%5) sub-select the range of frequencies we care about
fidx=[];
if ( ~isempty(opts.freqband) && size(X,2)>10 && ~isempty(opts.fs) )
  if ( numel(opts.freqband)>2 ) % convert the diff band spects to upper/lower
  frequencies
    if ( numel(opts.freqband)==3 ) opts.freqband=opts.freqband([1 3]);
    elseif(numel(opts.freqband)==4 ) opts.freqband=[mean(opts.freqband([1 2])) mean
    (opts.freqband([3 4]))];
    end
  end
  fprintf('5) Select frequencies\n');
```

```
  [ans,fidx(1)]=min(abs(freqs-opts.freqband(1))); % lower frequency bin
  [ans,fidx(2)]=min(abs(freqs-opts.freqband(2))); % upper frequency bin
  X=X(:,fidx(1):fidx(2),:); % sub-set to the interesting frequency range
end;

%5.5) Visualise the input?
if ( opts.visualize  && ~isempty(ch_pos) )
   uY=unique(Y);sidx=[]; labels=opts.class_names;
   for ci=1:numel(uY);
      mu(:,:,ci)=mean(X(:,:,Y==uY(ci)),3);
      if(~(ci>1 && numel(uY)<=2)) [auc(:,:,ci),sidx]=dv2auc((Y==uY(ci))*2-1,X,3,
      sidx); end;
      if ( isempty(labels) || numel(labels)<ci || isempty(labels{ci}) )  labels{ci
      }=sprintf('%d',uY(ci)); end;
   end
   if ( ~isempty(di) ) xy=cat(2,di.extra.pos2d); % use the pre-comp ones if there
   else xy = xyz2xy(ch_pos);
   end
   if (size(ch_pos,1)==3 ) xy = xyz2xy(ch_pos); else xy=[]; end; % convert 3d->2d
   co-ords
   erpfig=figure('Name','Data Visualisation: ERSP');
   yvals=freqs; if( ~isempty(fidx) ) yvals=freqs(fidx(1):fidx(2)); end
   image3d(mu,1,'plotPos',xy,'Xvals',ch_names,'ylabel','freq(Hz)','Yvals',yvals,
   'zlabel','class','Zvals',labels,'disptype','plot','ticklabs','sw','clabel','db');
   zoomplots;
   aucfig=figure('Name','Data Visualisation: ERSP AUC');
   image3d(auc,1,'plotPos',xy,'Xvals',ch_names,'ylabel','freq(Hz)','Yvals',yvals,
   'zlabel','class','Zvals',labels,'disptype','imaget','ticklabs','sw','clim',[.2
   .8],'clabel','auc');
   colormap ikelvin; zoomplots;
   drawnow;
end


%custom, calculate Center of Gravity based on relative ERD, Magnus Krogh
if(opts.cog)
   if(~exist('mu','var')) %check if mu has been calculated
      uY=unique(Y);sidx=[]; labels=opts.class_names;
      for ci=1:numel(uY);
         mu(:,:,ci)=mean(X(:,:,Y==uY(ci)),3);
         if(~(ci>1 && numel(uY)<=2)) [auc(:,:,ci),sidx]=dv2auc((Y==uY(ci))*2-1,X,3,
         sidx); end;
         if ( isempty(labels) || numel(labels)<ci || isempty(labels{ci}) )  labels{
         ci}=sprintf('%d',uY(ci)); end;
      end
      if ( ~isempty(di) ) xy=cat(2,di.extra.pos2d); % use the pre-comp ones if there
      else xy = xyz2xy(ch_pos);
      end
      if (size(ch_pos,1)==3 ) xy = xyz2xy(ch_pos); else xy=[]; end; % convert
```

```
      3d->2d co-ords
   end
   relERD=((mean(mu(:,:,2),2)-mean(mu(:,:,1),2))./mean(mu(:,:,1),2))';
   cW=1-relERD;
   cW(cW>1)=0;
   l=find(xy(1,:)<=0.00001); r=find(xy(1,:)>=0);
   cL=[sum(xy(1,l).*cW(l))/sum(cW(l)),sum(xy(2,l).*cW(l))/sum(cW(l))]; %Left
   hemisphere only
   cR=[sum(xy(1,r).*cW(r))/sum(cW(r)),sum(xy(2,r).*cW(r))/sum(cW(r))]; %Right
   hemisphere only
   cB=[sum(xy(1,:).*cW)/sum(cW),sum(xy(2,:).*cW)/sum(cW)]; %Both hemispheres
   cogfig=figure('Name','Data Visualisation: CoG');
   axis equal;
   grid on;
   axis([-2 2 -2 2]);
   hold on; scatter(cL(1),cL(2),'fill','d','b');
   hold on; scatter(cR(1),cR(2),'fill','d','r');
   hold on; scatter(cB(1),cB(2),'fill','d','g');
   r=.1;
   for i=1:size(ch_pos,2)
      hold on;
      rectangle('Position',[xy(1,i)-r xy(2,i)-r r*2 r*2],'Curvature',1);
      text(xy(1,i),xy(2,i),ch_names{i},'VerticalAlignment','Middle',
      'HorizontalAlignment','Center');
   end
end


%6) train classifier
fprintf('6) train classifier\n');
[clsfr, res]=cvtrainLinearClassifier(X,Y,[],opts.nFold,'zeroLab',1,varargin{:});

%7) combine all the info needed to apply this pipeline to testing data
clsfr.fs          = opts.fs;   % sample rate of training data
clsfr.detrend     = opts.detrend; % detrend?
clsfr.isbad       = isbadch;% bad channels to be removed
clsfr.spatialfilt = R;    % spatial filter used for surface laplacian

clsfr.filt        = []; % DUMMY -- so ERP and ERSP classifier have same structure
fields
clsfr.outsz       = []; % DUMMY -- so ERP and ERSP classifier have same structure
fields
clsfr.timeIdx     = timeIdx; % time range to apply the classifer to

clsfr.windowFn    = winFn;% temporal window prior to fft
clsfr.welchAveType= opts.aveType;% other options to pass to the welchpsd
clsfr.freqIdx     = fidx; % start/end index of frequencies to keep

clsfr.badtrthresh = []; if ( ~isempty(trthresh) ) clsfr.badtrthresh = trthresh(end
```

```
)*opts.badtrscale; end
clsfr.badchthresh = []; if ( ~isempty(chthresh) ) clsfr.badchthresh = chthresh(end
)*opts.badchscale; end
% record some dv stats which are useful
tstf = res.tstf(:,res.opt.Ci); % N.B. this *MUST* be calibrated to be useful
clsfr.dvstats.N   = [sum(res.Y>0) sum(res.Y<=0) numel(res.Y)]; % [pos-class
neg-class pooled]
clsfr.dvstats.mu  = [mean(tstf(Y==clsfr.spKey(1))) mean(tstf(Y==clsfr.spKey(2)))
mean(tstf)];
clsfr.dvstats.std = [std(tstf(Y==clsfr.spKey(1)))  std(tstf(Y==clsfr.spKey(2)))
std(tstf)];
%  bins=[-inf -200:5:200 inf]; clf;plot([bins(1)-1 bins(2:end-1)
bins(end)+1],[histc(tstf(Y>0),bins) histc(tstf(Y<=0),bins)]);

%custom
if(opts.cog)
   res.CoG           = struct('L',cL,'R',cR,'both',cB);
   res.extra         = struct('auc',auc,'mu',mu,'ch_names',{ch_names},'yvals',yvals
   ,'xy',xy);
end

if ( opts.visualize > 1 )
   b=msgbox({sprintf('Classifier performance : %s',sprintf('%4.1f ',res.tstbin(:,:,
   res.opt.Ci)*100)) 'OK to continue!'},'Results');
   while ( ishandle(b) ) pause(.1); end; % wait to close auc figure
   if ( ishandle(aucfig) ) close(aucfig); end;
   if ( ishandle(erpfig) ) close(erpfig); end;
   if ( ishandle(b) ) close(b); end;
   drawnow;
end

return;

%---------------------------------
function xy=xyz2xy(xyz)
% utility to convert 3d co-ords to 2-d ones
% search for center of the circle defining the head
cent=mean(xyz,2); cent(3)=min(xyz(3,:));
f=inf; fstar=inf; tstar=0;
for t=0:.05:1; % simple loop to find the right height..
   cent(3)=t*(max(xyz(3,:))-min(xyz(3,:)))+min(xyz(3,:));
   r2=sum(repop(xyz,'-',cent).^2);
   f=sum((r2-mean(r2)).^2); % objective is variance in distance to the center
   if( f<fstar ) fstar=f; centstar=cent; end;
end
cent=centstar;
r = abs(max(abs(xyz(3,:)-cent(3)))*1.1); if( r<eps ) r=1; end;  % radius
h = xyz(3,:)-cent(3);  % height
rr=sqrt(2*(r.^2-r*h)./(r.^2-h.^2)); % arc-length to radial length ratio
```

```
xy = [xyz(1,:).*rr; xyz(2,:).*rr];
return
%---------------------------------------
function testCase()
z=jf_mksfToy('Y',sign(round(rand(600,1))-.5));
[clsfr]=train_ersp_clsfr(z.X,z.Y,'fs',z.di(2).info.fs,'ch_pos',[z.di(1).extra.pos3d
],'ch_names',z.di(1).vals,'freqband',[0 .1 10 12],'visualize',1,'verb',1);
f=apply_ersp_clsfr(X,clsfr);
```

```
function [classifier,res,Y]=cvtrainLinearClassifier(X,Y,Cs,fIdxs,varargin)
% train a regularised linear classifier with reg-parameter tuning by cross
validation
%
% [classifier,res]=trainLinearClassifier(X,Y,Cs,fIdxs,varargin)
%
% N.B. use applyLinearClassifier to apply the learned model to new data.
%
% Inputs:
%  X - [n-d float] the data to classify/train on
%  Y - [size(X,dim) x 1] set of 1:nSp per trial labels
%      OR
%      [size(X,dim) x nSp] set of -1/0/+1 per-subproblem labels, where 0 indicates
an ignored point
%  Cs      - [1 x nCs] set of penalties to test
([10^(-3:3) 0])
%  fIdxs   - [size(Y,1) x nFold] logical matrix indicating which trials
%            to use in each fold,
%               -1 = training trials, 0 = excluded trials,  1 = testing trials
%            OR
%            [1 x 1] number of folds to use (only for Y=trial labels).     (10)
%            or
%            [size(Y) x nFold x nCls] logical matrix indicating trials for each
sub-prob per fold
% Options:
%  dim    - [int] the dimension(s) of X which contain the trials
(ndims(X))
%  objFn  - [str] which objetive function to optimise,
('klr_cg')
%  Cscale - [float] scaling parameter for the penalties
(.1*var(X))
%            N.B. usually auto computed from the data, set to 1 to force input Cs
%  balYs  - [bool] balance the labels of sets                                (0)
%  spType - [str] sub-problem decomposition to use for multi-class. one-of '1v1'
'1vR' ('1v1')
%  spKey  - [Nx1] set of all possible label values                           ([])
%  spMx   - [nSp x nClass] encoding/decoding matrix to map from class labels
to/from binary
%           subProblems                                                      ([])
% Outputs:
%  classifier -- [struct] containing all the information about the linear classifier
%           |.w -- [size(X) x nSp] weighting over X (for each subProblem)
%           |.b -- [nSp x 1] bias term
%           |.dim -- [ind] dimensions of X which contain the trails
%  res    -- [struct] results structure as returned by cvtrainFn
opts=struct('objFn','klr_cg','dim',[],'spType','1v1','spKey',[],'spMx',[],'zeroLab'
,0,...
            'balYs',0,'verb',0,'Cscale',[],'compKernel',1);
[opts,varargin]=parseOpts(opts,varargin);
```

```
if( nargin < 3 ) Cs=[]; end;
if( nargin < 4 || isempty(fIdxs) ) fIdxs=10; end;

dim=opts.dim; if ( isempty(dim) ) dim=ndims(X); end;
dim(dim<0)=dim(dim<0)+ndims(X)+1; % convert negative to positive indicies

if( ndims(Y)==2 && size(Y,1)==1 && size(Y,2)>1 ) Y=Y'; end; % col vector only
% build a multi-class decoding matrix
spKey=opts.spKey; spMx =opts.spMx;
if ( ~(isempty(spKey) && isempty(spMx)) ) % sub-prob decomp already done, so trust
it
  if ( ~all(Y(:)==-1 | Y(:)==0 | Y(:)==1) )
    error('spKey/spMx given but Y isnt an set of binary sub-problems');
  end
elseif ( size(Y,2)==1 && all(Y(:)==-1 | Y(:)==0 | Y(:)==1) && ~(opts.zeroLab && any
(Y(:)==0)) ) % already a valid binary problem
    spKey=[1 -1]; % binary problem
    spMx =[1 -1];
else
  [Y,spKey,spMx]=lab2ind(Y,spKey,spMx,opts.zeroLab); % convert to binary
  sub-problems
end
spDesc=mkspDesc(spMx,spKey);

% build a folding -- which is label aware, and aware of the sub-prob encoding type
if ( numel(fIdxs)==1 ) fIdxs=gennFold(Y,fIdxs,'dim',numel(dim)+1); end;
if ( opts.balYs ) [fIdxs] = balanceYs(Y,fIdxs); end % balance the folding if wanted

% estimate good range hype-params
Cscale=opts.Cscale;
if ( isempty(Cscale) || isequal(Cscale,'12') )  Cscale=CscaleEst(X,2,[],0);
elseif ( isequal(Cscale,'11') )                 Cscale=sqrt(CscaleEst(X,2,[],0));
end
if ( isempty(Cs) ) Cs=[5.^(3:-1:-3)]; end;

oX=X; odim=dim; szX=size(X); szY=size(Y); szF=size(fIdxs);
if ( numel(dim)>1 ) % make n-d problem into 1-d problem
  X=reshape(X,[prod(szX(1:min(dim)-1)) prod(szX(dim))]);
  Y=reshape(Y,[prod(szY(1:numel(dim))) szY(numel(dim)+1:end) 1]);
  % scale up fIdxs to Y size if necess
  if ( any(szF(1:numel(dim))==1) && any(szF(1:numel(dim))~=szY(1:numel(dim))) )
     fIdxs=repmat(fIdxs,[szY(1:numel(dim))./szF(1:numel(dim)) ones(1,ndims(fIdxs)-
     numel(dim))]);
     szF=size(fIdxs); % new size
  end
  fIdxs=reshape(fIdxs,[prod(szY(1:numel(dim))) szF(numel(dim)+1:end) 1]);
  dim=2; % now trial dim is 2nd dimension
end
```

```
% compute the kernel if needed for kernel methods
if ( opts.compKernel )
   % compute kernel
   if ( opts.verb>0 ) fprintf('CompKernel..');  end;
   X = compKernel(X,[],'linear','dim',dim);
   if ( opts.verb>0 ) fprintf('..done\n'); end;
   % call cvtrain to do the actual work
   % N.B. note we use dim 2 because of the kernel transformation
   res=cvtrainFn(opts.objFn,X,Y,Cscale*Cs,fIdxs,'dim',2,'verb',opts.verb,varargin
   {:});
else
   % call cvtrain to do the actual work
   res=cvtrainFn(opts.objFn,X,Y,Cscale*Cs,fIdxs,'dim',dim,'verb',opts.verb,varargin
   {:});
end


% Extract the classifier weight vector(s)
% best hyper-parameter for all sub-probs, N.B. use the same C for all sub-probs to
ensure multi-class is OK
[opttstbin,optCi]=max(mean(res.tstbin,2)+mean(res.tstauc,2),[],3);
for isp=1:size(Y,2); % get soln for each subproblem
   if ( isfield(res,'opt') && isfield(res.opt,'soln') ) % optimal calibrated
   solution trained on all data
      soln  = res.opt.soln{isp};
   else
      soln  = res.soln{isp,optCi(isp)};
   end
   W(:,isp) = soln(1:end-1); b(isp)=soln(end);
end
if ( ~opts.compKernel ) % input space classifier, just extract
   W=reshape(W,[szX(1:min(odim)-1) size(W,2)]);
else % kernel method. extract the weights
   if ( numel(odim)>1 ) W=reshape(W,[szX(odim) size(W,2)]); end;
   Xidx=1:ndims(X); Xidx(odim)=-odim; % convert from dual(alpha) to primal (W)
   W   = tprod(oX,Xidx,W,[-odim ndims(X)+1]);
end

% put all the parameters into 1 structure
classifier = struct('W',W,'b',b,'dim',dim,'spMx',spMx,'spKey',spKey);
return;
%--------------------------------------------------------------------------
function testCase()

[X,Y]=mkMultiClassTst([-1 0 0 0; 1 0 0 0; .2 .5 0 0],[400 400 50],[.3 .3 0 0; .3 .3
 0 0; .2 .2 0 0],[],[-1 1 1]);
[classifier,res]=cvtrainLinearClassifier(X,Y,[],10);
% 2d features
X=reshape(X,[2 2 size(X,2)]);
```

```
[classifier,res]=cvtrainLinearClassifier(X,Y,[],10);
[classifier,res]=cvtrainLinearClassifier(X,Y,[],10,'objFn','lr_cg','compKernel',0);
 % non-kernel method
% 2d epochs
szX=size(X); X=reshape(X,[szX(1:end-1) szX(end)/2 2]); Y=reshape(Y,size(Y,1)/2,2);
[classifier,res]=cvtrainLinearClassifier(X,Y,[],10,'dim',[-2 -1]);
[classifier,res]=cvtrainLinearClassifier(X,Y,[],10,'objFn','lr_cg','compKernel',0,
'dim',[-2 -1]);

f=applyLinearClassifier(X,classifier);



[ans,optCi]=max(res.tstbin,[],3);  % check the results are identical
clf;plot([res.f(:,1,optCi),f2(:)]);

% multi-class test
[X,Y]=mkMultiClassTst([-1 0; 1 0; .2 .5],[400 400 50],[.3 .3; .3 .3; .2 .2],[],[1 2
 3]);[dim,N]=size(X);
[classifier,res]=cvtrainLinearClassifier(X,Y,[],10,'spType','1vR');
[classifier,res]=cvtrainLinearClassifier(X,Y,[],10,'spType','1v1');
fldD = n2d(res.fold.di,'fold'); spD = n2d(res.fold.di,'subProb');
cvmcPerf(Y,res.fold.f,[1 spD fldD],res.fold.di(fldD).info.fIdxs,classifier.spMx,
classifier.spKey)
```